SOME PROBLEMS IN THE SLOSHING OF LIQUID IN MOVING CONTAINERS

by
RADHESHYAM KHANDELWAL

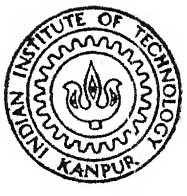

DEPARTMENT OF AERONAUTICAL ENGINEERING
INDIAN INSTITUTE OF TECHNOLOGY KANPUR

JANUARY 1980

SOME PROBLEMS IN THE SLOSHING OF LIQUID IN MOVING CONTAINERS

A Thesis Submitted
In Partial Fulfilment of the Requirements
for the Degree of
DOCTOR OF PHILOSOPHY

by
RADHESHYAM KHANDELWAL

to the
DEPARTMENT OF AERONAUTICAL ENGINEERING
INDIAN INSTITUTE OF TECHNOLOGY KANPUR
JANUARY 1980

AE-1900-D-KHA-SOM

TO

MAA INDIRA

CERTIFICATE

This is to certify that the thesis entitled "SOME PROBLEMS IN THE SLOSHING OF LIQUID IN MOVING CONTAINERS" by Radheshyam Khandelwal is a record of work carried out under my supervision and has not been submitted elsewhere for a degree.

N. C. NIGAM
Professor
Department of Aeronautical Engineering
Indian Institute of Technology, Kanpur

Kanpur

ACKNOWLEDGEMENTS

The author wishes to express his gratitude and sincere thanks to Professor N. C. Nigam for his guidance throughout the course of this work.

The author is grateful to Professors P. N. Murthy, N.G.R. Iyengar and Dr. S. Narayanan for their kind encouragement.

Drs. G. Kameshwar Rao, B. Kunwar, S.R.H. Rizvi and Messrs Laxman Pandey, A. Anwar, O. P. Singh, J. K. Sharma have earned the sincere thanks of the author for their help to compile this work. The instant and unassuming help offered by Mr. K.S. Mudappa, whenever needed, is gratefully acknowledged.

There is nothing valuable to repay in kind as a mark of sincere service for the sacrifice and sufferings undergone by author's mother. He expresses his respects and indebtedness with all his heart to her.

For typing the manuscript Mr. Nihal Ahmad is acknowledged thankfully.

Radheshyam Khandelwal

CONTENTS

LIST OF TABLES

LIST OF FIGURES

LIST OF PRINCIPAL SYMBOLS

a	length of container
a_1	length of wagon, container
b	breadth of container, wagon
$B_1, B_2, \ldots$	constants of integration
c	damping constant for plate
C_{rs}	damping constant for the plate mode r,s
c_1, c_2	damping constant for vehicle front and aft axles
c_v	damping constant for pendulum
$[c]$	damping matrix
C	railway track roughness constant
C_o	constant acceleration in horizontal direction
$d_1, d_2, d_3 \ldots$	initial conditions for displacements
D	bending rigidity of plate
$[D]$	dynamic matrix
$e_1, e_2, \ldots e_5$	eccentricity
E	Young's modulus
$E[\cdot]$	expectation operator
f_c, f	cut-off frequency in cycle/sec, frequency in cycle/ft
$\{f\}$	force vector
$\{F\}$	augmented forcing function vector
F_x	force in x-direction exerted by fluid
F_s	shear force
$F(\Omega)$	orthogonal function related to track roughness
g	acceleration due to gravity

g_o	amplitude of applied period acceleration
$\{g_i\}$	augmented forcing function vector in time domain
$\{G_i\}$	augmented forcing function vector in space domain
h	depth of liquid
h_l	height of container, liquid
h_i	impulse response function
$H(\Omega)$	frequency response function
I_{ov}	fixed mass moment of inertia
I_{sy}	moment of inertia of solidified mass of fluid
I_l	moment of inertia of empty vehicle mass about the centre of gravity of loaded vehicle
$[I]$	identity matrix
j	imaginary unit = $\sqrt{-1}$
k_1, k_2	vehicle suspension spring constant for front and aft axles
k_{ij}	eigenvalue for i, j mode of fluid
$[k]$	stiffness matrix
$[K]$	augmented mass and stiffness matrix
l_i	length of the pendulum for ith liquid slosh mode
l_v	length of the pendulum for first liquid slosh mode
l_1, l_2	are front and aft axle distance from the loaded vehicle c.g.
L_o	fixed mass distance from liquid c.g.
L_i	pivot point of the pendulum for ith liquid slosh mode
L	base length of the vehicle = l_1+l_2
m_p	mass/unit area of the plate
m_i	slosh mass for the ith mode of the liquid
m_v	mass of the pendulum = First slosh mass of the liquid = m_1

m_{ov}	fixed fluid mass
m_e	mass of the unloaded vehicle
$[m]$	mass matrix
$[M]$	augmented mass and damping matrix
M_{rs}	generalized mass in r,s mode of the plate
M_o	total mass of the fluid
M_b	bending moment
M_{Ty}	moment about the y-axis exerted by the liquid
p	pressure exerted by fluid
p_c	total pressure exerted by fluid on plate
P^*_{rs}	generalized force exerted by fluid on plate in r,s mode
$\{q\}$	augmented response vector
q_{rs}	generalized co-ordinate for plate
r_k	random phase distributed uniformly between 0 and 2π
R	aspect ratio of the container = h/a
$R_1, R_2, \ldots$	system constants in response evaluation
s	vehicle position along the track
t	time
t_o	natural period of oscillation of the vehicle
t_p	plate thickness, typical time period
T	total kinetic energy
$[U]$	modal matrix of eigen-vectors
$[u]$	partial eigen-vector of $[U]$
U	total potential energy
v	varying velocity of the vehicle

v_o	constant, initial velocity of the vehicle
$v_1, v_2, \ldots$	initial conditions for velocity response
V_x, V_y, V_z	velocity of fluid in x,y,z directions
W	transverse deflection of plate
$x_1, x_2, \ldots$	generalized co-ordinates for vehicle system
$y(t)$	track roughness as a function of time t
$Y(s)$	track roughness as a function of distance s.
$\bar{Z}$	generalized displacement vector, response vector
$[\alpha]$	eigen value matrix
$\alpha_1, \alpha_2, \alpha_3 \ldots$	eigenvalues
λ	reciprocal of eigenvalue = $1/\alpha$
β	damping ratio for vehicle
β_{rs}	damping ratio for r,s mode of the plate
γ	constant in track-profile power spectral density
Δ	determinant
ε	non-dimensional parameter for acceleration = $\ddot{z}_o/g$
ζ	free surface displacement
η	normal mode in x-direction for plate
ξ	normal mode in y-direction for plate
$\kappa_{zz}(s_1, s_2)$	covariance function of random process z(s)
ρ	density of fluid
μ_z	mean of random process z
ν	Poisson's ratio
φ	velocity potential
$\Phi_{YY}(\Omega)$	power spectral density of the process, Y
$\{\phi_i\}$	eigenvector
ω	frequency, rad/sec

ω_{rs}	natural frequency of plate in r,s mode
Ω	spatial frequency, rad/ft, rad/meter
Ω_c	cut-off frequency, rad/ft, rad/meter
Ω_{ij}	fluid natural frequency in i,j mode
Ω_i	natural ith slosh frequency
$(\cdot)$	differentiation w.r.t. time, t
$(')$	differentiation w.r.t. space variable, s.

SYNOPSIS

RADHESHYAM KHANDELWAL
Ph.D.
INDIAN INSTITUTE OF TECHNOLOGY, KANPUR
JANUARY, 1980

SOME PROBLEMS IN THE SLOSHING OF LIQUID IN MOVING CONTAINERS

The sloshing of liquids in partially filled moving containers occurs in a diverse class of problems. The moving container may be a fuel tank of an aircraft, a launch vehicle or an automobile; a ground based vehicle, such as, a truck, a railway wagon or an ocean going ship carrying liquid as cargo; an overhead tank, lake or dam, during ground motion, due to an earthquake. The container motion causes the contained liquid to oscillate. The oscillating liquid causes time dependent forces and moments to act on the container walls. Further, if the container walls are flexible, then there is an interaction between liquid oscillation and vibration of the container walls. For the structural design of the container, it is necessary to know the time-history of the forces and moments acting on the container walls due to sloshing. In the case of vehicles carrying liquid, the sloshing may be induced due to acceleration or deceleration of the vehicle and/or, the vibration of the vehicle. The sloshing of liquid generates time dependent forces and moments,

which in turn affect the vehicle vibration. Thus sloshing is coupled with vehicle vibration and forms an integral part of the overall vehicle dynamics. Under certain conditions the liquid in a container may undergo increasingly large amplitude oscillations leading to an interesting class of problems of instability.

For a mathematical treatment of the sloshing of liquid in a container, it is necessary to derive the equations governing the motion of the container and the liquid. The governing equations consist of a system of coupled equations of hydrodynamics and the equations of vibration of the container system. The exact nature of equations depends upon the physical problem. Generally, however, the equations are coupled, non-linear, partial and ordinary differential equations. Under certain assumptions, the equations of hydrodynamics can be linearized. Even these linearized equations are not always amenable to analytical treatment. For a large class of problems, particularly those concerning vehicle dynamics, it is convenient to replace the oscillating liquid by an equivalent discrete element mechanical model. For such a model, the governing equations consist of a system of coupled ordinary differential equations. These equations again may be nonlinear and may be further linearized or solved numerically.

The sloshing of liquid in containers mounted on ground based vehicles, constitutes a special class of problems. In these problems, the basic sources of vibration are the acceleration or deceleration of the vehicle and/or, the ground induced excitation due to the unevenness of the

prepared surface, such as, road, railway track or runway. Due to random nature of the unevenness of the prepared surfaces on which the vehicle rolls, the ground induced excitation is random in nature. The unevenness of prepared surfaces can be treated as a homogeneous one-dimensional random process with the space co-ordinate along the direction of motion as the indexing parameter. If the vehicle moves with a constant velocity, the base induced excitation is stationary and the vehicle response may be determined using the well known techniques of random vibration. If the vehicle moves with variable velocity, the base induced excitation becomes non-stationary. An analytical treatment of the non-stationary problem is much more difficult. Since the underlying process is homogeneous in space co-ordinates, the concept of evolutionary random process can be applied by transforming the governing equations from time to space co-ordinates. On such a transformation, the differential equations have variable co-efficients, but the excitation is homogeneous. The equations can now be solved either analytically in the frequency domain, using the concept of evolutionary spectra, or through simulation.

The present investigation deals with following problems in the sloshing of liquid in moving containers:

(i) Investigation of the stability of the plane free surface of liquid in a rectangular container with flexible bottom, under periodic vertical excitation.

(ii) Development of a mechanical model for liquid sloshing in a rectangular container under the simultaneous action of vertical excitation and horizontal motion.

(iii) Study of the dynamics of a vehicle carrying liquid as cargo and comparison of the results with a vehicle carrying an equivalent solidified mass of the liquid under identical random track induced excitation.

An incompressible inviscid liquid in a rectangular container with flexible bottom is subjected to longitudinal periodic excitation. Liquid motion is assumed to be linear. The container bottom is assumed to be simply supported plate on all edges and undergoes elastic deformations under thin plate approximations. The coupled differential equations have been solved to determine the regions of parametric instabilities. Numerical results have been presented to determine the primary and secondary instability regions for different cases of natural frequencies of liquid and bottom wall of the container and compared with stability regions for a container with rigid bottom.

An equivalent mechanical model is constructed for the liquid sloshing in a rigid rectangular container. The container is subjected to a constant horizontal acceleration and a periodic longitudinal acceleration. The liquid is assumed to be incompressible and inviscid. The governing hydrodynamic equations are linearized. The equivalent

mechanical model is determined by the equivalence of forces and moments developed by the sloshing liquid on the walls of the container. The mechanical model has a rigid mass and infinite number of oscillating pendulum masses. The analogy is valid for stable free surface conditions of the liquid.

In the last phase of the investigation, the dynamic response of a railway wagon carrying liquid as a cargo is studied. Two models of the wagon are considered. In the first the wagon is assumed to respond under the heave mode and in the second it responds under the heave and pitch modes. Two types of motions of the wagon are considered: (a) motion with constant acceleration, and (b) motion with constant velocity.

The equations governing the vibration of the wagon models are nonlinear. These equations are solved for the heave model moving with constant acceleration, through simulation. The track unevenness is simulated on a digital computer assuming a suitable power spectral density of the track. The liquid cargo is replaced by an equivalent mechanical model as described earlier. The equations governing the vehicle-fluid system are coupled and nonlinear. The response is determined by numerical integration in time domain for different heights of the liquid in the container. It is found that the vehicle response is a non-stationary narrow band random process. The liquid response reaches a

steady state quite early and the relative wave height, at the free surface of the liquid in the container, decreases with increase in the depth of the liquid. The coupling effect is found to be negligible.

The response of the wagon is also determined for a model having heave and pitch degrees of freedom. The liquid cargo is replaced by its equivalent mechanical analog. Equations of motion of the vehicle-fluid system are nonlinear and coupled. They contain inertial, velocity and restoring force nonlinearities. Equations of motion are linearized by one of the methods of stochastic linearization. The linearized equations of motion are transformed in space domain. The base excitation is assumed to be homogeneous in space domain. Assuming a suitable power spectral density of the track unevenness, the solution is obtained in the frequency domain. The response statistics are determined and compared with the vehicle system which has an equivalent solidified mass of the liquid.

The wagon is assumed to move with constant velocity and constant acceleration. For constant velocity case, the results obtained through the analytical form of the response statistics are presented. For constant acceleration case the equations of motion are solved numerically using the simulation technique.

When the wagon moves with constant velocity, the vehicle response statistics vary rapidly in the neighbourhood of small vehicle velocities. The response settles down with increase in vehicle velocity. At large vehicle velocities the response of the vehicle, in heave and pitch modes, tends to be independent of vehicle velocity. The relative wave height of the liquid at the free surface is found to increase with decrease in depth of the contained liquid. The relative wave height of the liquid increases with the increase in the eccentricity of the container c.g. placed with respect to vehicle c.g. The same is true for the shear force and bending moment developed by the sloshing liquid at the bottom edge of the side wall of the container.

On comparing the response of vehicle-liquid system with that of the vehicle-solidified mass system, it is found that the sloshing of liquid has the effect of reducing the vehicle response over most of the velocity range of interest. At some velocities, sloshing of liquid causes increase in vehicle response, but the range of such velocities is narrow and occurs at small vehicle velocities. The decrease in vehicle response is due to absorber-effect. The liquid absorbs the energy from the vehicle thus reducing the response, which in turn affects the liquid sloshing. The absorber-effect increases with increase in eccentricity of the container c.g. placed with respect to vehicle c.g. For a vehicle moving with constant

acceleration the overall vehicle and liquid response is similar to the constant velocity case. The reduction in vehicle response due to transfer of energy to the liquid is significant at high vehicle velocities. It is concluded that neglecting liquid sloshing provides conservative estimates of forces and displacements for under carriage design.

CHAPTER 1

INTRODUCTION

1.1 The Sloshing of Liquids

The dynamic behavior of liquids in moving containers, also known as sloshing, is of considerable interest to engineers, scientists, geophysicists, seismologists and other scientific workers. The spilling of a partially filled container carried hurriedly from one place to another is a common experience. Drinking a cup of tea or coffee can be a frustrating experience while riding on a vehicle moving over an uneven surface. Similar phenomena of liquid sloshing are observed in fuel tanks of aircrafts, rockets, automotive vehicles, large ocean going ships and rail-road tank cars. The motion of water in wells, lakes and dams during earthquakes constitutes large scale sloshing of a confined liquid mass.

The phenomena of liquid motion within a containing vessel presented a challenge to the hydrodynamicists of the past century. Their interest was stimulated by the need to study the earthquake effects on large dams, gasoline oil tanks, water reservoirs and elevated water tanks [31,49,50]. In applying the terrestrial molten core theory,

geophysicists have been interested in the study of motion of liquids in rotating containers [33]. The design of Boiling-Water-Reactor (BWR) [3] requires that the water level does not drop below a certain level under earthquake excitation. This is primarily due to the danger of escaping superheated steam through the inlet pipe. Similarly, the dynamic response analysis of a fast breader reactor should consider the sloshing of liquid sodium, used as coolant, in containers [9].

The problem of liquid fuel response in containers of aircrafts, rockets and missiles and its effect on vehicle dynamics has received considerable attention during the last three decades. Dynamic stability, flutter, controllability, attitude stabilization, elastic deformations produced due to forces created by fuel are some of the problems of continuing interest in aerospace applications.

Ground based vehicles often carry liquid as fuel or cargo. These include the rockets during their motion on a sled, aircrafts during taxi, take-off and landing; automotive vehicles and railway wagons. These vehicles are subjected mainly to two types of excitations. The first is the vertical base excitation of the vehicle through the points of contact on an uneven surface on which the vehicle is moving. The second is the

horizontal acceleration due to varying velocity of the vehicle. The dynamic analysis of such vehicles is considered primarily to understand the design aspects of the vehicle structure, passenger comfort, cargo safety and controllability of the vehicle.

As pointed out earlier, the liquid in a container mounted on a vehicle is subjected to a vertical excitation due to surface unevenness. This causes parametric excitation of the fluid mass and under certain conditions the free surface may undergo violent oscillations. This may result in disintegration of the surface and entrainment of small vapor bubbles may cause choking of the pipes connected to the container. Thus a study of the stability of the free surface of fluid in a container is also of considerable interest [1-3,8].

1.1.1 The design and dynamics of vehicles

The modern trend in vehicle design is towards higher speed, increased structural flexibility, light weight, low cost and longer life. The design of vehicle structure is strongly influenced by the dynamic loads due to vehicle motion. Structural components of vehicles, such as, landing gear and wing root in aircrafts, are prone to fracture or fatigue failure due to dynamic loading.

A vehicle should offer, psychological and physical comfort and safety to the passengers. The induced acceleration and the range of frequency are the two important parameters affecting the safety and comfort. Certain cargo, such as fragile materials, cannot withstand vibration effects beyond a certain level. In such a situation, operating vehicle speed becomes an important design constraint and this in turn influences the design of the undercarriage. Controllability and manoeuvrability of the vehicle by the driver are other important design aspects. Generally, gradual loss of control is followed by increasing velocity. Similarly, the manoeuvrability is reduced whenever there is a loss of ground contact or contact pressure of the wheels.

Ground based vehicles usually roll over an uneven surface and are subjected to base excitation. The characteristics of base excitations are determined by the type of contact, ground unevenness and vehicle speed. Due to random nature of ground unevenness, a vehicle moving on such a surface is subjected to random excitation. It is, therefore, necessary to carry out a random vibration analysis to determine the dynamic response of vehicles.

The vehicle dynamic response is determined by the nature of base excitation and the dynamic characteristics

of the vehicle, primarily, its natural frequency, modeshapes and damping. In vehicles carrying fluid in containers, vehicle motion and ground induced excitations cause fluid to oscillate; which in turn causes time varying loads to act on the vehicle. Thus, there is a coupling between liquid sloshing and vehicle response. Under certain conditions, this interaction may be significant both from the point of view of vehicle dynamics and liquid sloshing.

1.2 Review of Previous Work

The present work deals with some aspects of liquid sloshing and, also its effects on vehicle dynamics. A brief review of previous work in liquid sloshing and vehicle dynamics is given in the following sections:

1.2.1 Hydrodynamic effects induced in containers

The governing equations of motion for the liquid sloshing are generally non-linear in nature [1,2,8,17]. However, under certain approximations these equations can be linearized [1,8,31]. There are several interesting aspects of liquid sloshing, such as, liquid behavior under gravitational force, the bubble formation and growth, fluid-elastic interaction, vortex formation in draining containers, spinning containers, connected containers and other related problems. Cooper [17] and Abramson [2] have given a detailed

review of dynamic behavior of liquids in moving containers. A comprehensive review and analysis is given in Ref. [1]. In the sequel, a brief review of linearized liquid behavior in a container is given under the gravitational force.

1.2.1.1 Linear inviscid fluid oscillations in rigid containers

Scientists [31,41,8], seismologists [24], aerospace engineers [22,29,36] have shown considerable interest in developing comprehensive linearized theory of fluid oscillations in containers. For an incompressible fluid, Graham et al. [22] gave a detailed analysis based on horizontal, translation, pitching about a horizontal axis and rolling about a vertical axis for a partially filled rectangular container. Similar analysis for cylindrical containers is reported in [1-3,17, 29]. Workers in reservoir and reservoir-dam systems also have shown keen interest to take into account the hydrodynamic effects on dams during earthquake excitations for incompressible [49] and compressible [15,38] nature of water.

1.2.1.2 Equivalent mechanical models

To study the dynamic forces coming on the liquid-filled structures, it is convenient to replace the liquid by an equivalent mechanical system. The reason is that the discrete mass, stiffness and damping elements are more conveniently included in the equations of motion for the entire system.

Generally, an equivalent mechanical system is constructed by the equivalence of forces and moments developed by the fluid on the walls of the container. Such mechanical systems have been developed by number of investigators [1,2,17]. Graham et al. [22] have presented a sophisticated mechanical analog, for a rectangular container under lateral excitation, consisting of a fixed mass and infinite number of spring supported masses. This model has since been used extensively, specially in aircrafts, to study the dynamic behavior of fuel motion. Another mechanical model based on a fixed mass and infinite number of oscillating pendulum masses is reported in [29] for a circular cylinder undergoing lateral excitation. The advantage of the latter analogy is that the parameters of the model do not change with change in vertical acceleration. Experimental verifications of the theoretical results based on the models have been also reported [1,2,17].

A mechanical model, for liquid sloshing under vertical or simultaneously under lateral and vertical excitations of a container, is required for vehicle response studies. Such a model is not available in the literature [1].

1.2.1.3 Stability of free-surface of liquid

When a container filled with liquid, such as water, undergoes vertical periodic excitation, a pattern of stationary or standing waves can be observed on the free

surface. The governing equation of motion of free surface is characterized by parametric excitation and in a rigid container is described by Mathieu's equation [8,1]. The standing wave may have subharmonic, harmonic or superharmonic frequencies of oscillations. The stability of the free surface is accordingly influenced.

Workers in the past have studied the stability of free surface under vertical excitation mainly for rigid containers [1,2,17]. Benjamin and Ursell [8] have tried to generalize the linearized theory of stability of free surface under vertical periodic acceleration in rigid containers. For a particular case of circular cylinder, they also conducted experiments to confirm the theory. It is of interest to extend the linearized theory of stability of free surface to containers with flexible walls.

1.2.1.4 Damping of liquid motions in rigid containers

Damping has a profound effect on control and stability of liquid free surface. This is particularly true when the control system natural frequencies are close to the liquid natural frequencies. The damping of liquid is affected by the liquid height, liquid kinematic viscosity, size and the kind of wall prepared for the container. Liquids, like water, have negligible damping in containers with smooth

walls [1,8,16]. Theoretical and experimentally verified damping law of liquid motions are reported for containers with smooth, baffled and compartmented walls [1,2,16].

1.2.1.5 Fluid-elastic interaction

Due to external excitations, the generated hydrodynamic pressure deforms a container with flexible walls, which in turn affects the hydrodynamic pressure. This kind of fluid-elastic interaction occurs in several ways, such as, bending and breathing motion of container bottom and side walls.

In some studies, a simple beam bending mode is assumed for container walls and the sloshing is treated as a forced motion problem [1,7,17,35]. Both theory and experiments confirm that the presence of free liquid surface results in an increase of wall bending resonant frequency over the container of a capped liquid. On the other hand, the flexibility of the bottom of the container reduces the natural frequencies of the system [1,7,11].

Studies on fluid-elastic interaction have been carried out by assuming liquid as compressible also. Such studies include breathing vibration of containers [10,12,43] and lateral oscillations of liquids [9]. Workers of reservoir and reservoir dam systems have also considered the fluid-elastic interaction problem [15,38].

1.2.2 Vehicle dynamics

The trend in the design of transportation systems is increasingly towards achieving shortest travel time with maximum comfort for passengers and transport of maximum volume of cargo with safety and ease. To meet these requirements vehicles are required to provide better riding quality, higher velocity and larger capacity to carry the load. For the design of ground based vehicles, therefore, a better understanding of the dynamic behavior of the vehicle rolling over the ground surface is of considerable interest.

Since ground unevenness is the source of excitation for the rolling vehicles, the characteristics of the prepared ground surfaces such as roads, runways, railway track, etc. have been studied by many workers. Surface profiles are generally assumed to be one dimensional homogeneous Gaussian stochastic process in space and can be represented through their power spectral density. Such profiles include runways [23,51], highways [18,19,46], railway tracks [21].

Equations governing the vehicle dynamics may have nonlinearities in inertia, velocity and restoring force terms. If the vehicle operates in random environment, it is possible to approximate the equations of motion in a linear form by approximate methods. These methods include Fokker-Planck equation, small perturbation approach [46]

and equivalent statistical linearization method [14,32]. The equivalent statistical linearization method has been proposed and extensively used by Caughey [14] for a single degree of freedom model [4,26,32]. Later this method has been extended to multi-degree-of-freedom system by Iwan and Yang [26]. Another method applicable to multi-degree-of-freedom system is proposed by Atalik and Utku [4]. Limitations of each of these methods have been discussed in detail by Atalik and Utku [4]. Iwan and Yang's method is suited for spring-mass systems, but fails to linerize inertial nonlinearities. The more direct and simple method of stochastic linearization is the one suggested by Atalik and Utku [4]. By this method a multi-degree-of-freedom system in inertial, velocity and restoring forces can be linearized.

Analytical investigations for vehicle dynamics are possible both in time and frequency domain [51]. As the profile unevenness is assumed homogeneous, the input excitation process becomes stationary for vehicles moving with constant velocity [48,51]. For the linear model of the vehicle, the response becomes a stationary process. Both heave and pitch degrees of freedom have been considered for single point and two point excitations respectively by these investigators.

For an accelerating vehicle rolling over an uneven surface, the input excitation becomes non-stationary. In Refs. [46,48,51], the response of accelerating vehicles has been presented. Ref. [51] has presented a frequency domain approach using the concept of evolutionary spectra suggested by Priestley [39].

To analyze properly the dynamic performance of the vehicle carrying liquid as cargo, it is desirable to consider the sloshing aspects of the liquid in a container [1]. The dynamics of such vehicles is of interacting nature and is difficult to carry out. However, if one replaces the sloshing-liquid by its equivalent mechanical model, as discussed earlier, then the dynamic analysis of the vehicle system can be simplified. Also, by selecting only a few significant oscillating masses of the model, the analysis is further simplified. One can choose an analytical method to solve the equations of motion for vehicles, such as a railway wagon carrying a liquid cargo, as discussed above.

1.3 Objective and Scope of the Present Study

The objectives of the present study can be broadly classified as:

(i) To study the stability of the plane free surface in a flexible container under periodic vertical excitation,

(ii) to develop a mechanical model for liquid sloshing in a container under the simultaneous action of vertical and horizontal excitations, and.

(iii) to study the dynamics of the vehicle carrying liquid as cargo and comparing the results with equivalent solidified mass of the liquid carried by the vehicle under the same random environment.

In the first part of the work, an incompressible inviscid fluid in a rectangular container with flexible bottom is subjected to longitudinal periodic excitation. Linearized equations of motion and boundary conditions for the fluid oscillations are assumed. The flexible bottom plate undergoes elastic deformations under thin plate approximations and is assumed to be simply supported on all edges. The mathematical treatment for the coupled differential equations of motion is carried out by the method suggested by Bolotin [13]. This has been presented in Chapter 1.

In the second part of the work, described in Chapter 2, a mechanical model representing the liquid sloshing behavior in a rigid rectangular container is presented. The container is subjected to simultaneous action of a constant horizontal acceleration and a periodic longitudinal acceleration. Linearized equations of motion and boundary conditions are

assumed for the inviscid, incompressible fluid undergoing the presumed excitations. The equivalent mechanical model consists of a rigid mass and infinite number of oscillating pendulum masses. The oscillating masses are found to be independent of the parameters of excitations involved. Each oscillating mass is representative of the corresponding fluid mode. The fixed mass represents the mass of fluid which remains unaffected by the applied excitations. The analogy is valid for stable free surface conditions.

Chapters 4 and 5 present the results of the investigation of the dynamic response of a railway wagon carrying liquid as a cargo. The response is determined for the wagon moving with constant velocity and constant acceleration.

Chapter 4 describes the simulation of the track unevenness on a digital computer and determination of the response of a non-linear vehicle-fluid system model through numerical integration. The mathematical expression, for power spectral density of railway track, given in Ref. [21] is modified and tested. An analytically convenient mathematical expression is chosen such that it closely approximates the given power-spectral-density of Ref. [21] by least-square-fit procedure. The random process is generated by Monte-Carlo method suggested in [44,45] using the given power spectral density. The power spectral density of the simulated process

is determined and tested. It is found that the target and simulated spectra are close to each other.

The vehicle is assumed to respond under heave mode only. The liquid cargo is replaced by an equivalent mechanical model described in Chapter 3. The governing equations of motion of the vehicle system are described through 2-nonlinear coupled differential equations. Equations of motion are solved numerically by Runge-Kutta algorithm. The input process is generated as described earlier. It is found that the vehicle response is a narrow band nonstationary random process. The coupling effect between the vehicle response and liquid sloshing is found to be negligible. The liquid response is determined for three different heights of the liquid in the container. For different heights of the liquid it is found that the relative wave height of the liquid reduces with increase in the liquid depth in the container.

Chapter 5 describes the vehicle dynamics for a model with heave and pitch degrees of freedom. The vehicle dynamics is influenced by the sloshing of liquid. The dynamic behavior of liquid is represented through the mechanical analog developed in Chapter 3. The power spectral density of the track unevenness is assumed as in Chapter 4. The equations of motion describing the vehicle system dynamics are nonlinear and coupled. They contain

inertial, velocity and restoring force nonlinearities. The equations of motion are linearized by the method suggested by Atalik and Utku [4]. This method, as pointed out earlier, has an advantage of linearizing the nonlinearities in inertial terms as well. The linearized coupled equations are decoupled using the method of Foss [20]. The uncoupled equations are transformed from time domain to space domain. Finally the solution is obtained in frequency domain using the theory of random vibration. This is possible as the base excitation process is homogeneous in space domain. The response statistics for displacement and velocity are determined as a function of vehicle velocity. The response statistics are compared with the vehicle system which has an equivalent solidified mass of the liquid. Nine different vehicle-container configurations are considered for the study.

The vehicle chosen is a railway wagon which is assumed to move with constant velocity and constant acceleration. The base excitation to the vehicle is provided through the rail-road roughness whose form has been described in Chapter 4.

For constant velocity case, the response statistics are obtained in analytical form. The results obtained are presented and compared with the equivalent solid mass-vehicle system. It is found that the response statistics

vary rapidly in the neighbourhood of small vehicle velocities. The response settles down with increase in velocity. At large vehicle velocities the response of the vehicle, in heave and pitch modes, tends to be independent of vehicle velocity. Similar characteristics are found for the free surface response. The relative wave height of the fluid at the free surface increases with decrease in fluid depth. It further increases with the increase in eccentricity of the container c.g. placed with regard to vehicle c.g. Similar observations are made for the shear force and bending moment developed by the sloshing liquid at the bottom edge of the side wall of the container.

The response of vehicle-fluid system with that of the vehicle-solidified mass system are compared. It is found that the sloshing of liquid causes reduction in the vehicle response over most of the velocity range of interest. At some velocities, the sloshing of liquid causes increase in vehicle response. The range covered in such cases is narrow and towards small velocities. The decrease in vehicle response is due to absorber effect. The liquid absorbs the energy from the vehicle, thus reducing the response, which in turn affects the liquid sloshing. The absorber effect is found to increase with increase in eccentricity of the container placed with respect to the vehicle c.g.

For the constant acceleration case, the governing equations of motion for vehicle-fluid system and vehicle-solidified mass system are solved numerically using the simulation technique as described in Chapter 4 for the same rail-road roughness. It is found that the overall vehicle and liquid response is similar to the constant velocity case.

CHAPTER 2

PARAMETRIC INSTABILITIES OF THE PLANE FREE SURFACE OF A LIQUID IN A CONTAINER WITH FLEXIBLE BOTTOM UNDER VERTICAL PERIODIC MOTION

2.1 Introduction

Vertical vibrations of a container filled with liquid occur in several cases. In rockets and missiles, vertical vibrations occur due to dynamic coupling between the structure and the engine thrust. In aircrafts vertical excitation of fuel container occurs during taxi, landing and take-off and also during flight because of air turbulence. Containers filled with liquid in automobiles are also subjected to vertical excitation due to road roughness. Other examples of interest are containers subjected to vertical excitation during earthquake and include dams, overhead tanks etc. In vertically excited containers patterns of standing waves are observed. At certain forcing frequencies the surface may respond in a large amplitude standing wave and sometimes may disintegrate, forming a dense spray. It has been also observed that at a large input levels of vibrations, the surface motion

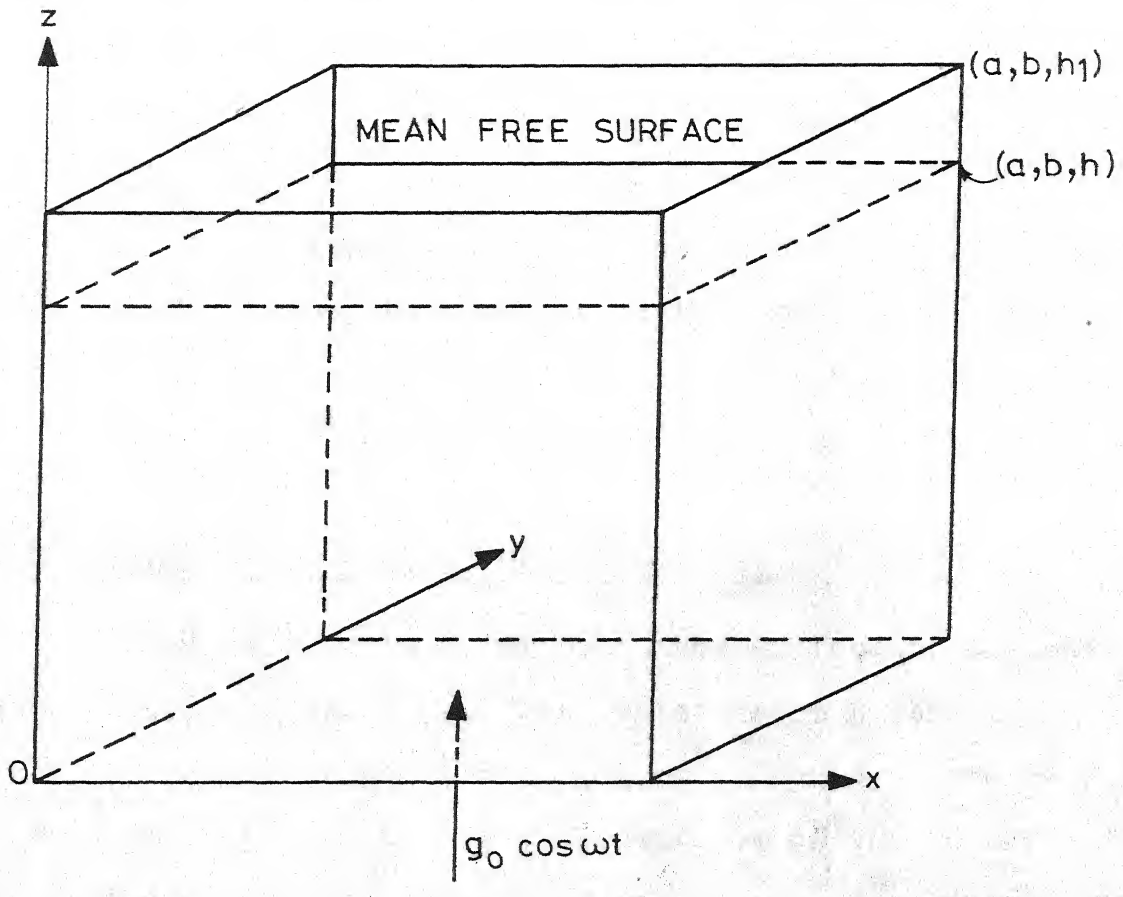

Fig. 2.1 CO-ORDINATE SYSTEM AND PARTIALLY FILLED RECTANGULAR CONTAINER GEOMETRY.

becomes violent and bubble formation may result. Literature on such behaviors of sloshing liquid has been widely reported [1,2,8,17].

In a prior investigation [8], the linearized theory of liquid motion is developed to study the stability of the plane free surface in rigid containers. In the present analysis the linearized theory of liquid motion is extended to study the stability of the plane free surface in a container having flexible bottom and rigid side walls.

2.2 Mathematical Formulation of the Problem

Consider a rectangular container of length, a, breadth, b and depth, h_1 (Fig. 2.1). The container is partially filled with an incompressible, inviscid liquid to the height, h as shown in the Fig. (2.1). Dimensions of the container are such that surface tension is neglected. The side walls of the container are rigid while the bottom is flexible and is assumed to be simply supported on all edges. The container is excited vertically upwards with acceleration $g_o \cos \omega t$, where g_o is constant. The fixed coordinate axes (x,y,z) are attached to the bottom corner of the container. Within the liquid the velocity potential must satisfy the Laplace's equation, viz.,

$$\frac{\partial^2\varphi}{\partial x^2} + \frac{\partial^2\varphi}{\partial y^2} + \frac{\partial^2\varphi}{\partial z^2} = 0 \qquad (2.1)$$

The velocity in the three directions x,y,z are given as

$$(V_x, V_y, V_z) = \left(\frac{\partial\varphi}{\partial x}, \frac{\partial\varphi}{\partial y}, \frac{\partial\varphi}{\partial z}\right) \qquad (2.2)$$

2.2.1 Boundary conditions

On the free surface of the liquid two conditions are to be satisfied. The first is the dynamic condition which demands that the pressure on the free surface must equal the pressure outside the liquid, which is assumed to be zero without loss of generality. Mathematically, it is given by [8],

$$\left[\frac{\partial\varphi}{\partial t} + (g - g_o \cos\omega t)\zeta\right]_{z=h} = 0, \qquad (2.3)$$

where $z = \zeta(x,y,t)$ defines the free surface and g is the acceleration due to gravity. And the second condition is the kinematic which requires that a particle on the free surface moves with the velocity of the free surface. Hence

$$\left[\frac{\partial\varphi}{\partial z} = \frac{\partial\zeta}{\partial t}\right]_{z=h} \qquad (2.4)$$

In deriving last two equations, products of small quantities are neglected [8]. Hence the formulation given here is restricted to small motions.

The normal component of velocity to the rigid wall is to be zero. Hence

$$\frac{\partial \varphi}{\partial x} = 0, \quad \text{at } x = 0, a \tag{2.5}$$

$$\frac{\partial \varphi}{\partial y} = 0, \quad \text{at } y = 0, b \tag{2.6}$$

Finally, if the flow does not cavitate, the particles of the liquid in contact with the flexible bottom and the bottom itself must move with the same velocity. If $W(x,y,t)$ denotes bottom plate displacement then the last boundary condition is given by

$$\frac{\partial \varphi}{\partial z}\Big]_{z=0} = \frac{\partial W}{\partial t} \tag{2.7}$$

In deriving the last boundary condition the products of nonlinear terms are neglected and the liquid velocity is evaluated at the undisturbed position of the bottom plate. The approximations are consistent with those of free surface conditions.

2.2.2 Equation of motion of the bottom plate

The differential equation for the motion of a thin elastic rectangular plate is

$$D\left[\frac{\partial^4 W}{\partial x^4} + 2\frac{\partial^4 W}{\partial x^2 \partial y^2} + \frac{\partial^4 W}{\partial y^4}\right] + c\dot{W} + m_p\ddot{W} = -p_c(x,y,t) \tag{2.8}$$

where,

W = transverse deflection of the plate,

$$D = Et_p^3/12(1 - \nu^2), \tag{2.9}$$

E = Young's modulus,

t_p = plate thickness, ν is Poisson's ratio, m_p is the mass per unit area of the plate, c is damping constant. $p_c(x,y,t)$ is the total pressure acting on the plate and is given by

$$p_c(x,y,0,t) = \rho h\,(g-g_o \cos\omega t) - \rho \frac{\partial \varphi}{\partial t}\Big]_{z=0} \qquad (2.10)$$

The last term in this equation is referred to as dynamic pressure [8] and ρ is the density of the liquid. The right hand member of (2.8) has a negative sign because positive pressure acts on the plate in a direction opposite to that of the positive plate deflection. Here simply supported bottom plate on its all edges is considered although the formulation holds good for other edge conditions. For a simply supported rectangular bottom plate the displacement $W(x,y,t)$ is given as follows,

$$W(x,y,t) = \sum_r \sum_s \eta_r(x) \cdot \xi_s(y)\, q_{rs}(t) \qquad (2.11)$$

where $$\eta_r(x) = \sin\left(\frac{r\pi}{a}x\right), \qquad (2.12)$$

$$\xi_s(y) = \sin\left(\frac{s\pi}{b}y\right),$$

are the normal modes in x and y directions and $q_{rs}(t)$ is the generalized co-ordinate for the modes r and s. In this co-ordinate system the differential equation for the plate vibrations is characterized as follows.

$$M_{rs}[\ddot{q}_{rs}(t) + 2\beta_{rs}\omega_{rs}\dot{q}_{rs} + \omega^2_{rs}\, q_{rs}(t)] = -P^*_{rs} \quad (2.13)$$

where, $M_{rs} = m_p \int_0^a \int_0^b \sin^2 \frac{r\pi}{a}x \cdot \sin^2(\frac{s\pi}{b}y)\,dxdy$

$$= m_p \frac{ba}{4}$$

$$C_{rs} = c \int_0^a \int_0^b \sin^2(\frac{r\pi}{a}x)\ \sin^2(\frac{s\pi}{b}y)\,dxdy$$

$$= \frac{cba}{4}, \quad (2.14)$$

$$\beta_{rs} = \frac{C_{rs}}{2M_{rs}\ \omega_{rs}},$$

$$\omega_{rs} = \pi^2 [(\frac{r}{a})^2 + (\frac{s}{b})^2]\sqrt{(\frac{D}{m_p})},$$

$$P^*_{rs}(t) = \int_0^b \int_0^a p_c(x,y,0,t)\ \sin \frac{r\pi}{a}x \cdot \sin \frac{s\pi}{b}y\ dxdy$$

2.2.3 Solution of the coupled boundary value problem

Following functions [8] satisfy the boundary conditions (2.5) and (2.6),

$$\varphi(x,y,z,t) = \sum_i \sum_j \cos(\frac{i\pi}{a}x)\ \cos(\frac{j\pi}{b}y)\ F_{ij}(z,t) \quad (2.15)$$

$$\zeta(x,y,t) = \sum_i \sum_j \cos(\frac{i\pi}{a}x)\ \cos(\frac{j\pi}{b}y)\ Q_{ij}(z,t) \quad (2.16)$$

The functions $F_{ij}(z,t)$ and $Q_{ij}(z,t)$ are to be determined. On substituting (2.15) into (2.1), (2.7) one gets

$$\frac{\partial^2 F_{ij}(z,t)}{\partial z^2} - k_{ij}^2 F_{ij}(z,t) = 0 \qquad (2.17)$$

where $k_{ij}^2 = r^2 \left[\left(\frac{i}{a}\right)^2 + \left(\frac{j}{b}\right)^2\right]$ (2.18)

and

$$\sum_i \sum_j \cos\left(\frac{i\pi}{a}x\right) \cos\left(\frac{j\pi}{b}y\right) \frac{\partial F_{ij}}{\partial z}\Big]_{z=0} = W(x,y,t) \qquad (2.19)$$

To make the last boundary condition (2.19) applicable, one multiplies both sides of it by $\cos(\frac{i\pi}{a}x)$ and $\cos(\frac{i\pi}{b}y)$ and then integrates with respect to x and y between the limits of $x = (0,a)$ and $y = (0,b)$ respectively. Finally one gets using (2.11)

$$\frac{\partial F_{ij}(z,t)}{\partial z}\Big]_{z=0} = \sum_r \sum_s C_{ij}^{rs} \dot{q}_{rs}(t) \qquad (2.20)$$

where, $C_{ij}^{rs} = \dfrac{16rs}{\pi^2(r^2-i^2)(s^2-j^2)}$.

Relation (2.20) is valid for odd-even combinations of (r,i) and (s,j). For all other combinations of (r,i) and (s,j) one has

$$\frac{\partial}{\partial z} F_{ij}(z,t)\Big]_{z=0} = 0 \qquad (2.21)$$

The other boundary condition is obtained from (2.3) and (2.4) using (2.15) and (2.16)

$$\frac{\partial F_{ij}(z,t)}{\partial t}\Big]_{z=h} + (g - g_o \cos \omega t)\, Q_{ij}(t) = 0 \qquad (2.22)$$

and

$$\frac{\partial F_{ij}(z,t)}{\partial z}\Big]_{z=h} = \frac{dQ_{ij}(t)}{dt} \qquad (2.23)$$

The boundary condition (2.21) corresponds to the case in which there is no coupling between fluid and elastic modes of plate. The solution of (2.17) corresponding to boundary conditions (2.21) and (2.22), (2.23) has been already dealt with [8]. Here solution corresponding to the coupled boundary conditions (2.20) and (2.22), (2.23) is treated for (2.17).

The general solution of (2.17) is given by,

$$F_{ij}(z,t) = A_{ij}(t) \cosh(k_{ij}z) + B_{ij}(t)\sinh(k_{ij}z) \qquad (2.24)$$

Boundary condition (2.20) gives

$$B_{ij}(t) = \frac{\sum_r \sum_s C_{ij}^{rs}\, \dot{q}_{rs}(t)}{k_{ij}} \qquad (2.25)$$

b.c. (2.22) and (2.23) determine respectively

$$\dot{A}_{ij}(t) \cosh (k_{ij}h) + \dot{B}_{ij}(t) \sinh (k_{ij}h) + (g-g_o \cos \omega t)\, Q_{ij}(t) = 0 \qquad (2.26)$$

and

$$k_{ij} A_{ij}(t) \sinh (k_{ij}h) + k_{ij} B_{ij}(t) \cosh (k_{ij}h) = \dot{Q}_{ij}(t) \qquad (2.27)$$

To determine $Q_{ij}(t)$ one needs to eliminate $A_{ij}(t)$ or its derivatives from (2.26) and (2.27). By multiplying (2.26) and (2.27) with $k_{ij}\sinh(k_{ij}h)$ and $\cosh(k_{ij}h)$ respectively and then differentiating (2.27) w.r.t. t one gets after subtraction from these two equations

$$\ddot{Q}_{ij} + (g-g_o\cos\omega t)\, k_{ij}\tanh(k_{ij}h)\, Q_{ij}(t) = \frac{k_{ij}\dot{B}_{ij}(t)}{\cosh(k_{ij}h)} .$$

Substituting for $\dot{B}_{ij}(t)$ using (2.25) one gets,

$$\ddot{Q}_{ij}(t) + k_{ij}\tanh(k_{ij}h)(g-g_o\cos\omega t)\, Q_{ij}(t) = \frac{\sum_r \sum_s C_{ij}^{rs}\, \ddot{q}_{rs}(t)}{\cosh(k_{ij}h)} \qquad (2.28)$$

Using specified initial conditions equation (2.28) is solvable for $Q_{ij}(t)$ provided $q_{rs}(t)$ is known. Further $Q_{ij}(t)$ and $q_{rs}(t)$ are coupled. At this point, the velocity potential for all the plate and fluid modes is written using (2.15), (2.24), (2.25) as follows.

$$\varphi(x,y,z,t) = \sum_i \sum_j \cos\left(\frac{i\pi}{a}x\right)\cos\left(\frac{j\pi}{b}y\right)\left[A_{ij}(t)\cosh(k_{ij}z) + \frac{\sum_r \sum_s C_{ij}^{rs}\, \dot{q}_{rs}(t)}{k_{ij}}\sinh(k_{ij}z)\right] \qquad (2.29)$$

in which $A_{ij}(t)$ is known either from (2.26) or (2.27) on the assumption that $Q_{ij}(t)$ is also known from (2.28). The function $q_{rs}(t)$ is determined using (2.10), (2.13) and (2.14). Using (2.10) and (2.29) one gets,

$$p_c(x,y,0,t) = \rho h(g-g_o\cos\omega t) - \rho \sum_i \sum_j \cos(\frac{i\pi}{a}x) \cos(\frac{j\pi}{b}y) \cdot \dot{A}_{ij}(t)$$

in which $\dot{A}_{ij}(t)$ is known either using (2.26) or (2.25) and is given by

$$\dot{A}_{ij}(t) = -[(g-g_o\cos\omega t)Q_{ij}(t) + \frac{\sum_r \sum_s C_{ij}^{rs} \ddot{q}_{rs}}{k_{ij}} \sinh k_{ij}h] \frac{1}{\cosh(k_{ij}h)}$$

Thus,

$$p_c(x,y,0,t) = +\rho h(g-g_o\cos\omega t) + \rho \sum_i \sum_j \cos\frac{i\pi}{a}x \cdot \cos\frac{j\pi}{b}y$$

$$[(g-g_o\cos\omega t)\, Q_{ij}(t) + \frac{[\sum_{r_1} \sum_{s_1} C_{ij}^{rs} \ddot{q}_{r_1 s_1}] \sinh k_{ij}h}{k_{ij}}] \frac{1}{\cosh(k_{ij}h)} \cdot \qquad (2.30)$$

Using (2.30) one gets from (2.14)

$$P_{rs}^*(t) = \frac{\rho h\, ab}{\pi^2 rs}[(-1)^r-1][(-1)^s-1](g-g_o\cos\omega t)$$

$$+\rho \sum_i \sum_j \frac{ab}{4} \frac{C_{ij}^{rs}}{k_{ij}\cosh(k_{ij}h)} [k_{ij}(g-g_o\cos\omega t)\, Q_{ij}(t)$$

$$+ \sinh(k_{ij}h) \sum_{r_1} \sum_{s_1} C_{ij}^{r_1 s_1} \ddot{q}_{r_1 s_1}(t)] \qquad (2.31)$$

On substituting (2.31) into (2.13) one gets

$$M_{rs}[\ddot{q}_{rs}(t) + 2\beta_{rs}\omega_{rs}\dot{q}_{rs}(t) + \omega_{rs}^2 q_{rs}(t)]$$

$$= -\left[\frac{\rho h ab\,((-1)^r-1)((-1)^s-1)}{\pi^2 rs}(g-g_o\cos\omega t)\right.$$

$$+\rho \sum_i \sum_j \frac{ab}{4} \frac{C_{ij}^{rs}}{k_{ij}\cosh(k_{ij}h)} \left(k_{ij}(g-g_o\cos\omega t)Q_{ij}(t)\right.$$

$$\left.\left. + \sinh k_{ij}h \sum_{r_1}\sum_{s_1} C_{ij}^{r_1 s_1} \ddot{q}_{r_1 s_1}(t)\right)\right] \qquad (2.32)$$

Rewriting for convenience, Eq. (2.28) one has

$$\ddot{Q}_{ij}(t) + k_{ij}\tanh(k_{ij}h)\cdot(g-g_o\cos\omega t)Q_{ij}(t) = \frac{\sum_r\sum_s C_{ij}^{rs}\ddot{q}_{rs}(t)}{\cosh(k_{ij}h)} \qquad (2.33)$$

Last two equations are sufficient to determine as many unknowns as in $Q_{ij}(t)$ and $q_{rs}(t)$ depending upon the initial conditions specified for the same number of unknowns. Thus, the problem is well defined for the unknowns $Q_{ij}(t)$ and $q_{rs}(t)$. It has been also noted earlier that (i,r) and (j,s) individually should have odd-even combinations so that C_{ij}^{rs} is other than zero for a coupled boundary value problem. For other combinations, C_{ij}^{rs} does not exist and belongs to uncoupled boundary value problem. It is clear that the solution involving all the fluid and elastic modes is difficult if not impossible. Therefore to gain insight, the problem is treated for one elastic and one fluid mode only.

One of the many possible combinations of (i,r), (j,s) may be either r=s=1 for plate and i=j=2 for fluid modes, or, r=s=2 for plate and i=j=1 for fluid modes.

Presently as an example, r=s=1 and i=j=2 are assumed. Further for simplification the plate damping, β_{rs}, is assumed zero and hence one gets from (2.32) and (2.33) the two coupled equations as follows.

$$\left(M_{11} + \frac{\rho ab (C_{22}^{11})^2 \tanh k_{22}h}{4 k_{22}}\right) \ddot{q}_{11}(t) + M_{11}\omega_{11}^2 q_{11}(t)$$

$$= -\left(\frac{4\rho hab}{\pi^2} + \frac{\rho ab\, C_{22}^{11}\, Q_{22}(t)}{4 \cosh (k_{22}h)}\right) (g - \varepsilon_o \cos \omega t)$$

$$\ddot{Q}_{22}(t) + k_{22} \tanh(k_{22}h)\cdot(g - g_o \cos \omega t) Q_{22}(t) = \frac{C_{22}^{11} \ddot{q}_{11}(t)}{\cosh(k_{22}h)}$$

On rearranging the last two equations one gets

$$\ddot{q}_{11} + \omega_{11}^{*2} q_{11}(t) + D_2(1-\varepsilon \cos \omega t) Q_{22}(t) = -D_1(1-\varepsilon \cos \omega t) \tag{2.34}$$

$$-D_3 \ddot{q}_{11}(t) + \ddot{Q}_{22}(t) + \Omega_{22}^2 (1-\varepsilon \cos \omega t)\, Q_{22}(t) = 0 \tag{2.35}$$

where,

$$\omega_{11}^{*2} = \frac{M_{11}}{M_{11}^*} \omega_{11}^2, \quad \Omega_{22}^2 = g\, k_{22} \tanh (k_{22}h)$$

$$M_{11}^* = M_{11} + \frac{\rho (C_{22}^{11})^2 \cdot ab \tanh(k_{22}h)}{4 k_{22}},$$

$$C_{22}^{11} = \frac{16}{9\pi^2}, \quad \varepsilon = \frac{g_o}{g}, \tag{2.36}$$

$$D_1 = \frac{4\, h_o ab}{\pi^2 M_{11}^*} g, \quad D_2 = \frac{\rho C_{22}^{11} ab}{4 M_{11}^* \cosh(k_{22} h)} g ,$$

$$D_3 = \frac{C_{22}^{11}}{\cosh(k_{22} h)} . \tag{2.36}$$

Combining equations (2.34) and (2.35) in the matrix form as follows.

$$\underline{C}\, \ddot{\underline{F}} + (\underline{I} - \underline{A} - \varepsilon\, \underline{B} \cos \omega t)\, \underline{F} = \underline{D} \tag{2.37}$$

where

$$\underline{C} = \begin{bmatrix} 1 & 0 \\ -D_3 & 1 \end{bmatrix}, \quad \underline{I} = \begin{bmatrix} 1 & 0 \\ 0 & 1 \end{bmatrix},$$

$$\underline{A} = \begin{bmatrix} 1-\omega_{11}^{*2} & -D_2 \\ 0 & 1-\Omega_{22}^2 \end{bmatrix}, \quad \underline{B} = \begin{bmatrix} 0 & D_2 \\ 0 & \Omega_{22}^2 \end{bmatrix}, \tag{2.38}$$

$$\underline{F} = \begin{Bmatrix} q_{11} \\ Q_{22} \end{Bmatrix}, \quad \underline{D} = \begin{Bmatrix} -D_1(1-\varepsilon \cos \omega t) \\ 0 \end{Bmatrix}.$$

Equation (2.37) will be used to study the parametric instabilities of the liquid surface.

2.3 The Parametric Instabilities

The parametric instabilities of a liquid surface mainly differ from the forced vibration response in following respects.

(i) The parametric instability may occur at frequencies other than the natural frequency of the free-surface oscillations.

(ii) For transverse excitation of tank, the frequency of the free surface is precisely the same as that of the forcing frequency and resonance occurs at discrete frequencies. In contrast to this, the parametric resonance exists over a continuous regions of excitations (regions of dynamic instabilities) in which we are interested [13].

Parametric instabilities are classified [13] as primary and secondary instabilities. If a system has natural frequencies $\Omega_n (n = 1,2,3,\ldots)$, then the primary instabilities occur at $\omega = \frac{2}{k}\Omega_n$ with $k = 1,3,5,\ldots$, as the excitation parameter tends to zero, where ω is the frequency of periodically varying parameter. Similarly, the secondary instabilities occur at $\omega = \frac{2}{k}\Omega_n$ with $k = 2,4,6,\ldots$, as the excitation parameter tends to zero. Further distinction in parametric instability is made when k=1 and 2 and corresponding instabilities are termed as principal primary and principal secondary instabilities respectively. Bolotin [13] has suggested that principal instability is the most critical one among all others and has greatest physical importance. Principal primary instability region is also known as the principal region of dynamic instability.

2.3.1 Determination of regions of dynamic instabilities

To study the dynamic instability the homogeneous part of equation (2.37) is considered viz.,

$$\underline{C}\,\ddot{\underline{F}} + (\underline{I} - \underline{A} - \varepsilon\underline{B}\cos\,\omega t)\,\underline{F} = 0 \qquad (2.39)$$

Bolotin [13] has shown that the regions of unbounded solutions are separated from the regions of bounded solutions by the periodic solutions with period T and 2T, where $T = \frac{2\pi}{\omega}$ (Ref. Appendix A). More explicitly, the region of instability is bounded by two solutions of identical periods whereas the region of stability is bounded by two solutions of different periods. The regions of primary instability are contained by the solutions with period 2T and secondary instability regions are contained by the solutions with period T.

2.3.1.1 Primary instability regions

To determine the regions of primary instability of the system (2.39) one assumes [13]

$$\underline{F} = \sum_{k=1,3,5} [\underline{a}_k \sin\,(\tfrac{k}{2}\,\omega t) + \underline{b}_k \cos\,(\tfrac{k}{2}\,\omega t)], \qquad (2.40)$$

where $\underline{a}_k$ and $\underline{b}_k$ are unknown vectors and are independent of time. Substituting (2.40) into (2.39) and comparing coefficients of $\sin(\frac{k\omega t}{2})$ and $\cos(\frac{k\omega t}{2})$ on both sides of the equation one obtains the following system of matrix equations.

$$(\underline{I} - \underline{A} + \tfrac{1}{4}\varepsilon\,\underline{B} - \tfrac{\omega^2}{4}\,\underline{C})\,\underline{a}_1 - \tfrac{1}{2}\,\varepsilon\,\underline{B}\,\underline{a}_3 = \underline{0},$$

$$(\underline{I} - \underline{A} - \tfrac{1}{4}k^2\omega^2\,\underline{C})\,\underline{a}_k - \tfrac{1}{2}\varepsilon\,\underline{B}\,(\underline{a}_{k-2} + \underline{a}_{k+2}) = \underline{0},$$

$$(\underline{I} - \underline{A} - \tfrac{1}{2}\varepsilon\,\underline{B} - \tfrac{1}{4}\omega^2\,\underline{C})\,\underline{b}_1 - \tfrac{1}{2}\varepsilon\,\underline{B}\,\underline{b}_3 = \underline{0},$$

$$(\underline{I} - \underline{A} - \tfrac{1}{4}k^2\omega^2\,\underline{C})\,\underline{b}_k - \tfrac{1}{2}\varepsilon\,\underline{B}\,(\underline{b}_{k-2} + \underline{b}_{k+2}) = \underline{0},$$

with $k = 3,5, \ldots$ (2.41)

Combining all these infinite set of matrix equation one gets,

$$\begin{bmatrix} G_{11} & G_{12} & G_{13} & G_{14} & \cdots \\ G_{21} & G_{22} & G_{23} & G_{24} & \cdots \\ G_{31} & G_{32} & G_{33} & G_{34} & \cdots \\ G_{41} & G_{42} & G_{43} & G_{44} & \cdots \\ \vdots & & & & \end{bmatrix} \begin{Bmatrix} \underline{a}_1 \\ \underline{b}_1 \\ \underline{a}_3 \\ \underline{b}_3 \\ \vdots \end{Bmatrix} = \{\underline{0}\}, \qquad (2.42)$$

where

$G_{11} = \underline{I} - \underline{A} + \frac{1}{2}\varepsilon\,\underline{B} - \frac{\omega^2}{4}\,\underline{C}$, $G_{12} = 0$, $G_{13} = \frac{1}{2}\,\varepsilon\,\underline{B}$, $G_{14} = 0, \ldots$

$G_{21} = 0$, $G_{22} = \underline{I} - \underline{A} - \frac{1}{2}\varepsilon\,\underline{B} - \frac{\omega^2}{4}\,\underline{C}$, $G_{23} = 0$, $G_{24} = -\frac{1}{2}\varepsilon\,\underline{B}, \ldots$

$G_{31} = -\frac{1}{2}\varepsilon\,\underline{B}$, $G_{32} = 0$, $G_{33} = \underline{I} - \underline{A} - \frac{9}{4}\omega^2\underline{C}$, $G_{34} = 0, \ldots$

$G_{41} = 0$, $G_{42} = -\frac{1}{2}\varepsilon\,\underline{B}$, $G_{43} = 0$, $G_{44} = \underline{I} - \underline{A} - \frac{25}{4}\,\omega^2\underline{C}, \ldots$

etc.

The system of equations (2.42) has solutions other than trivial provided the determinant of the co-efficient matrix,

[G], is zero. This will ensure the determination of frequencies bounding the instability regions. The determinant, $|G|$, is of infinite order. It can be shown that, $|G|$, belongs to the class of normal[t] determinant and is absolutely convergent [13]. The direct application of $|G|$ to determine the exact instability regions is practically inconvenient. Hence, approximately the regions of instability are obtained by truncating the series in equation (2.40) at k=1. This is equivalent to consider the determinant circumscribed with dashed lines in (2.42). The approximation, k=1, necessarily yields the principal instability regions. For a better approximation and also to determine the higher order regions of instability one has to truncate the series in equation (2.40) at higher values of k. Bolotin [13] has shown through an example of a beam subject to a periodic axial force that

---

t The determinant

$$\Delta = \begin{vmatrix} 1+C_{11} & C_{12} & C_{13} & \cdots \\ C_{21} & 1+C_{22} & C_{23} & \cdots \\ C_{31} & C_{32} & 1+C_{33} & \cdots \\ \cdots\cdots & & & \end{vmatrix}$$

is called normal if the double series $\sum_{i=1}^{\infty} \sum_{k=1}^{\infty} C_{ik}$ is absolutely convergent.

for values of ε upto 0.6, the regions of principal primary instability obtained by k=1 approximation, are within one percent of those obtained by k=3 approximation. In another example of coupled equations Bolotin has shown that the width of the regions of dynamic instability rapidly decreases as the number of regions increases. The width of the instability region reduces as ε^r, where r is the number corresponding to the first, second etc. instability regions. Thus, the first region of instability has the greatest width.

2.3.1.2 Secondary instability regions

To determine the regions of secondary instability, which are separated by solution of period T, one assumes [13]

$$\underline{F} = \frac{1}{2}\underline{b}_o + \sum_{k=2,4,6} \left[\underline{a}_k \sin\frac{k\omega t}{2} + \underline{b}_k \cos\frac{k\omega t}{2}\right] \qquad (2.43)$$

Substituting this equation into (2.39) and comparing the co-efficients of $\sin(\frac{k\omega}{2}t)$ and $\cos(\frac{k\omega}{2}t)$, yields the equation of the form (2.42) with the column vector $\begin{Bmatrix} b_o \\ a_2 \\ b_2 \\ a_4 \\ \vdots \end{Bmatrix}$ and the matrix [G] having the elements as follows.

$G_{11} = \underline{I} - \underline{A}$, $G_{12} = 0$, $G_{13} = -\varepsilon\underline{B}$, $G_{14} = 0$, ...

$G_{21} = 0$, $G_{22} = \underline{I} - \underline{A} - \omega^2\underline{C}$, $G_{23} = 0$, $G_{24} = -\frac{1}{2}\varepsilon\underline{B}$, ...

$G_{31} = -\frac{1}{2}\varepsilon\underline{B}$, $G_{32}=0$, $G_{33} = \underline{I}-\underline{A}-\omega^2\underline{C}$, $G_{34}=0$,

$G_{41} = 0$, $G_{42} = -\frac{1}{2}\varepsilon\underline{B}$, $G_{43} = 0$, $G_{44} = (\underline{I} - \underline{A} - 4\omega^2\underline{C})$, ...

.....

etc.

The determinant corresponding to k=2 approximation is

$$\begin{vmatrix} G_{11} & G_{12} & G_{13} \\ G_{21} & G_{22} & G_{23} \\ G_{31} & G_{32} & G_{33} \end{vmatrix}, \qquad (2.44)$$

and when equated to zero, determines the regions of secondary instability approximately.

2.4 Results and Discussions

2.4.1 Computations performed

Using the analysis presented in the earlier sections, the following computations have been performed. Regions of primary and secondary instabilities associated with the first mode of the plate (1,1) and second mode of the fluid (2,2) are determined so that coupling effect is retained. The instability regions have been presented as plots of the non-dimensional frequency versus the excitation parameter ε. The non-dimensional frequency is the ratio of exciting frequency to fluid natural frequency associated with the fluid mode under discussion. The excitation parameter is the ratio of vertical acceleration to acceleration due to gravity. Values of ε up to 0.9 have been considered for both primary and secondary instability regions.

The regions of instability have been obtained for three ratios of plate to fluid natural frequencies. These ratios

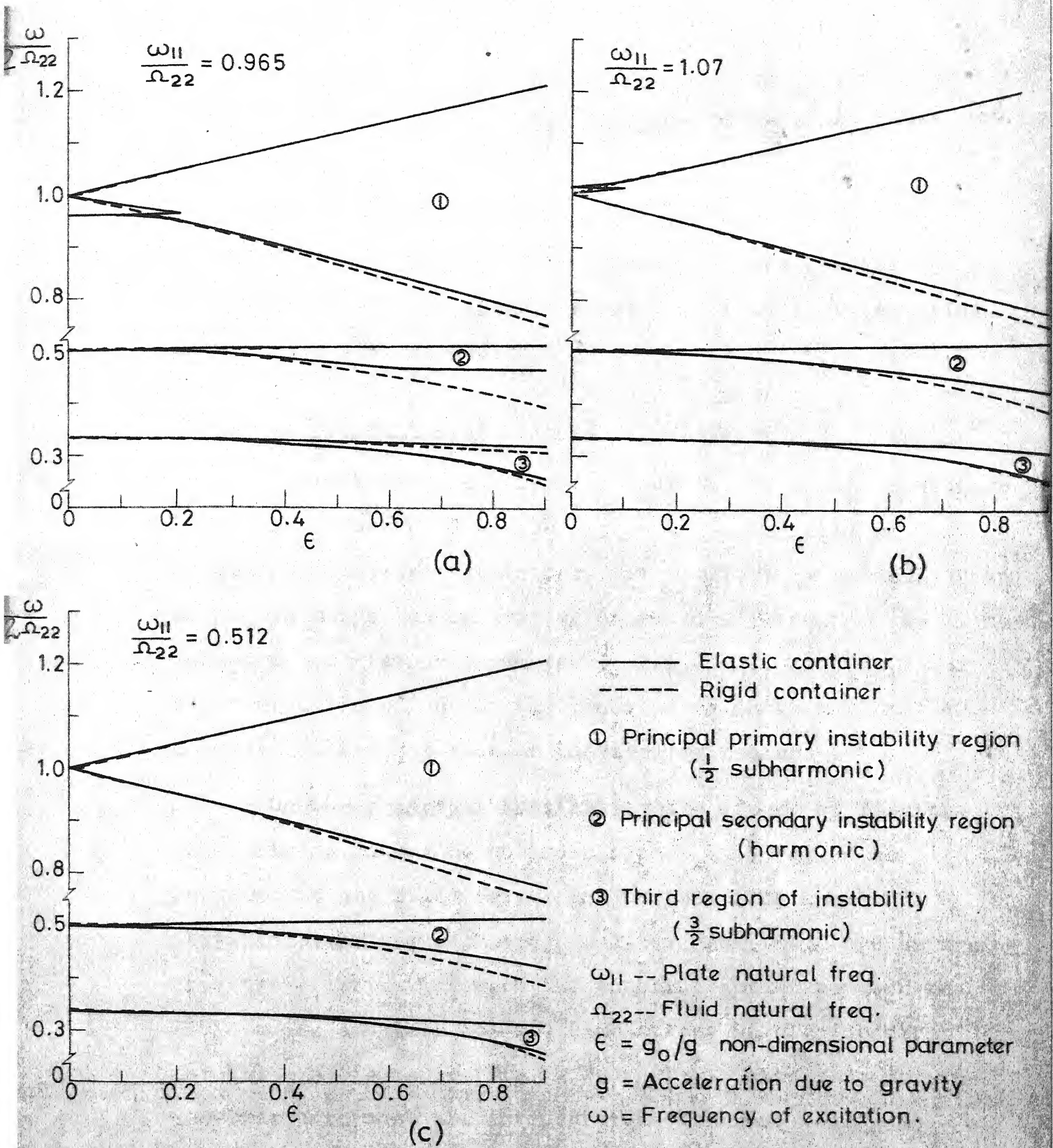

FIG.2.2 REGIONS OF INSTABILITIES ASSOCIATED WITH PLATE MODE (1,1) AND FLUID MODE (2,2)

have been chosen as to cover the range of interest 0.965, 1.07, 0.512.

For the determination of primary instability region equation (2.42) with the circumscribed matrix and for secondary instability region expression (2.44), by equating it to zero, are assumed.

2.4.2 Effect of flexibility of container wall on stability

As expected the effect of flexibility of the container bottom is to narrow down the region of instability with respect to the rigid container. This effect is markedly seen on the principal secondary region specially towards the higher values of excitation parameter ε (Fig. 2.2). At the lower value of ε the effect on instability region is marginal as compared to rigid container instability region.

On the principal instability the effect of flexible bottom is to introduce one more instability region as compared to the rigid case. One of them lies near the plate natural frequency and the other near the fluid natural frequency. This indicates the coupling action between the fluid modes and wall modes. Same effect is also observed for the $\frac{3}{2}$ subharmonic (Fig. 2.2a). It is seen that for the $\frac{3}{2}$ subharmonic case the introduction of second region is almost invisible. It is to be noted that the introduction

of second region of instability is visible only when the natural frequencies of fluid and plate are close to each other (Fig. 2.2(a),(b)) whereas for differing values of natural frequencies of liquid and plate, such as shown in Fig. 2.2(c), the likely second region of instability is almost indistinguishable. The ratio of plate to liquid natural frequency is chosen for Fig. (2.2(c)) is 0.512. In this particular case the principal primary region is not appreciably affected by the flexible bottom. Whereas the effect on principal secondary region is seen to reduce it markedly towards the higher values of ε.

To sum up the flexible container base wall in general reduces the instability region of the fluid free surface as compared to the rigid container. Closer the natural frequency of fluid surface to the container wall natural frequency, the greater is the coupling effect between the modes of the two. Correspondingly greater is the effect on the stability of fluid surface and the tendency is to narrow down the instability region as compared to rigid container. For a wider difference between the natural frequencies, the fluid surface behaves as in a rigid container.

CHAPTER 3

A MECHANICAL MODEL FOR LIQUID SLOSHING IN A CONTAINER UNDER THE SIMULTANEOUS ACTION OF LONGITUDINAL AND HORIZONTAL EXCITATIONS

3.1 Introduction

The motion of liquid in partially filled container affects the dynamics of many physical systems, such as, aircrafts, missiles, railway wagons carrying fluid cargo, overhead tanks and dams during earthquake excitation. In such systems, there exists an interaction between the overall structural dynamics and sloshing of fluid. To solve the complete dynamics problem, it is convenient to represent the sloshing liquid by a simple mechanical system.

Some investigations have been carried out in the past to represent the sloshing of liquid by a mechanical model under lateral excitation [1,22,24,29]. Graham et al. [22] have given a comprehensive analogy for lateral sloshing of liquid by moving spring supported masses and a rigid mass in a container. In Ref. [29], the sloshing liquid is represented by moving pendulum masses and a rigid mass for the lateral excitation. The choice of a particular representation depends on the physical problem and analytical convenience.

Ground based vehicles are subjected mainly to two types of excitations. The first is the vertical excitation due to surface unevenness and the second is the horizontal acceleration due to varying velocity of the vehicle. The dynamic analysis of such vehicles is considered mainly to understand the design aspects of the vehicle structure, passenger comfort, cargo safety and controllability of the vehicle. Due to travel over an uneven surface, the vehicle dynamics is random in nature. The problem of dynamic analysis is further complicated, if the cargo is liquid. This is due to interaction between the sloshing liquid and the vehicle structure. The analysis can be simplified, if the sloshing fluid is replaced by equivalent mechanical model.

Developing a mechanical model for a generalized vertical and horizontal excitation of a sloshing fluid, is relatively complex and difficult. Under vertical excitation, the governing differential equations for the liquid motion are characterized by parametric excitation. The response of the liquid motion may have stable or unstable subharmonic, harmonic or superharmonic nature [1,8]. Therefore an equivalent mechanical model should attempt to reproduce these responses. A comprehensive analysis is not reported in the literature even for simple cases. An attempt

has been made in the following analysis to represent a sloshing liquid in a rigid rectangular tank, under simultaneous action of vertical and horizontal excitations, by an equivalent mechanical system. The analysis is valid for stable system.

3.2 Mathematical Formulation of the Problem

Consider a rigid rectangular container partially filled with incompressible, inviscid liquid to the height, h as shown in the Fig. 2.1. Dimensions of the tanks are such that the surface tension is neglected. The coordinates are moving, as shown in the Fig. 2.1, with the container such that the mean fluid free surface has the equation z=h. The container is excited vertically upwards with an acceleration $g_o \cos\omega t$, where g_o is constant. The container also moves horizontally with a constant acceleration C_o. The Eulerian equations of motion [31] for the fluid are given by

$$\frac{\partial V_x}{\partial t} + V_x \frac{\partial V_x}{\partial x} + V_y \frac{\partial V_x}{\partial y} + V_z \frac{\partial V_x}{\partial z} = -\frac{1}{\rho}\frac{\partial p}{\partial x} + C_o,$$

$$\frac{\partial V_y}{\partial t} + V_x \frac{\partial V_y}{\partial x} + V_y \frac{\partial V_y}{\partial y} + V_z \frac{\partial V_y}{\partial z} = -\frac{1}{\rho}\frac{\partial p}{\partial y}, \qquad (3.1)$$

$$\frac{\partial V_z}{\partial t} + V_x \frac{\partial V_z}{\partial x} + V_y \frac{\partial V_z}{\partial y} + V_z \frac{\partial V_z}{\partial z} = -\frac{1}{\rho}\frac{\partial p}{\partial z} - (g - g_o \cos\omega t).$$

The equation of continuity is

$$\frac{\partial V_x}{\partial x} + \frac{\partial V_y}{\partial y} + \frac{\partial V_z}{\partial z} = 0 . \qquad (3.2)$$

If the motion was originally started from rest, there is a velocity potential such that $(V_x, V_y, V_z) = (\frac{\partial}{\partial x}, \frac{\partial}{\partial y}, \frac{\partial}{\partial z})\varphi$. The equations of motion then have the integral

$$\frac{\partial \varphi}{\partial t} + \frac{1}{2}(V_x^2 + V_y^2 + V_z^2) + \frac{p}{\rho} + (g - g_o \cos\omega t)(z-h) - C_o x = F(t), \qquad (3.3)$$

where $F(t)$ is independent of (x,y,z) and may be put equal to zero [8,31,47]. Equation (3.2) may be written as Laplace equation

$$\frac{\partial^2 \varphi}{\partial x^2} + \frac{\partial^2 \varphi}{\partial y^2} + \frac{\partial^2 \varphi}{\partial z^2} = 0 , \qquad (3.4)$$

3.2.1 Boundary conditions

If the equation of free surface is $z = \zeta(x,y,t)$, the kinematic surface condition is

$$\frac{\partial \zeta}{\partial t} + V_x \frac{\partial \zeta}{\partial x} + V_y \frac{\partial \zeta}{\partial y} - V_z = 0 . \qquad (3.5)$$

If the deflexion and slope of the free surface is small, then the products of V_x, V_y, V_z, ζ and their squares can be neglected. Thus the linearized free surface conditions are obtained from (3.3) and (3.5) as

$$\frac{\partial \varphi}{\partial t} + (g \pm g_o \cos \omega t)\zeta - C_o x = 0 \qquad (3.6)$$

$$\frac{\partial \zeta}{\partial t} = \frac{\partial \varphi}{\partial z} \qquad (3.7)$$

Other boundary conditions require that the relative velocity normal to the wall be zero. Hence

$$\frac{\partial \varphi}{\partial x} = 0, \quad \text{at } x = 0,a \qquad (3.8)$$

$$\frac{\partial \varphi}{\partial y} = 0, \quad \text{at } y = 0,b \qquad (3.9)$$

$$\frac{\partial \varphi}{\partial z} = 0, \quad \text{at } z = 0 . \qquad (3.10)$$

3.2.2 Solution of the problem

It can be proved that ζ and φ can be expressed in terms of the same set of eigenfunctions [8]. Thus one assumes that

$$\zeta(x,y,t) = \sum_{i=0}^{\infty} \sum_{j=0}^{\infty} r_{ij}(t)\, S_{ij}(x,y) \qquad (3.11)$$

$$\varphi(x,y,z,t) = \sum_{i=0}^{\infty} \sum_{j=0}^{\infty} \dot{r}_{ij}(t) \frac{\cosh(k_{ij}z)}{k_{ij} \sinh(k_{ij}h)} S_{ij}(x,y) \qquad (3.12)$$

where $S_{ij}(x,y) = \cos\left(\frac{i\pi x}{a}\right) \cos\left(\frac{j\pi y}{b}\right)$

$$k_{ij}^2 = \pi^2 \left(\frac{i^2}{a^2} + \frac{j^2}{b^2}\right) \text{ such that } k_{ij} \neq 0 . \qquad (3.13)$$

It is to be noted that the boundary conditions (3.8) to (3.10) are satisfied. The free surface kinematic condition (3.7) is also satisfied. For the second free surface condition (3.6) one finds that

$$\sum\sum \ddot{r}_{ij}(t) \frac{\cosh(k_{ij}z)}{k_{ij}\sinh(k_{ij}h)} S_{ij}(x,y) + (g-g_o\cos\omega t)\, r_{ij}(t)$$

$$S_{ij}(x,y) = C_o x$$

As the right hand side is independent of y, modes corresponding to j=0 are only possible. On multiplying both sides by $\cos(\frac{i\pi}{a}x)$ and integrating over x=0,a one finds that

$$\ddot{r}_i(t) + gk_i \tanh(k_i h)(1 - \varepsilon\cos\omega t) r_i = -A_i \Omega_i^2, \text{ for } i = 1,3,5\ldots$$

$$= 0, \text{ for } i = 0, 2,4,6,\ldots$$

where, $A_i = \dfrac{4C_o}{a \cdot gk_i^2}$

$$\Omega_i^2 = g\, k_i^2 \tanh(k_i h) \qquad (3.14)$$

$$\varepsilon = \frac{g_o}{g}, \quad |\varepsilon| < 1 \ .$$

The summation sign over j drops out. If $r_i(t)$ is determined from (3.14) with the prescribed initial conditions then all of the boundary conditions are satisfied. The resulting expression for velocity potential for zero initial conditions of $r_i(t)$ is given by

$$\varphi(x,z,t) = \sum_{i=1,3,5\ldots}^{\infty} r_i(t) \frac{\cosh k_i z}{k_i \sinh(k_i h)} \cos(k_i x) \qquad (3.15)$$

where $r_i(t)$ is given (see Appendix B) for small ε as

$$r_i(t) = -\Omega_i^2 A_i \left[\frac{1}{\Omega_i^2}(1-\cos\Omega_i t) + \varepsilon\left(\frac{-3\Omega_i^2}{(\Omega_i^2-\omega^2)(4\Omega_i^2-\omega^2)}\cos\Omega_i t\right.\right.$$

$$+ \frac{\cos\omega t}{(\Omega_i^2-\omega^2)} + \frac{1}{2}\left(\frac{\cos(\Omega_i+\omega)t}{\omega(2\Omega_i+\omega)} - \frac{\cos(\Omega_i-\omega)t}{\omega(2\Omega_i-\omega)}\right)\Big)$$

$$+ \varepsilon^2 \frac{\Omega_i^2}{2}\left(\frac{3}{(\Omega_i^2-\omega^2)(4\Omega_i^2-\omega^2)}\left\{1 - \frac{\Omega_i^2}{\omega^2}\left(\frac{\cos(\Omega_i-\omega)t}{(2\Omega_i-\omega)} - \frac{\cos(\Omega_i+\omega)t}{(2\Omega_i+\omega)}\right)\right\}\right.$$

$$- \frac{1}{8\omega^2}\left(\frac{\cos(\Omega_i+2\omega)t}{(2\Omega_i+\omega)(\Omega_i+\omega)} + \frac{\cos(\Omega_i-2\omega)t}{(2\Omega_i-\omega)(\Omega_i-\omega)}\right) + \frac{\cos 2\omega t}{(\Omega_i^2-\omega^2)(\Omega_i^2-4\omega^2)}$$

$$\left.\left. + \frac{\Omega_i^2 - 9\omega^2}{\omega^2(4\Omega_i^2-\omega^2)(\Omega_i^2-4\omega^2)}\cos\Omega_i t\right)\right)\Big] \qquad (3.16)$$

3.2.3 Determination of forces and moments

The total pressure acting at any point is the sum of static pressure and dynamic pressure. This is given by Eq. (3.3). After neglecting the second order terms, as done to arrive at (3.6), and putting $F(t) = 0$ one gets

$$p = \rho(g-g_o\cos\omega t)(h-z) - \rho\frac{\partial\varphi}{\partial t} + C_o x\rho \qquad (3.17)$$

Total force acting in x-direction per unit width of the container is given by

$$F_x = \int_A p\,dA$$

where A is the area of the wall. Thus

$$F_x = M_o C_o + 2\rho \sum_{i=1,3,5\ldots}^{\infty} \ddot{r}_i(t)/k_i^2 \qquad (3.18)$$

where $M_o = \rho ah$ is the total mass of the fluid per unit width of the container.

Moment of the continuum model

The moment exerted by the sloshing fluid is determined about the centre of gravity (c.g.) of the fluid. The counterclockwise moment is assumed to be positive when viewed in positive y-direction. The total moment, due to forces acting on the walls of the container having unit width, is given as

$$M_{Ty} = -\oint p\,(z - \frac{h}{2})\,dz$$

$$= -\int_h^o \rho[g-g_o\cos\omega t)(h-z) - \frac{\partial\varphi}{\partial t} + C_o x\rho](z - \frac{h}{2})dz$$

$$- \int_o^a \rho[(g-g_o\cos\omega t)h - \frac{\partial\varphi}{\partial t} + C_o x\rho](x - \frac{a}{2})\,dx$$

$$- \int_o^h \rho[(g-g_o\cos\omega t)h - \frac{\partial\varphi}{\partial t} + C_o x\rho]\,(z - \frac{h}{2})dz$$

$$= -\frac{\rho C_o a^3}{12} - \rho \sum_{i=1}^{\infty} (1-(-1)^i)\,\frac{\ddot{r}_i(t)}{k_i^2}.$$

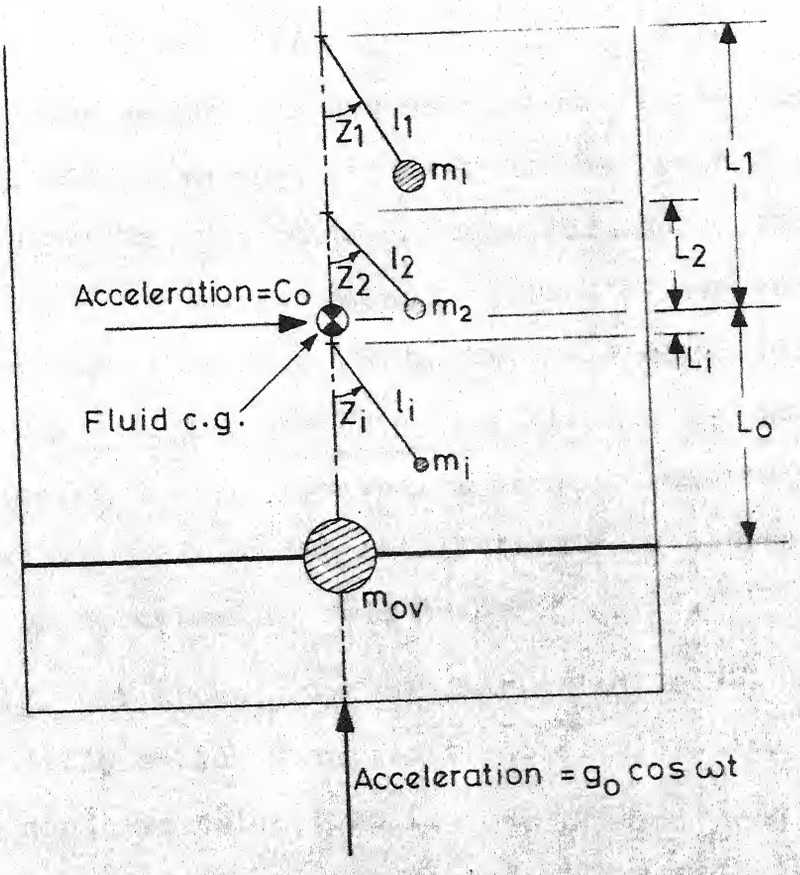

FIG. 3.1 MECHANICAL MODEL WITH ONE FIXED MASS AND INFINITE NUMBER OF SLOSHING MASSES REPRESENTING FLUID MOTION UNDER SIMULTANEOUS ACTION OF VERTICAL AND HORIZONTAL EXCITATION OF CONTAINER MOTION.

3.3 Mechanical Model

The criteria for constructing the model to be equivalent to the fluid motion in the container are chosen as follows. The mechanical system must exert the same force and total moment on the container as the fluid does for the type of container motion under consideration. The fluid may have infinite number of modes. Hence corresponding to each sloshing fluid mode there must be a oscillating mass. In this way infinite number of oscillating mechanical masses are required. However, a detailed analysis would show that the size of the oscillating mass decreases rapidly with increasing mode number [22,29].

Fig. 3.1 shows a typical mechanical model representing the fluid motion under vertical acceleration, $g_o \cos\omega t$, and horizontal acceleration C_o. The oscillating mass, m_i, is attached through a pendulum rod with length l_i. The fixed mass, M_{ov} is placed at a distance, L_o, from the fluid c.g. The pendulum mass, m_i, is confined to move in vertical plane. The pivot of the pendulum is placed at a distance, L_i from the fluid c.g.

3.3.1 Determination of model parameters

The length of the pendulum, l_i, is determined on the basis of the assumption that the natural frequency of the

pendulum is the same as that of the corresponding fluid mode. Hence

$$\Omega_i^2 = g/l_i \tag{3.20}$$

The equation of motion of the pendulum is written as

$$l_i^2 m_i \ddot{z}_i + m_i l_i g (1 - \varepsilon \cos \omega t) z_i = -m_i l_i C_o \tag{3.21}$$

The solution of equation (3.21) can be obtained for zero initial conditions using the results of Appendix B. Similarity between Eq. (3.14) and (3.21) may be noted.

The mechanical masses are determined by equating the total horizontal force exerted by the mechanical model and continuum model. The total horizontal force of the mechanical model is given by

$$F_x' = m_{ov} C_o + \sum_{i=1}^{\infty} m_i C_o + \sum_{i=1}^{\infty} m_i l_i \ddot{z}_i(t) \tag{3.22}$$

As the horizontal force for the two systems is same hence one gets after comparing (3.18) and (3.22) the following

$$M_o C_o = m_{ov} C_o + \Sigma m_i C_o$$

$$\text{or,} \quad m_{ov} = M_o - \sum_i m_i \tag{3.23}$$

and,

$$\sum m_i l_i \ddot{z}_i = 2\rho \sum_{i=1,3,5\ldots} \frac{\ddot{r}_i(t)}{k_i^2} .$$

As each fluid mode is independent of the other and corresponding to each fluid mode there is a mechanical pendulum hence

$$m_i l_i \ddot{z}_i = 2\rho \frac{\ddot{r}_i(t)}{k_i^2} \qquad (3.24)$$

On substituting the expressions of $\ddot{z}_i$ and $\ddot{r}_i(t)$ using the results of Appendix B one can have

$$m_i[---] C_o = 2\rho \frac{\Omega_i^2}{k_i^2} A_i [---] \qquad (3.25)$$

The terms in the brackets on the two sides of the equation are same. Hence on substituting for A_i, Ω_i from (3.14) one gets

$$\frac{m_i}{M_o} = \frac{8 \tanh (k_i h)}{\pi^3 i^3 R} \qquad (3.26)$$

where, R = aspect ratio of the container = $\frac{h}{a}$.

Moment of the Mechanical Model

The distance of the masses are measured positive above the c.g. Thus the positive counterclockwise moment about the c.g. is given by

$$M'_{Ty} = -[m_{ov} L_o C_o + \sum_i^\infty m_i L_i C_o + \sum_i^\infty m_i l_i L_i \ddot{z}_i] \qquad (3.27)$$

If the two systems generate the same moment then on comparing (3.19) and (3.27) one obtains,

$$m_i l_i L_i \ddot{z}_i = \frac{\rho}{k_i^2} B_i \ddot{r}_i \tag{3.28}$$

where

$$B_i = (1 - (-1)^i) \left[\frac{h}{2} + \frac{2}{k_i \sinh(k_i h)} - \frac{1}{k_i \tanh(k_i h)}\right] \tag{3.29}$$

Using (3.24) and (3.28) one obtains

$$L_i = \frac{B_i}{2} \tag{3.30}$$

Finally comparing (3.19) and (3.27) one obtains the fixed mass distance, L_o, as

$$m_{ov} L_o + \Sigma m_i L_i = \frac{\rho a^3}{12}$$

or,
$$L_o = \frac{1}{m_{ov}} \left[M_o \frac{a^2}{12h} - \sum_{i=1,3,5,\ldots}^{\infty} m_i L_i\right] \tag{3.31}$$

The moment of inertia, I_{ov}, of the fixed mass, m_{ov} is determined by pitching the tank about the axis, y passing through c.g. of the fluid. The analysis is available in Ref. [22]. Thus one obtains, I_{ov} from the following.

$$I_{ov} + m_{ov} L_o^2 + \sum_{i=1,3,5\ldots} m_i (L_i - l_i)^2 = I_{sy} \left[1 - \frac{4}{1+R^2} + \frac{768}{R(1+R^2)\pi^5} \sum_{n=o}^{\infty} \frac{\tanh (2n+1) \frac{\pi}{2} R}{(2n+1)^5}\right] \tag{3.32}$$

where I_{sy} is the moment of inertia of the solidified liquid mass about the y axis passing through c.g. of the fluid. Thus all the parameters of the mechanical model are known.

CHAPTER 4

DIGITAL SIMULATION OF THE DYNAMIC RESPONSE OF LIQUID IN A CONTAINER MOUNTED ON A VEHICLE MOVING ON AN UNEVEN SURFACE

4.1 Introduction

Liquid is often carried by vehicles as a cargo or fuel. The unrestrained free surface of the liquid in a container has a tendency to respond quickly even to a small motion of the container. Hence, the response of liquid in a container mounted on a moving vehicle is of considerable interest. Vehicles operating on the ground are subjected to base excitation due to ground unevenness. The undulations in prepared ground surfaces, such as, roads, railway tracks, runways are random in nature and, therefore, a vehicle moving on such a surface is subjected to random excitation. A random vibration analysis of vehicle-fluid system is therefore required. Usually the mathematical equations characterizing such a system, are nonlinear and involve time-dependent-parametric excitations. Due to such complexities, an analytical treatment of random vibration analysis is not always possible. In such cases, the digital simulation offers a convenient approach to determine the response.

Basically, digital simulation techniques [40] involve generation of random processes on digital computer to match some of the statistical properties of the natural phenomena. The simulated process is treated as an input to the system and the response is calculated by numerical integration of the governing equations. An important advantage of simulation technique is that it can handle fairly complicated systems. The disadvantage lies in the fact that it may require large computer time. However, this practical difficulty is overcome by present day high speed digital computers.

In the following analysis, the Monte-Carlo technique has been employed [45] to determine the response. The input base excitation is simulated corresponding to a given rail-road power spectral density [21], and fed to the nonlinear system. The response is determined by numerical integration of governing equations. The system is described later in the present chapter.

4.2 Representation of Power-Spectral-Density of Rail-Road-Roughness

In Fig. 6 of Ref. [21] the one sided power spectral density of rail road roughness has been given. The same is reproduced on a different scale in Fig. 4.1 for reference.

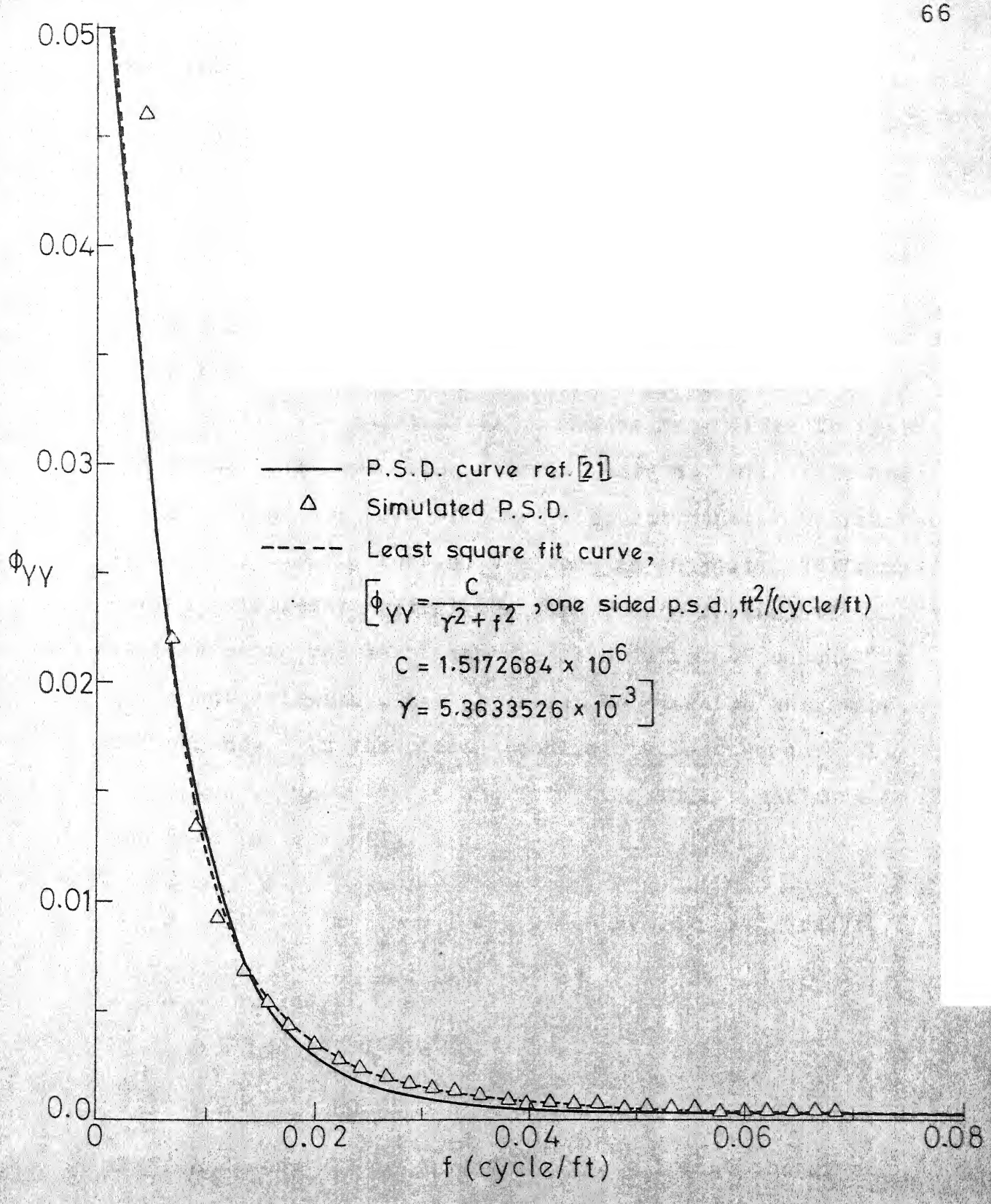

FIG. 4.1 TARGET AND SIMULATED SPECTRA OF THE RAIL ROAD PROFILE.

Ref. [21] has discussed various forms of rail-road-spectrum. Following form of one-sided power-spectral-density is used for the analysis employed in Ref. [21].

$$\Phi_{YY}(\Omega) = \frac{2\pi A_v \Omega_c^2}{(\Omega^2 + \Omega_c^2)\,\Omega^2}, \text{ in}^2/(\text{rad/ft}) \qquad (4.1)$$

where $\Omega_c = 0.2513$ rad/ft, is the cut-off spatial frequency. A_v is the constant which may be determined from the plot. The value of the constant, A_v, changes from track to track. The track roughness changes as it wears out with time and usage. While the form of power spectral density (hereafter written as p.s.d.) remains the same as in (4.1), the constant, A_v, increases with time. The choice of analytical expression to represent measured p.s.d. is not unique. A different expression may be chosen to suit the analytical convenience. In the present analysis a least-square-fit procedure is used to fit the following analytical form to the data in Ref. [21].

$$\Phi_{YY}(\Omega) = \frac{C}{\gamma^2 + \Omega^2}, \text{ one sided p.s.d., ft}^2/(\text{rad/ft}),$$

where Ω in rad/ft and,

$$C = (9.533277)\ 10^{-6},$$

$$\gamma = (3.3698937)\ 10^{-2} \qquad (4.2)$$

are constants. It is seen from Fig. 4.1 that the given p.s.d. curve of Ref. [21] and the least-square-fit curve (4.2)

are quite close to each other. It differs marginally towards the higher frequency range. Hence the p.s.d. represented by (4.2) is accepted to be used in the subsequent analysis.

4.3 Target and Realized Power Spectrum

The specified power spectral density is called the target power spectral density. The spectral density estimated from the simulated data is called realized power spectral density. In the present analysis, the target p.s.d. is specified by relation (4.2). The spatial function Y(s) is simulated as follows [44,45],

$$Y(s) = \sqrt{2} \sum_{k=1}^{N} A_k \cos(\Omega_k s - r_k), \tag{4.3}$$

where

$$A_k^2 = \int_{(k-1)\Delta\Omega}^{k\Delta\Omega} \Phi_{YY}(\Omega)\, d\Omega \doteq \Phi_{YY}(\Omega_k)\Delta\Omega \quad , \tag{4.4}$$

and r_k are random phase distributed uniformly between 0 and 2π. $\Phi_{YY}(\Omega)$ is defined by (4.2). The degree of approximation of the realized function (4.3) depends upon the cut-off frequency, Ω_c, and whether $\Delta\Omega$ is small enough to hold (4.4). Generally the cut-off frequency, Ω_c, is chosen such that contribution to the total power beyond Ω_c is negligible. The degree of approximation between the theoretical spatial function and the realized spatial function is ensured further as follows. A series of digitized

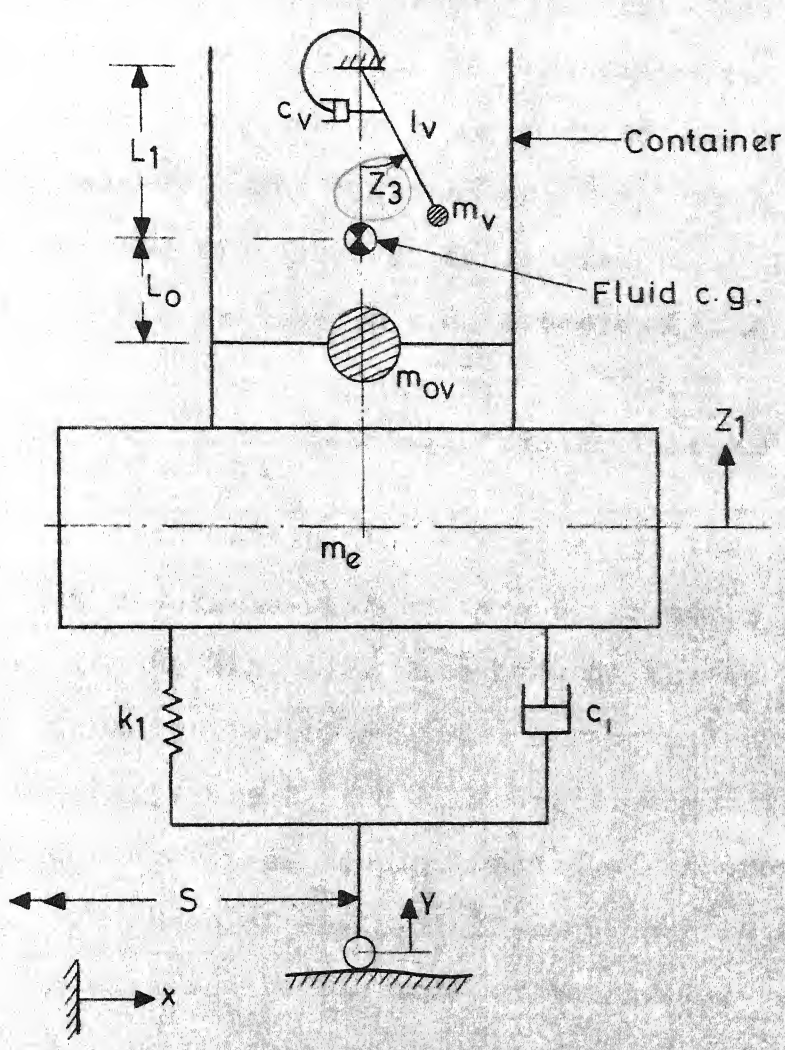

FIG. 4.2 A CONTAINER MOUNTED ON A VEHICLE, WITHOUT TYRE, MOVING OVER A SURFACE.

sample function is generated using (4.3). The realized power spectrum is estimated from the realized sample function series [5,6,27]. In the present analysis the Blackman-Tukey procedure of power spectrum determination is employed. The smoothing of power spectrum is carried out using Parzen spectral window. The realized power spectrum and the target power spectrum are compared as in Fig. 4.1. It is seen that the target and realized p.s.d. are close to each other.

4.4 Response of Liquid-Filled-Container Mounted on Moving-Vehicle

A rigid rectangular container filled with liquid is mounted on a vehicle-without-tyre which moves over a surface as shown in the Fig. 4.2. The mass of the empty vehicle is m_e. It is supported by a linear spring and a viscous damper whose constants are k_1 and c_1 respectively. The vehicle is subjected to vertical displacement Y(s) as shown in the figure. The mass of empty rigid-container is assumed to be small as compared to the mass of the loaded vehicle and is neglected. The liquid in the container is idealized by a pendulum with mass m_v, length l_v, and a fixed mass, m_{ov}. The expressions of these masses and their respective positions, as shown in the Fig. 4.2, are given by Eqs. (3.20) to (3.32). The pendulum is attached to a damper with damping constant, c_v [16], as shown in the figure.

4.4.1 Equations of motion

The equations of motion, for the moving vehicle model as shown in Fig. 4.2, are given by

$$(m_e + m_{ov} + m_v)\,\ddot{z}_1 + m_v l_v\,(\ddot{z}_3 \sin z_3 + \dot{z}_3^2 \cos z_3) + c_1\,(\dot{z}_1 - \dot{y}) + k_1\,(z_1 - y) = 0, \tag{4.5}$$

$$m_v l_v^2\,\ddot{z}_3 + m_v l_v\,\ddot{z}_1 \sin z_3 + c_v \dot{z}_3 + m_v l_v g \sin z_3 = 0. \tag{4.6}$$

These equations are nonlinear and are coupled.

4.4.2 Solution of the equations of motion

Equations (4.5) and (4.6) are solved numerically as follows. The input excitation, y(t), is the surface roughness of the track over which the vehicle moves. For the present analysis, the surface roughness is chosen according to the p.s.d. of the rail-road roughness given by (4.2). Y(s) is generated with the help of Eq. (4.3) and the procedure outlined in Section 4.3. The vertical velocity, $\dot{y}(t)$, is given by

$$\begin{aligned} \dot{y}(t) &= \frac{dY(s)}{ds} \cdot \frac{ds}{dt}, \\ &= Y' \cdot v, \end{aligned} \tag{4.7}$$

where v is the velocity of the vehicle and the spatial derivative Y' is known from (4.3). With the known initial

conditions for z_1, $\dot{z}_1$ and z_3, $\dot{z}_3$ one can solve the equations (4.5) and (4.6) numerically using the fourth order Runge-Kutta integration method. Since the input excitation is random in nature, it is necessary to calculate the response as an ensemble average of n samples. Further averaging is necessary in terms of moving average over n consecutive step readings [6,27]. The step length corresponding to a suitable step length of integration may be chosen for Runge-Kutta algorithm.

4.5 Results and Discussions

4.5.1 Simulation

In Section 4.3, the procedure for simulating the random process is outlined. The spacing $\Delta\Omega$ is chosen for Eq. (4.3) in view of the approximation (4.4). There are two ways to determine the number of spacings N in the frequency domain. The first is to assume the spacing, $\Delta\Omega$ as constant. The second is to assume the variable spacing. In the second, finer spacings are chosen in those domains of frequency where the fluctuation of the spectral density is more rapid and coarser spacings elsewhere [44]. Number of simulation terms, N, will be decisively less with the second method. To save the computer time, the advantage lies with the second method. In the present analysis, the

second method is employed to select the terms N.

From Fig. 4.1, it is considered sufficient to choose the cut-off spatial frequency to be 1/8 cycle/ft. Beyond this value, the p.s.d. is close to zero. Accordingly, total number of 51 variable spacings are considered sufficient. The random phase angles, r_k, are generated by using the built in subroutine RAN of DEC system 1090.

4.5.2 Parameters of vehicle, mechanical model and initial conditions

The vehicle under consideration is the one of Ref. [42]. Important data of the wagon are listed in Table 4.1. For the sloshing of liquid, in a rectangular container representing a wagon, a mechanical model is assumed. The mechanical model parameters are determined through the Eqns. (3.20) to (3.32). As the fundamental mode of sloshing liquid is more important than other modes [22], the pendulum mass corresponding to fundamental mode is considered. The parameters of the mechanical model necessary for the present analysis are given in Table 4.2. The damping ratio for the pendulum is assumed to be 0.0034 as suggested in Ref. [16].

The vehicle is assumed to maintain constant acceleration. Results are presented for the case in which vehicle attains a velocity of 150 km/hour over 1 km distance from rest. The distance and velocity at any time, t, can be

calculated as follows.

$$s = v_o t + \frac{1}{2} C_o t^2 , \qquad (4.8)$$

$$v^2 = v_o^2 + 2C_o s , \qquad (4.9)$$

where C_o is the constant acceleration, s and v are the distance covered and velocity at time t. v_o is the initial velocity which is zero at t=0.

Initial conditions

Calculations are carried out for the zero initial conditions of the variables involved in Eqn. (4.5) and (4.6).

4.5.3 Numerical integration and averaging

The equations of motion (4.5), (4.6) are solved using the fourth order Runge-Kutta integration method. The step length of integration is usually taken as [6,27]

$$\Delta t = \frac{1}{2f_c} , \qquad (4.10)$$

where f_c is the cut-off frequency in cycle/sec. In the present case, the cut-off spatial frequency considered is 1/8 cycle/ft. Hence the step length of integration in spatial domain is $\Delta s = 4$ ft. Hence

$$\Delta t = \frac{\Delta s}{v} \text{ second}, \qquad (4.11)$$

where v is the velocity in ft/second. In the present analysis

the vehicle has variable velocity run. Hence a suitable step size is required to integrate the equations of motion.

From Table 4.2, one notes the following. For all the heights of fluid considered in the container, the completely full container offers the least ratio of pendulum to vehicle natural period and is found to be approximately 5.7366282. Accordingly, the step size, Δt, equivalent to one-tenth of the vehicle natural period, is considered sufficient in the present analysis.

Since the input excitation function is random in nature, it is necessary to take the ensemble average of sample functions. It was found sufficient to take ensemble average over five sample functions. Further averaging is carried out over the five consecutive readings of the sample response function.

4.5.4 Vehicle response

Vehicle response with varying fluid height in the container is studied. The mean square response of vertical displacement with non-dimensional time is presented in Fig. 4.3 for zero initial conditions. t_o is the natural period of the vehicle system at a given load. The fluid heights considered are corresponding to 1, 1/2 and 1/4 height of the container. The natural frequency of the

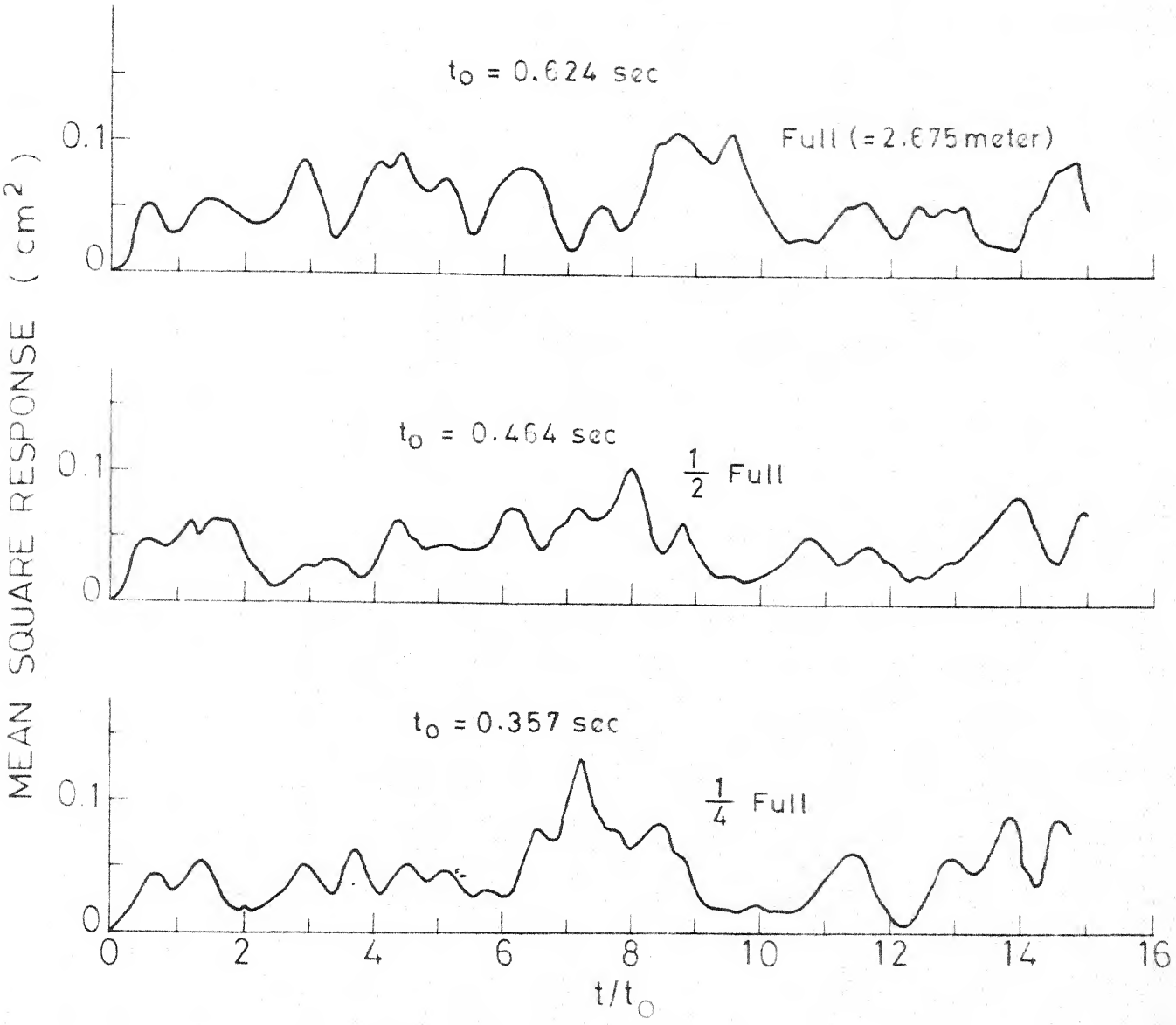

FIG. 4.3 TIME Vs. MEAN SQUARE RESPONSE OF THE C.G. OF THE VEHICLE MOVING WITH CONSTANT ACCELERATION (0.868 5555 m/sec^2).

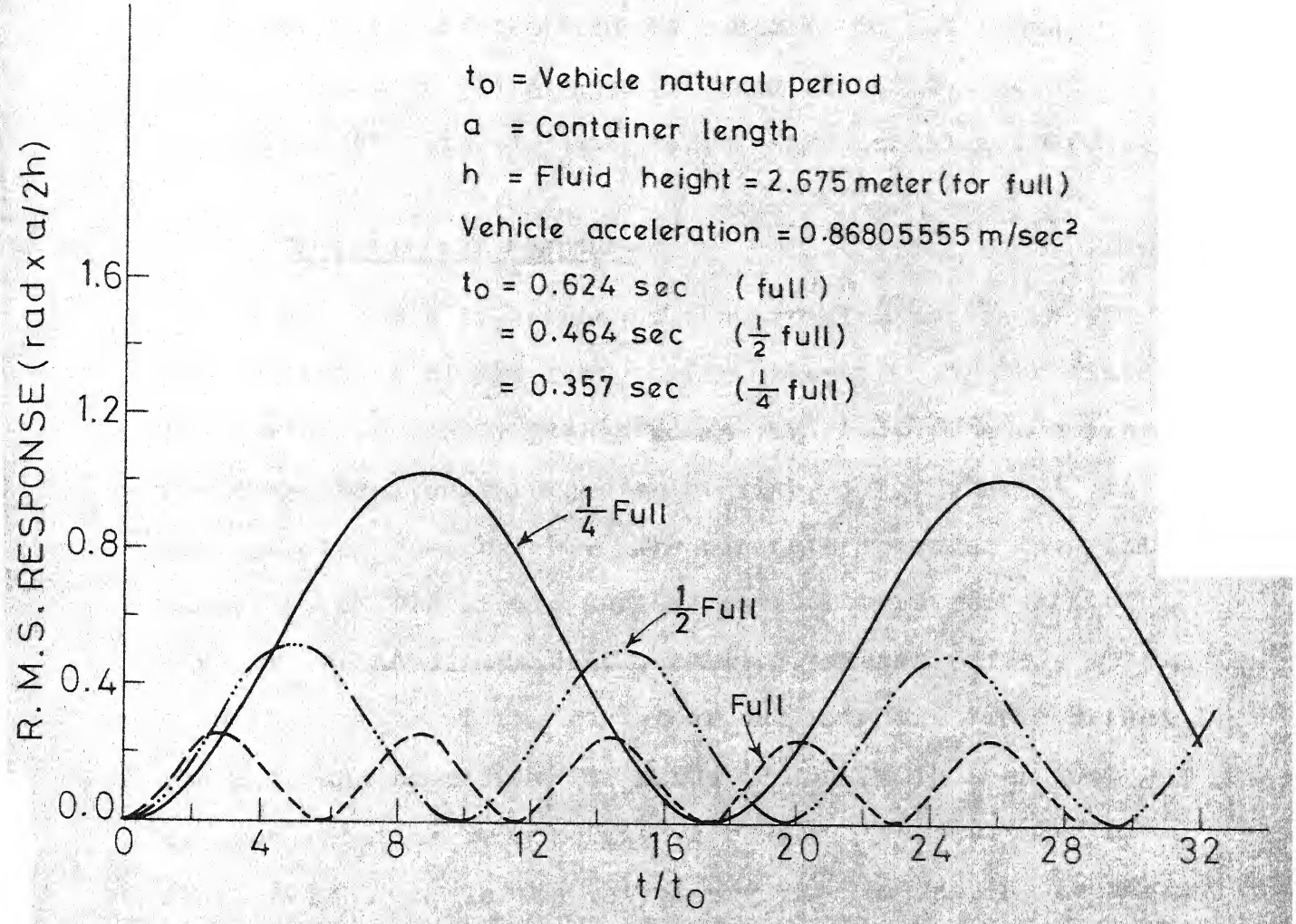

FIG. 4.4 TIME Vs. R.M.S. RESPONSE OF FREE SURFACE FOR DISPLACEMENT.

vehicle, when the fluid mass is assumed solidified, is given in Table 4.2. As expected, the vehicle response is a narrow band random process. From Fig. 4.3, it appears that the characteristics of the vehicle response do not change appreciably with fluid height. This is indicative of negligible coupling between vehicle and pendulum response.

4.5.5 Free surface response

The r.m.s. response of the pendulum motion is the representative of the free surface elevation of the fluid in the container and is presented in Fig. 4.4. The abscissa is the non-dimensional parameter of time, t/t_o, where t_o is same as discussed before. The ordinate measures the relative magnitude of the liquid surface wave. It is represented through the nondimensional parameter, radian (a/2h), where, a, is the length of the container and, h, is the fluid height. The response appears to be sinusoidal. It is seen that the maximum relative wave height increases with decrease in fluid height, h, in the container. As the damping is small, the maximum response does not decay appreciably over time. The steady state response occurs quite early. Numerically the maximum response is small enough to approximate the pendulum as linear. Although this aspect is not considered here but will be used in later analysis

Table 4.1

Data for 2 Axle Vehicle CR-28251

Drawing No. SK-71605, Ref. [42]

1.	Length	7.89 meters
2.	Breadth	2.946 "
3.	Height	2.675 "
4.	Wheel-Base	4.9 "
5.	Total sprung designed load	=36.84 tons
6.	Total sprung weight with no load	= 7.2 tons
7.	Damping ratio, β	= 0.2
8.	Stiffness on each wheel axle	0.358 tons/mm
9.	Moment of inertia about the empty vehicle c.g.	4245.1208 Kg-mass-meter^2

Note : Only necessary data have been listed in the table for the present and subsequent analysis.

Table 4.2

Vehicle and Mechanical Model Parameters

Pendulum damping ratio = 0.0034, Ref. [16]

Tank dimensions (7.89 x 2.946 x 2.675) meters.

Fluid Height (meter)	Fixed-mass (kg)	Pendulum mass for fundamental mode (kg)	Pendulum Rod Length (meter)	Natural frequency of pendulum (rad/sec)	Natural frequency of vehicle system (rad/sec)
2.675	2539.16	3799.01	3.188	1.754	10.062
1.338	818.45	2350.63	5.1534	1.3797	13.544
0.669	329.68	1254.86	9.653	1.008	17.575

CHAPTER 5

THE DYNAMIC RESPONSE OF A VEHICLE CARRYING LIQUID CARGO ON AN UNEVEN SURFACE

5.1 Introduction

In the preceding chapter the effect of liquid sloshing on vehicle dynamics was investigated for an idealised model restricted to heave motion and subjected to a single point excitation due to track unevenness. The response was determined by numerical integration of the non-linear equations of motion to simulated track unevenness. It was shown that for such a model, effect of sloshing on vehicle dynamics is not significant. In this chapter, a more realistic model incorporating heave and pitch degrees of freedom with two point excitations is considered. The liquid is replaced by an equivalent mechanical model consisting of a fixed mass and a pendulum representing sloshing motion. The equations of motion of the system are non-linear. The track unevenness is assumed to be a homogeneous random process in space co-ordinate along the track. For a vehicle moving on the track with constant velocity, the excitation is stationary. For a vehicle moving with variable velocity, the excitation

becomes non-stationary. The equations of motion are linearized using the stochastic linearization technique. The linearized equations are transformed into a system of first order equations in 2n-dimensional space. Through a canonical transformation, these equations are reduced to a set of 2n uncoupled first order equations. The equations are now transformed from time to space domain and response statistics are obtained in closed form for vehicles moving with constant velocity. For vehicles moving with variable velocity the excitation and the response are non-stationary and the associated matrices are unsymmetric. These equations are transformed from time to space domain. The input process is now homogeneous, but the co-efficients are functions of space co-ordinate. The response statistics are determined numerically. The response of the vehicle is also determined treating the liquid to be frozen and the two responses are compared to determine the effect of sloshing of liquid on vehicle dynamics.

5.2 Description of the Moving Vehicle System

A two axle railway wagon carrying a rigid rectangular container filled with liquid is considered as shown in Fig. 5.1. The vehicle moves horizontally over the track and is subjected to two point ground excitations. The moving vehicle is assumed to have heave and pitch degrees of freedom about its c.g.

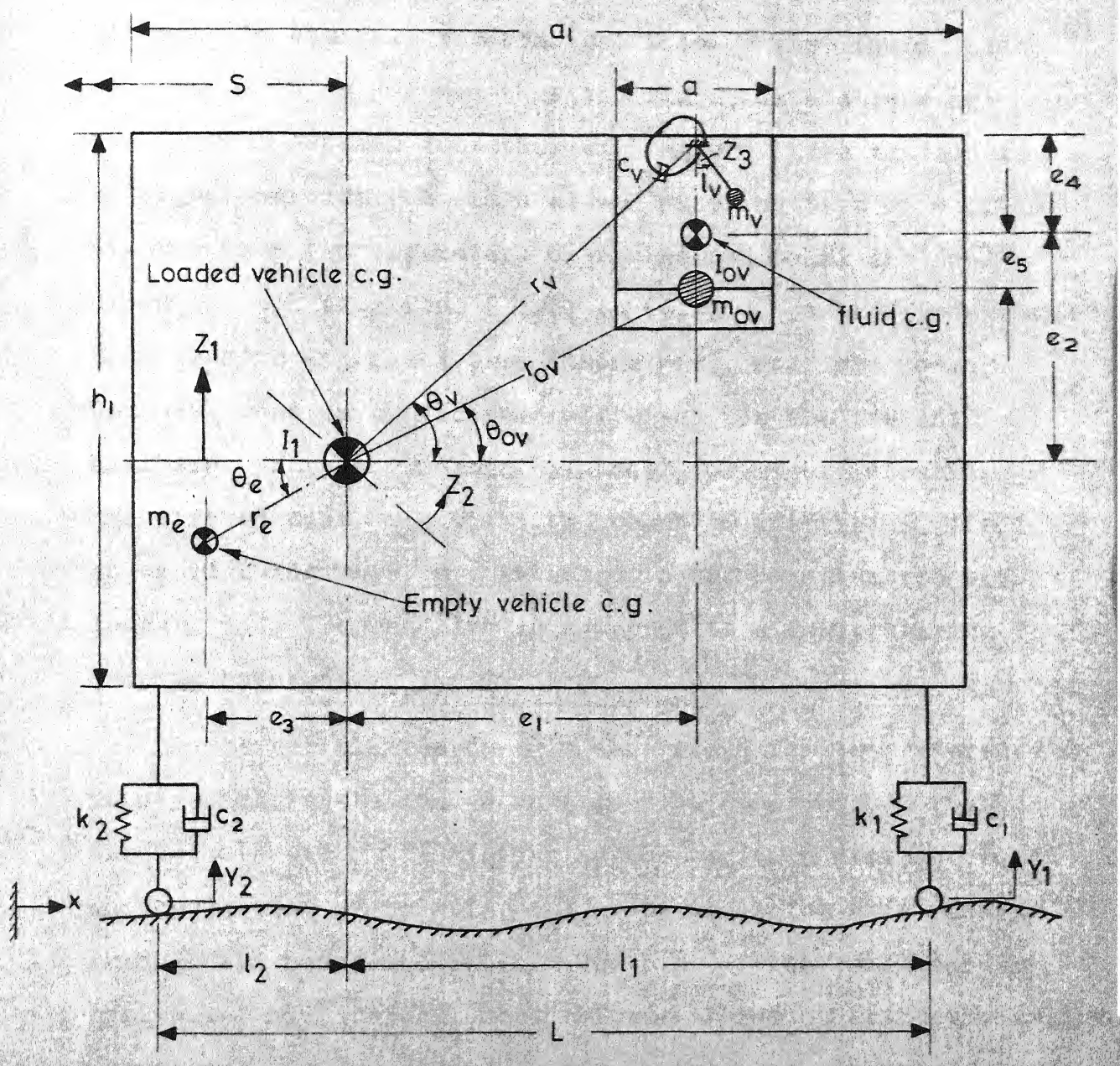

FIG. 5.1 A CONTAINER MOUNTED ON A TWO-AXLE VEHICLE WITHOUT TYRE, MOVING OVER A SURFACE.

The sloshing of liquid in the container is considered through its equivalent mechanical model. The liquid chosen is water. It is assumed that the fluid oscillations are small under assumed container excitations. The container undergoes vertical, horizontal and pitching type of excitations. Thus the parameters of mechanical model are determined through equations (3.20) to (3.32). As the fundamental mode is more important than others [22], only one moving pendulum mass is considered sufficient for the present analysis. Thus the mechanical model for liquid sloshing has a fixed mass, m_{ov}, with its moment of inertia, I_{ov}, and an oscillating mass, m_v, attached to the pendulum rod with length, l_v. The pendulum is attached to a damper having damping constant, c_v.

The vehicle response is determined for the reference point which is the loaded vehicle c.g. The mass, m_e, of the vehicle without container is located at a distance, e_3, and has moment of inertia, I_1, about the pitch axis passing through the reference point. The c.g. of the container has horizontal and vertical eccentricities e_1 and e_2 respectively. The vehicle is mounted on linear springs and dampers located at the corresponding axles. The spring constants are k_1, k_2 and damping constants c_1, c_2 at the fore and aft axles respectively. The whole vehicle system moves in positively increasing direction of x over an uneven surface as depicted in Fig. 5.1.

5.3 Equations of Motion

The general equations of motion are determined through Lagrange's equations. The loaded vehicle c.g. has vertical displacement, z_1, and rotation, z_2. The pendulum has rotational displacement, z_3 measured from its rest position as shown in Fig. 5.1.

The total kinetic energy (k.e.), T, and potential energy (p.e.), U, of the vehicle system is given by

$$\begin{aligned} T &= \tfrac{1}{2} m_e \dot{s}^2 + \tfrac{1}{2}(m_e \dot{z}_1^2 + I_1 \dot{z}_2^2) + \tfrac{1}{2} I_{ov} \dot{z}_2^2 \\ &+ \tfrac{1}{2} m_{ov} [(\dot{z}_1 + r_{ov} \dot{z}_2 \cos(\theta_{ov}+z_2))^2 + (\dot{s} - r_{ov} \dot{z}_2 \sin(\theta_{ov}+z_2))^2] \\ &+ \tfrac{1}{2} m_v [(\dot{z}_1 + r_v \dot{z}_2 \cos(\theta_v+z_2) + l_v \dot{z}_3 \sin z_3)^2 \\ &+ (\dot{s} + l_v \dot{z}_3 \cos z_3 - r_v \dot{z}_2 \sin(\theta_v+z_2))^2] \end{aligned} \qquad (5.1)$$

$$\begin{aligned} U &= \tfrac{1}{2} k_1 (z_1 + l_1 z_2 - y_1)^2 + \tfrac{1}{2} k_2 (z_1 - l_2 z_2 - y_2)^2 \\ &+ m_v g [r_v(\sin(\theta_v+z_2) - \sin\theta_v) + l_v(1-\cos z_3)] \\ &+ m_{ov} g r_{op} (\sin(\theta_{ov}+z_2) - \sin\theta_{ov}) + m_e g r_e[-\sin(\theta_e+z_2) \\ &+ \sin\theta_e] \end{aligned} \qquad (5.2)$$

where s is the displacement of the loaded vehicle c.g. at any time t in horizontal direction.

The equations of motion for the system can be represented through Lagrange's equations [25] as

$$\frac{d}{dt}\left(\frac{\partial T}{\partial \dot{z}_i}\right) - \frac{\partial T}{\partial z_i} + \frac{\partial U}{\partial z_i} - Q_{Di} = Q_{Ai}, \quad i = 1,2,3. \qquad (5.3)$$

where Q_{Ai} are externally applied forces and Q_{Di} are damping forces. Using (5.3), (5.1) and (5.2) one writes the equations of motion as follows.

$$(m_e+m_{ov}+m_v)\ddot{z}_1 + [m_{ov}r_{ov}\cos(\theta_{ov}+z_2) + m_v r_v \cos(\theta_v+z_2)]\ddot{z}_2$$
$$+ m_v l_v \sin z_3 \cdot \ddot{z}_3 + m_v l_v \cos z_3 \cdot \dot{z}_3^2 - [m_{ov}r_{ov}\cos(\theta_{ov}+z_2)$$
$$+ m_v r_v \cos(\theta_v+z_2)]\dot{z}_2^2 + (c_1+c_2)\dot{z}_1 + (c_1l_1-c_2l_2)\dot{z}_2$$
$$+ (k_1+k_2)z_1 + (k_1l_1-k_2l_2)z_2 = k_1y_1+k_2y_2+c_1\dot{y}_1+c_2\dot{y}_2 \qquad (5.4)$$

$$[m_{ov}r_{ov}\cos(\theta_{ov}+z_2) + m_v r_v \cos(\theta_v+z_2)]\ddot{z}_1$$
$$+(I_1+I_{ov}+m_{ov}r_{ov}^2+m_v r_v^2)\ddot{z}_2 + (m_v l_v r_v \sin(\theta_v+z_2-z_3))\ddot{z}_3$$
$$+(m_v l_v r_v \cos(\theta_v+z_2-z_3))\dot{z}_3^2 - \{(m_{ov}r_{ov}\sin(\theta_{ov}+z_2)) + m_v r_v \sin(\theta_v+z_2)\}\ddot{s}$$
$$+(c_1l_1-c_2l_2)\dot{z}_1 + (c_1l_1^2+c_2l_2^2)\dot{z}_2 + (k_1l_1-k_2l_2)z_1$$
$$+(k_1l_1^2+k_2l_2^2)z_2 + g[m_v r_v \cos(\theta_v+z_2) + m_{ov}r_{ov}\cos(\theta_{ov}+z_2)$$
$$-m_e r_e \cos(\theta_e+z_2)] = k_1l_1y_1 - k_2l_2y_2 + c_1l_1\dot{y}_1 - c_2l_2\dot{y}_2 \qquad (5.5)$$

$$m_v l_v^2 \ddot{z}_3 + \ddot{z}_1 \cdot m_v l_v \sin z_3 + (m_v l_v r_v \sin(\theta_v+z_2-z_3))\ddot{z}_2$$
$$-(m_v l_v r_v \cos(\theta_v+z_2-z_3))\dot{z}_2^2 + c_v\dot{z}_3 + m_v l_v g \sin z_3 = 0 \qquad (5.6)$$
$$+ m_v l_v \ddot{s}\cos z_3$$

If the c.g. of the mechanical model is assumed to be the same as that of the liquid in the container and z_2 as small

then one can approximate

$$g[m_v r_v \cos(\theta_v + z_2) + m_{ov} r_{ov} \cos(\theta_{ov} + z_2) - m_e r_e \cos(\theta_e + z_2)]$$
$$\simeq - g\, m_v l_v\, z_2.$$

Equations (5.4) to (5.6) are non-linear and coupled. These equations have nonlinearities in displacement, velocity and also in inertial terms. An analytical solution of these equations is not feasible. Hence the following stochastic linearization technique is used to linearize these equations.

5.4 Stochastic Linearization of Equations of Motion

There are deterministic and statistical methods to linearize the equations of motion. Each has its own advantages and disadvantages. These are discussed in detail in Ref. [4]. For the random excitation, statistical or stochastic linearization is preferred. Broadly speaking two methods of stochastic linearization are available. The first one was suggested by Iwan and Yang [26] and the other by Atalik and Utku [4]. In the former the nonlinearities in damping and stiffness are considered but inertial nonlinearities are excluded. In the latter [4], nonlinearities of inertial terms are also included and hence it is more powerful. Accordingly, in the present analysis, the method of Ref. [4] is adapted.

5.4.1 The stochastic linearization method (Ref. [4])

The nonlinear multi-degree-of-freedom system

$$\bar{g}\,(\ddot{\bar{Z}},\ \dot{\bar{Z}},\ \bar{Z}) \;=\; \bar{f}(t) \tag{5.7}$$

is linearized to

$$[m]\,\ddot{\bar{Z}} + [c]\,\dot{\bar{Z}} + [k]\,\bar{Z} \;=\; \bar{f}(t) \tag{5.8}$$

where,

$\bar{Z}$ is the generalized displacement vector,

$g_i(\ddot{\bar{Z}},\dot{\bar{Z}},\bar{Z})$ is the total internal force acting in the ith degree-of-freedom direction,

$\bar{f}(t)$ is the stationary Gaussian random excitation vector, with zero mean;

$[m],[c],[k]$ are mass, damping, stiffness matrices. The elements of these matrices are given by

$$\begin{aligned} m_{ij} &= E\left[\frac{\partial g_i}{\partial \ddot{z}_j}\right] \\ c_{ij} &= E\left[\frac{\partial g_i}{\partial \dot{z}_j}\right] \qquad i,j = 1,2,3; \\ k_{ij} &= E\left[\frac{\partial g_i}{\partial z_j}\right] \end{aligned} \tag{5.9}$$

where $E[\cdot]$ is the expectation operator.

5.4.2 Application to the present analysis

Nonlinear equations (5.4) to (5.6) are linearized using relations (5.7) to (5.9). It is assumed that z_2 and z_3 are small quantities so that $\sin z_2 \simeq z_2$, $\sin z_3 \simeq z_3$,

cos $z_2 \simeq 1.0$, cos $z_3 \simeq 1.0$. The squares and products of z_2 and z_3 are neglected. It is assumed that the excitation process, Y(s) is Gaussian in nature with zero mean. Hence z_i are Gaussian in nature with

$$E[z_i] = 0, \quad i = 1,2,3 \tag{5.10}$$

Using the properties of Gaussian process [32], the assumptions cited above and (5.10), one gets the linearized equations as

$$[m_{ij}]\{\ddot{z}_i\} + [c_{ij}]\{\dot{z}_i\} + [k_{ij}]\{z_i\} = \{f_i\}, \; i,j=1,2,3 \tag{5.11}$$

where

$$m_{11} = (m_e + m_{ov} + m_v), \; m_{12} = (m_{ov}+m_v)e_1, \; m_{13}=0,$$

$$m_{21}=m_{12}, \; m_{22} = I_1+I_{ov}+m_{ov}r_{ov}^2 + m_v r_v^2, \; m_{23} = m_v l_v (e_2+e_4),$$

$$m_{31} = m_{13}, \; m_{32} = m_{23}, \; m_{33} = m_v l_v^2 ;$$

$$c_{11} = (c_1+c_2), \quad c_{12} = (c_1 l_1 - c_2 l_2), \quad c_{13} = 0$$

$$c_{21} = c_{12}, \quad c_{22} = c_1 l_1^2 + c_2 l_2^2, \quad c_{23} = 0$$

$$c_{31} = 0, \quad c_{32} = 0, \quad c_{33} = c_v ;$$

$$k_{11} = k_1+k_2, \quad k_{12} = k_1 l_1 - k_2 l_2, \quad k_{13} = 0, \quad k_{21} = k_{12},$$

$$k_{22} = k_1 l_1^2 + k_2 l_2^2 - g m_v l_v - (m_{ov}+m_v)\, e_1\, E[\ddot{z}_1 z_2]$$

$$- m_v l_v (e_2+e_4)\, E[z_2 \ddot{z}_3] - (m_{ov}+m_v) e_1 \ddot{s},$$

$$k_{23} = m_v l_v (e_2+e_4)\, E[z_2 \ddot{z}_3], \quad k_{31} = 0$$

$$k_{32} = m_v l_v (e_2+e_4)\, E[\ddot{z}_2 z_3],$$

$$k_{33} = m_v l_v g - m_v l_v (e_2+e_4)\, E[z_3 \ddot{z}_2];$$

$$f_1 = k_1 y_1 + k_2 y_2 + c_1 \dot{y}_1 + c_2 \dot{y}_2$$

$$f_2 = k_1 l_1 y_1 - k_2 l_2 y_2 + c_1 l_1 \dot{y}_1 - c_2 l_2 \dot{y}_2$$

$$f_3 = 0.$$

For stationary processes z_i, z_j it can be proved that [37]

$$E[\ddot{z}_i z_j] = E[z_i \ddot{z}_j] \qquad (5.12)$$

Thus for stationary process z_i, the mass, damping and stiffness matrices are symmetric.

5.5 Uncoupling the Equations of Motion for the Vehicle Moving with Constant Velocity

A general method to uncouple damped linear system is reported in the literature [20, 25, 34, 51]. This method, suggested by Foss, is specially useful for systems with non-proportional damping and is used here.

Let the generalized co-ordinates are x_n, n=1, 2, ...6 with

$$z_i = \sum_{n=1}^{6} u_{in} x_n, \quad \dot{z}_i = \sum_{n=1}^{6} \alpha_n u_{in} x_n, \quad i = 1, 2, 3 ; \qquad (5.13)$$

where α_n are the eigenvalues and u_{in} are the elements of the modal column matrix

$$[U] = \begin{bmatrix} [\alpha u] \\ \vdots \\ [u] \end{bmatrix} \qquad (5.14)$$

of the 6 x 6 dynamic matrix

$$[D] = \begin{bmatrix} [0] & [I] \\ -[k]^{-1}[m] & -[k]^{-1}[c] \end{bmatrix} . \qquad (5.15)$$

where [k], [m], [c] are known from (5.11). The eigenvalues α_n are determined such that

$$\left| [D] - \lambda [I] \right| = 0, \quad \text{and } \lambda = \frac{1}{\alpha} \tag{5.16}$$

Eigenvalues and eigenvectors occur in complex conjugate pair. For a stable system, eigenvalues have negative real part.

If $\{\phi_1\}$, $\{\phi_2\}$, ... $\{\phi_6\}$ are the eigenvectors then

$$[u] = [\{\phi_1\}\{\phi_2\} \cdots \{\phi_6\}] \tag{5.17}$$

and
$$[\alpha u] = [\alpha_1 \{\phi_1\} \alpha_2\{\phi_2\} \cdots \alpha_6\{\phi_6\}] \tag{5.18}$$

are 3x6 rectangular matrices. It is assumed that [m], [c], [k] are symmetric and hence it can be proved that the modes are orthogonal [20,25,34]. Thus in generalized co-ordinates, the decoupled equations are [20,25,34]

$$\dot{x}_1 - \alpha_i x_i = F_i/R_i, \quad i = 1,2,\ldots 6 \tag{5.19}$$

where,

$$R_i = 2\alpha_i \{\phi_i\}^T [m] \{\phi_i\} + \{\phi_i\}^T [c] \{\phi_i\} \tag{5.20}$$

$$F_i = \{\phi_i\}^T \{f(t)\}$$

$$= (u_{1i} + l_1 u_{2i})(k_1 y_1 + c_1 \dot{y}_1) + (u_{1i} - l_2 u_{2i})(k_2 y_2 + c_2 \dot{y}_2) \tag{5.21}$$

5.5.1 Equations in space-domain

The decoupled equations of motion (5.19) in space domain become

$$\frac{ds}{dt} x_i' - \alpha_i x_i = \frac{1}{R_i} \left[(u_{1i} + l_1 u_{2i})(k_1 Y(s+l_1) + c_1 \frac{ds}{dt} Y'(s+l_1)) \right.$$
$$\left. + (u_{1i} - l_2 u_{2i})(k_2 Y(s-l_2) + c_2 \frac{ds}{dt} Y'(s-l_2)) \right],$$

where $x_i' = \frac{dx_i}{ds}$, $Y' = \frac{dY}{ds}$ (5.22)

5.6 Vehicle Motion

If s(t) is the distance covered by the vehicle along the track at time, t, then for constant velocity run one has

$$s = s_o + v_o t \tag{5.23}$$

where s_o is the initial distance at $t=0$ and v_o is the constant velocity. Thus

$$\frac{ds}{dt} = \dot{s} = v_o \tag{5.24}$$

5.7 Solution of Equations of Motion

For constant velocity run, using (5.24), (5.22) reduces to

$$v_o x_i' - \alpha_i x_i = \frac{1}{R_i} [(u_{1i} + l_1 u_{2i})(k_1 Y(s+l_1) + c_1 v_o Y'(s+l_1))$$
$$+ (u_{1i} - l_2 u_{2i})(k_2 Y(s-l_2) + c_2 v_o Y'(s-l_2))] \tag{5.25}$$

General solution of (5.25) is the sum of homogeneous and non-homogeneous parts. The homogeneous part is

$$x_{ih} = B_i e^{\alpha_i s / v_o} \tag{5.26}$$

where B_i are constants and are determined from initial conditions. The nonhomogeneous part in spatial frequency (Ω) domain is given by

then the constants of integration are given by

$$\{B\} = [U]^{-1} \begin{Bmatrix} v_1 \\ v_2 \\ v_3 \\ d_1 \\ d_2 \\ d_3 \end{Bmatrix} , \qquad (5.36)$$

where μ represents mean value.

5.7.1 Second order statistics of response

The mean values for displacement, first and second derivatives are evaluated, using (5.31) to (5.34), as follows

$$\mu_{z_i} = E[z_i(s)] = \sum_{n=1}^{6} u_{in} B_n e^{\alpha_n s/v_o} + \sum_{n=1}^{6} u_{in} \int_{-\infty}^{\infty} H_n(\Omega) e^{i\Omega s} .$$

$$E[dF(\Omega)] = \sum_{n=1}^{6} u_{in} B_n e^{\alpha_n s/v_o} \qquad (5.37)$$

Similarly,

$$\mu_{\dot{z}_i} = \sum_{n=1}^{6} \alpha_n u_{in} B_n e^{\alpha_n s/v_o} \qquad (5.38)$$

$$\mu_{\ddot{z}_i} = \sum_{n=1}^{6} \alpha_n^2 u_{in} B_n e^{\alpha_n s/v_o} \quad i = 1,2,3 \qquad (5.39)$$

The response, z_i and its derivatives, given by Eqs.(5.32) to (5.34), can be termed as oscillatory processes [39, section 3]. Hence, after transforming to zero mean, the evolutionary spectral density and the covariance function can be determined as suggested in Ref. [39, section 4]. Thus

$$\Phi_{z_i z_\ell}(\Omega) = \Phi_{YY}(\Omega) \left[\sum_{p=1}^{6} u_{ip} H_p(\Omega)\right]\left[\sum_{n=1}^{6} u_{\ell n} H_n(\Omega)\right]^*$$

$$= \Phi_{YY}(\Omega) \sum_{p=1}^{6}\sum_{n=1}^{6} u_{ip} u^*_{\ell n} H_p(\Omega) H^*_n(\Omega) \qquad (5.40)$$

where (*) denotes complex conjugate. Since the eigenvalues and eigenvectors occur in complex conjugate pair hence (5.40) can be written in a simpler form as

$$\Phi_{z_i z_\ell}(\Omega) = \Phi_{YY}(\Omega) \sum_{p=1}^{6}\sum_{n=1}^{6} u_{ip}\, u_{\ell n}\, H_p(\Omega)\, H_n(-\Omega) \qquad (5.41)$$

Similarly,

$$\Phi_{\dot{z}_i \dot{z}_\ell}(\Omega) = \Phi_{YY}(\Omega) \sum_{p=1}^{6}\sum_{n=1}^{6} \alpha_p \alpha_n u_{ip} u_{\ell n} H_p(\Omega)\, H_n(-\Omega) \qquad (5.42)$$

$$\Phi_{\ddot{z}_i \ddot{z}_\ell}(\Omega) = \Phi_{YY}(\Omega) \sum_{p=1}^{6}\sum_{n=1}^{6} \alpha_p \alpha_n u_{ip} u_{\ell n}\, \Omega^2 H_p(\Omega)\, H_n(-\Omega) \qquad (5.43)$$

$$i, \ell = 1, 2, 3.$$

The covariance function, for $s_1 \geq s_2$, is similarly expressed as

$$\kappa_{z_i z_\ell}(s_1, s_2) = \int_{-\infty}^{\infty} \Phi_{YY}(\Omega)\left[\sum_{p=1}^{6} u_{ip} H_p(\Omega)\right]\left[\sum_{n=1}^{6} u_{\ell n} H_n(\Omega)\right]^* e^{j\Omega(s_1 - s_2)} d\Omega$$

$$= \sum_{p=1}^{6}\sum_{n=1}^{6} u_{ip} u_{\ell n} \int_{-\infty}^{\infty} \Phi_{YY}(\Omega)\, H_p(\Omega)\, H_n(-\Omega)\, e^{j\Omega(s_1 - s_2)} d\Omega \qquad (5.44)$$

The complex conjugate operator has been dropped on the argument as given for (5.41). Similar expressions for covariance functions of velocity and acceleration can be obtained. If

$$I_{pn}(s_1,s_2) = \int_{-\infty}^{\infty} \Phi_{YY}(\Omega)\ H_p(\Omega)\ H_n(-\Omega)\ e^{j\Omega(s_1-s_2)}\, d\Omega, \quad (5.45)$$

then one has for $s_1 \geq s_2$

$$\kappa_{z_i z_\ell} = \sum_{p=1}^{6} \sum_{n=1}^{6} u_{ip}\ u_{\ell n}\ I_{pn} \quad (5.46)$$

$$\kappa_{\dot{z}_i \dot{z}_\ell} = \sum_{p=1}^{6} \sum_{n=1}^{6} \alpha_p\ \alpha_n\ u_{ip}\ u_{\ell n}\ I_{pn} \quad (5.47)$$

$$\kappa_{\ddot{z}_i \ddot{z}_\ell} = v_o^2 \sum_{p=1}^{6} \sum_{n=1}^{6} \alpha_p\ \alpha_n\ u_{ip}\ u_{\ell n}\ \frac{\partial^2 I_{pn}(s_1,s_2)}{\partial s_1\, \partial s_2} \quad (5.48)$$

$$\kappa_{\ddot{z}_i z_\ell} = v_o^2 \sum_{p=1}^{6} \sum_{n=1}^{6} u_{ip}\ u_{\ell n}\ \frac{\partial^2}{\partial s_1^2}(I_{pn}(s_1,s_2)) \quad (5.49)$$

Evaluation of $I_{pn}(s_1,s_2)$ and its derivatives

On substituting for $\Phi_{YY}(\Omega)$ from (4.2) and for $H(\Omega)$ from (5.27) into (5.45) one gets

$$I_{pn} = \frac{-C}{R_p R_n} \int_{-\infty}^{\infty} [(u_{1p}+l_1 u_{2p})(k_1+j\Omega c_1 v_o)e^{j\Omega l_1} + (u_{1p}-l_2 u_{2p})$$
$$(k_2+j\Omega c_2 v_o)e^{-j\Omega l_2}]\ [(u_{1n}+l_1 u_{2n})(k_1-j\Omega c_1 v_o)e^{-j\Omega l_1} + (u_{1n}-l_2 u_{2n}) \cdot$$
$$(k_2-j\Omega c_2 v_o)e^{j\Omega l_2}]\ \frac{e^{j\Omega(s_1-s_2)}}{(\gamma^2+\Omega^2)(j\Omega v_o-\alpha_p)(j\Omega v_o+\alpha_n)}\, d\Omega \quad (5.50)$$

The improper integral is evaluated by the contour integration [30] using residue theorem. As the eigenvalue has negative real part, there are two poles in the upper half plane. One is at $\Omega = j\gamma$ and the other at $\Omega = \alpha_p/jv_o$. Both are simple poles. Thus finally one gets for $s_1 \geq s_2$

$$I_{pn} = \frac{2\pi C}{R_p R_n} (F_{pn} + G_{pn}), \qquad (5.51)$$

where,

$$F_{pn} = \frac{(A_p D_1 + B_p D_2)(A_n D_3 + B_n D_4)}{2\gamma\,(\alpha_p + v_o\gamma)(\alpha_n - v_o\gamma)}\, e^{-\gamma(s_1 - s_2)}, \qquad s_1 \geq s_2$$

$$G_{pn} = \left[\frac{(A_p V_p + B_p W_p)(A_n X_p + B_n Y_p)}{(\alpha_p^2 - v_o^2\gamma^2)(\alpha_p + \alpha_n)}\right] v_o \cdot e^{\alpha_p (s_1 - s_2)/v_o},$$

$$D_1 = (k_1 - c_1\gamma v_o)\, e^{-\gamma l_1}, \quad D_2 = (k_2 - c_2\gamma v_o) e^{\gamma l_2},$$

$$D_3 = (k_1 + c_1\gamma v_o)\, e^{\gamma l_1}, \quad D_4 = (k_2 + c_2\gamma v_o) e^{-\gamma l_2},$$

$$A_p = (u_{1p} + l_1 u_{2p}), \qquad B_p = (u_{1p} - l_2 u_{2p}),$$

$$A_n = (u_{1n} + l_1 u_{2n}), \qquad B_n = (u_{1n} - l_2 u_{2n}),$$

$$V_p = (k_1 + \alpha_p c_1) e^{\alpha_p l_1/v_o}, \quad W_p = (k_2 + \alpha_p c_2) e^{-\alpha_p l_2/v_o},$$

$$X_p = (k_1 - \alpha_p c_1) e^{-\alpha_p l_1/v_o}, \quad Y_p = (k_2 - \alpha_p c_2) e^{\alpha_p l_2/v_o}.$$

5.7.2 Limiting cases

5.7.2.1 Small vehicle velocity

$$\lim_{v_o \to 0} I_{pn} = \frac{2\pi C}{R_p R_n} \lim_{v_o \to 0} (F_{pn} + G_{pn}),$$

$$\lim_{v_o \to 0} F_{pn} = \frac{(A_p k_1 + B_p k_2)(A_n k_1 + B_n k_2)}{2\gamma\ \alpha_p \cdot \alpha_n}\, e^{-\gamma(s_1 - s_2)},$$

$$\lim_{v_o \to 0} G_{pn} = \frac{1}{\alpha_p^2(\alpha_p + \alpha_n)} \lim_{v_o \to 0} v_o\, e^{\alpha_p (s_1 - s_2)/v_o} [k_1^2 + k_2^2 - \alpha_p^2 (c_1^2 + c_2^2)$$

$$+ (k_1 + \alpha_p c_1)(k_2 - \alpha_p c_2)\, e^{\alpha_p L/v_o} + (k_1 - \alpha_p c_1)(k_2 + \alpha_p c_2) e^{-\alpha_p L/v_o}], \qquad (5.52)$$

where $L = l_1 + l_2$.

As α_p has negative real part,

$$\lim_{v_o \to 0} v_o \, e^{\alpha_p (L+s_1-s_2)/v_o} \to 0, \text{ for all } s_1 \geq s_2.$$

$$\lim_{v_o \to 0} v_o \, e^{-\alpha_p (L-s_1+s_2)/v_o} \to 0 \text{ , if } L \leq (s_1-s_2) \text{ ,}$$

$$\to \infty \text{ , if } L > (s_1-s_2) \text{ ;}$$

as the exponential term increases much faster than v_o reduces. Hence

$$\lim_{v_o \to 0} G_{pn} \to \infty \text{ , if } L > (s_1-s_2)$$

$$\therefore \lim_{v_o \to 0} I_{pn} \to \infty \tag{5.53}$$

For mean square response $s_1=s_2$. This implies, from (5.46) to (5.48), that the mean square response in the neighbourhood of zero velocity is large.

5.7.2.2 Large vehicle velocity

(i) $$\lim_{v_o \to \infty} I_{pn} = \frac{2\pi C}{R_p R_n} \lim_{v_o \to \infty} (F_{pn} + G_{pn})$$

Looking to the expressions of F_{pn} and G_{pn}, from (5.51), one can easily prove that

$$\lim_{v_o \to \infty} F_{pn} = \frac{A_p A_n c_1^2 + B_p B_n c_2^2 + (A_p B_n e^{-\gamma L} + B_p A_n e^{\gamma L}) c_1 c_2}{2\gamma} \tag{5.54}$$

$$\lim_{v_o \to \infty} G_{pn} = 0$$

$$\therefore \lim_{v_o \to \infty} I_{pn} = \frac{\pi C}{R_p R_n \gamma} [A_p A_n c_1^2 + B_p B_n c_2^2 + c_1 c_2 (A_p B_n e^{-\gamma L} + B_p A_n e^{\gamma L})] \tag{5.55}$$

This implies, from (5.46) and (5.47), that at large velocity the mean square response for displacement and velocity tends to be independent of velocity.

$$\text{(ii)} \quad \lim_{v_o \to \infty} v_o^2 \frac{\partial^2 I_{pn}}{\partial s_1 \partial s_2} = \lim_{v_o \to \infty} \frac{-2\pi C}{R_p R_n} [\gamma^2 v_o^2 F_{pn} + \alpha_p^2 G_{pn}] \qquad (5.56)$$

Looking to the limits evaluated at (5.54), or directly one finds that this limit tends to ∞. This implies, from (5.48), that the mean square response for acceleration tends to be large at large velocity of travel.

5.8 Shear-Force and Bending Moment Response

Shear force and bending moment coming on the bottom corner of right container wall are determined assuming the wall to be a cantilever. The forces are assumed to act along the vertical centre line of the container wall which is fixed at the bottom. From Fig. 5.1, the shear force is given by

$$F_s = F_v + F_{ov} , \qquad (5.57)$$

where,

$$F_v = \frac{1}{2} m_v \frac{d}{dt} (l_v \dot{z}_3 \cos z_3 - r_v \dot{z}_2 \sin (\theta_v + z_2))$$

$$F_{ov} = \frac{1}{2} m_{ov} \frac{d}{dt} (\frac{ds}{dt} - r_{ov} \dot{z}_2 \sin (\theta_{ov} + z_2))$$

As z_2 and z_3 are small quantities one has

$$F_s = b_o + b_1 \ddot{z}_2 + b_2 \ddot{z}_3 + b_3 \ddot{z}_2 z_2 \qquad (5.58)$$

where,

$$b_o = \frac{1}{2} m_{ov} \ddot{s}, \quad b_1 = -\frac{1}{2}\left(m_v r_v \sin\theta_v + m_{ov} r_{ov} \sin\theta_{ov}\right),$$

$$b_2 = \frac{1}{2} m_v l_v, \quad b_3 = -\frac{1}{2}\left(m_v + m_{ov}\right) e_1 \qquad (5.59)$$

Similarly the bending moment is given by

$$M_b = \left(\frac{h}{2} + e_4\right) F_v + \left(\frac{h}{2} - e_5\right) F_{ov} \qquad (5.60)$$

where, h is the height of the liquid.

$$\text{Or, } M_b = r_o + r_1 \ddot{z}_2 + r_2 \ddot{z}_3 + r_3 \ddot{z}_2 z_2 \qquad (5.61)$$

where,

$$r_o = \left(\frac{h}{2} - e_5\right) b_o,$$

$$r_1 = -\frac{1}{2}\left[m_v\left(\frac{h}{2}+e_4\right) r_v \sin\theta_v + m_{ov}\left(\frac{h}{2}-e_5\right) r_{ov} \sin\theta_{ov}\right], \qquad (5.62)$$

$$r_2 = \left(\frac{h}{2}+e_4\right) b_2, \quad r_3 = -\frac{1}{2}\left[m_v\left(\frac{h}{2}+e_4\right) + m_{ov}\left(\frac{h}{2}-e_5\right)\right] e_1 .$$

5.8.1 Mean Value response

As the mean of z_i is zero hence

$$\mu_{F_s} = b_o + b_3 E[\ddot{z}_2 z_2]. \qquad (5.63)$$

For a stationary process z_2, one has

$$E[\ddot{z}_2 z_2] = -E[\dot{z}_2^2] . \qquad (5.64)$$

This is a second order term and is neglected.

$$\therefore \mu_{F_s} = b_o, \qquad (5.65)$$
$$= 0, \text{ for constant vehicle velocity.}$$

Similarly,

$$\mu_{M_b} = r_o$$
$$= 0 \text{ , for constant vehicle velocity.} \qquad (5.66)$$

5.8.2 Mean square response

Under Gaussian assumption one gets, after neglecting the second order terms,

$$E[(F_s-\mu_{F_s})^2] = b_1^2 E[\ddot{z}_2^2] + b_2^2 E[\ddot{z}_3^2] + 2b_1b_2E[\ddot{z}_2\ddot{z}_3]. \qquad (5.67)$$

Similarly,

$$E[(M_b-\mu_{M_b})^2] = r_1^2E[\ddot{z}_2^2] + r_2^2E[\ddot{z}_3^2] + 2r_1r_2E[\ddot{z}_2\ddot{z}_3]. \qquad (5.68)$$

5.9 Equations of Motion for the Vehicle System with Solidified Mass

The equations of motion for the vehicle system carrying equivalent solid cargo mass, M_o, having moment of inertia, I_{sy}, can be written as follows.

$$[m]\{\ddot{z}_i\} + [c]\{\dot{z}_i\} + [k]\{z_i\} = \{f_i\}, \; i = 1,2 \qquad (5.69)$$

where

$$[m]=\begin{bmatrix} m_e+M_o & 0 \\ 0 & I_1+I_{sy}+M_o(e_1^2+e_2^2) \end{bmatrix}, \; [c] = \begin{bmatrix} c_1+c_2 & c_1l_1-c_2l_2 \\ l_1c_1-l_2c_2 & c_1l_1^2+c_2l_2^2 \end{bmatrix}$$

$$[k]=\begin{bmatrix} k_1+k_2 & l_1k_1-l_2k_2 \\ l_1k_1-l_2k_2 & k_1l_1^2+k_2l_2^2 \end{bmatrix}, \; \begin{Bmatrix} f_1 \\ f_2 \end{Bmatrix} = \begin{Bmatrix} k_1y_1 + k_2y_2 + c_1\dot{y}_1 + c_2\dot{y}_2 \\ k_1l_1y_1-k_2l_2y_2+c_1l_1\dot{y}_1-c_2l_2\dot{y}_2 \end{Bmatrix}$$

These equations are linear and coupled with 2 degrees of freedom. The solution of these equations and response statistics can be obtained as pointed out in Sections (5.5) to (5.7).

5.10 Vehicle Moving with Constant Acceleration

The linearized equations of motion are given by (5.11). For the variable velocity case the response becomes non-stationary. In equation (5.11), the stiffness matrix contains expectation terms which are nonstationary. Hence stiffness matrix is unsymmetric and the equations of motion cannot be uncoupled by the procedure outlined in Section 5.5. The equation (5.11) can be transformed to

$$\{\dot{q}\} + [A]\{q\} = [M]^{-1}\{F(t)\} \tag{5.70}$$

where

$$[A] = [M]^{-1}[K],$$

$$\{q\} = \begin{Bmatrix}\{\dot{z}\}\\ \{z\}\end{Bmatrix}, \quad \{F(t)\} = \begin{Bmatrix}\{0\}\\ \{f(t)\}\end{Bmatrix},$$

$$[M] = \begin{bmatrix}[0] & [m]\\ [m] & [c]\end{bmatrix}, \quad [K] = \begin{bmatrix}-[m] & [0]\\ [0] & [k]\end{bmatrix}$$

$[m]$, $[c]$, $[k]$ are NxN square matrices whereas $[M]$, $[K]$, $[A]$ are 2Nx2N square matrices. $\{q(t)\}$ and $\{F(t)\}$ are vectors with 2N elements. Let

$$\{q\} = [U]\{x\} \tag{5.71}$$

On substituting (5.71) into (5.70) and premultiplying by $[U]^{-1}$ one obtains

$$\{\dot{x}\} - [\alpha]\{x\} = \{g(t)\} \tag{5.72}$$

where, $\{g(t)\} = U^{-1}\,[M]^{-1}\,\{F(t)\}$ (5.73)

$[\alpha] = -[U]^{-1}\,[A][U]$ (5.74)

The matrix $[\alpha]$ is a diagonal matrix if $[U]$ is the modal matrix of $[A]$. Thus the equation (5.72) represents a system of 2N first order uncoupled equations in time domain.

5.10.1 Solution of Uncoupled equations in space co-ordinate

Equations (5.72) in space co-ordinate reduce to

$$v\,x_i' - \alpha_i x_i = G_i(s), \quad i = 1,2,..2N \tag{5.75}$$

where

$$v = \frac{ds}{dt} = \sqrt{v_o^2+2C_o s}, \quad x_i' = \frac{dx_i}{ds} \tag{5.76}$$

and v_o is the initial velocity, C_o is the constant acceleration. $G_i(s)$ is the corresponding element of $g_i(t)$ when transformed in space co-ordinate. The homogeneous solution of (5.75) is given by

$$x_{ih} = B_i \exp\left(\alpha_i \sqrt{(v_o^2+2C_o s)}/C_o\right) \tag{5.77}$$

where B_i are constants of integration.

The nonhomogeneous solution is expressed in Duhamel integral form and is given by

$$x_{in} = \int_o^s h_i(s,p)\,G_i(p)\,dp \tag{5.78}$$

where the impulse response function $h_i(s,p)$ is given by

$$h_i(s,p) = \frac{1}{\sqrt{(v_o^2+2C_o p)}} \exp\left[\alpha_i\left(\sqrt{(v_o^2+2C_o s)} - \sqrt{(v_o^2+2C_o p)}\right)/C_o\right] \tag{5.79}$$

Thus the complete solution is given by

$$x_i(s) = x_{ih} + x_{in} \qquad (5.80)$$

Finally using the relations (5.70), (5.71), (5.80), one can obtain the response z_i.

5.11 Results and Discussions

The vehicle considered for the present study is the railway wagon whose data are given in Table 4.1. The fore and aft axle stiffness and damping ratio are same. The container is filled with water and is mounted on the vehicle. The response of the vehicle is determined for liquid cargo and also for the equivalent solidified mass. The liquid is replaced by an equivalent mechanical model whose parameters are given by Eqs. (3.20) to (3.32). Only the fundamental mode of liquid sloshing is considered as the contribution to the total wall forces and vehicle dynamics from higher modes is expected to be small [1,22]. In the present analysis, the fixed mass location of the mechanical model is determined such that the c.g. of the model is the same as that of the liquid in the container. The base excitation to the vehicle is provided by the vertical track roughness whose p.s.d. is given by Eq. (4.2).

5.11.1 Vehicle moving with constant velocity

The vehicle response is studied for nine different configurations of the container. The c.g. of the empty

vehicle is taken as the origin (0,0). The c.g. of the container is referred to the origin as (x,y), where the first co-ordinate refers to the horizontal distance and the second co-ordinate refers to the vertical distance. For example, ($a_1/4$, $h_1/4$) refers to a container with its c.g. at a distance of $a_1/4$ to the right of the origin and at a distance of $h_1/4$ above the origin. The nine cases considered are given below:

Case	Length	Liquid-depth	Container c.g.
1	a_1	h_1	(0, 0)
2	"	$h_1/2$	(0, $-h_1/4$)
3	"	$h_1/4$	(0, $-3h_1/8$)
4	$a_1/2$	$h_1/2$	($a_1/4$, 0)
5	"	$h_1/4$	($a_1/4$, $h_1/8$)
6	"	$h_1/2$	($a_1/4$, $h_1/4$)
7	$a_1/4$	$h_1/4$	($a_1/4$, $h_1/8$)
8	"	$h_1/2$	($a_1/4$, $h_1/4$)
9	"	$h_1/4$	($a_1/4$, $3h_1/8$)

where a_1 = 7.89 meter, h_1 = 2.675 meter.

It has been seen in Sec. 5.7.2 that the response tends to a large value in the neighbourhood of zero vehicle velocity due to a mathematical singularity. Therefore, the velocity of interest has been chosen beyond 5 m/sec. The upper limit of the velocity is kept at 95 m/sec as it is considered sufficiently large for the vehicle of interest.

Iterative procedure

It is seen from Eq. (5.11) that the elements of mass and damping matrices are constant. Some of the elements of the stiffness matrix include expectation terms. These terms are not known initially. Hence, for response calculations, following iterative steps are undertaken to determine the expectation terms involved:

(i) Initially the expectation terms are assumed to be zero;

(ii) the response is determined and the terms involving expectations are evaluated;

(iii) with the expectation terms of step (ii), the response is determined and also the expectation quantities;

(iv) expectation quantities of steps (ii) and (iii) are compared to establish the convergence;

(v) if the convergence is not achieved, within specified limits, steps (ii) to (iv) are repeated.

For all the vehicle configurations, it was found sufficient to keep the limit of convergence within 1 percent of the quantities of interest and 2 to 3 iterations were found sufficient.

The vehicle response for the case of solidified mass of liquid is determined using the equations of motion outlined in Section (5.9).

The two cases of cargo as liquid and the same as solidified mass, are distinguished with the letters 's' and 'N' in

various figures to present the results. The superscript 's' refers to the case of sloshing liquid and the superscript 'N' refers to the case of solidified mass of the liquid, i.e. the case with no-sloshing. In each figure, which accompanies a table, the numbers indicate the container location, size and liquid height.

5.11.1.1 R.M.S. heave response for displacement and velocity

In Fig. (5.2a,b), the r.m.s. displacement and velocity response for heave mode of the loaded vehicle c.g. are presented for nine different cases. It is seen that at small velocities, the response fluctuates rapidly for all the cases considered. For vehicle velocities more than 15 m/sec, the r.m.s. value of the displacement response increases slowly with velocity. The r.m.s. velocity response fluctuates up to 30 m/sec. It increases rapidly up to 60 m/sec and then increases gradually. Both the responses tend to be independent of vehicle velocity at its large value. This is in accordance with the limits discussed in Sec. 5.7.2.

For centrally mounted container, (cases 1,2,3), the equations of liquid sloshing and vehicle vibration in heave mode are uncoupled. Hence sloshing has no effect on vehicle response in heave mode as is evident from Fig. (5.2a,b).

For eccentrically mounted container the r.m.s. response for sloshing case is invariably less, as much as 45 to 50%,

Empty vehicle c.g. at (o , o)
for liquid in container:

	Length	Height	c.g.
1	a_l	h_l	(o , o)
2	,,	$\frac{h_l}{2}$	(o , $-\frac{h_l}{4}$)
3	,,	$\frac{h_l}{4}$	(o , $-\frac{3}{8}h_l$)
4	$\frac{a_l}{2}$	$\frac{h_l}{2}$	($\frac{a_l}{4}$, o)
5	,,	$\frac{h_l}{4}$	($\frac{a_l}{4}$, $\frac{h_l}{8}$)
6	,,	$\frac{h_l}{2}$	($\frac{a_l}{4}$, $\frac{h_l}{4}$)

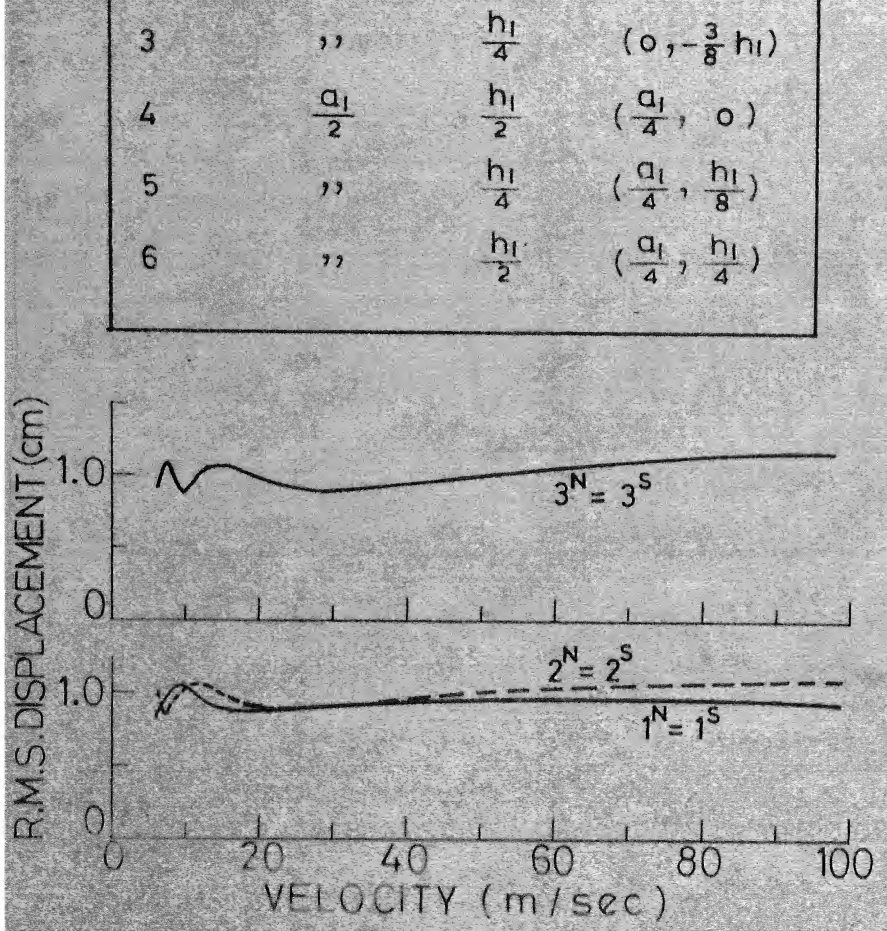

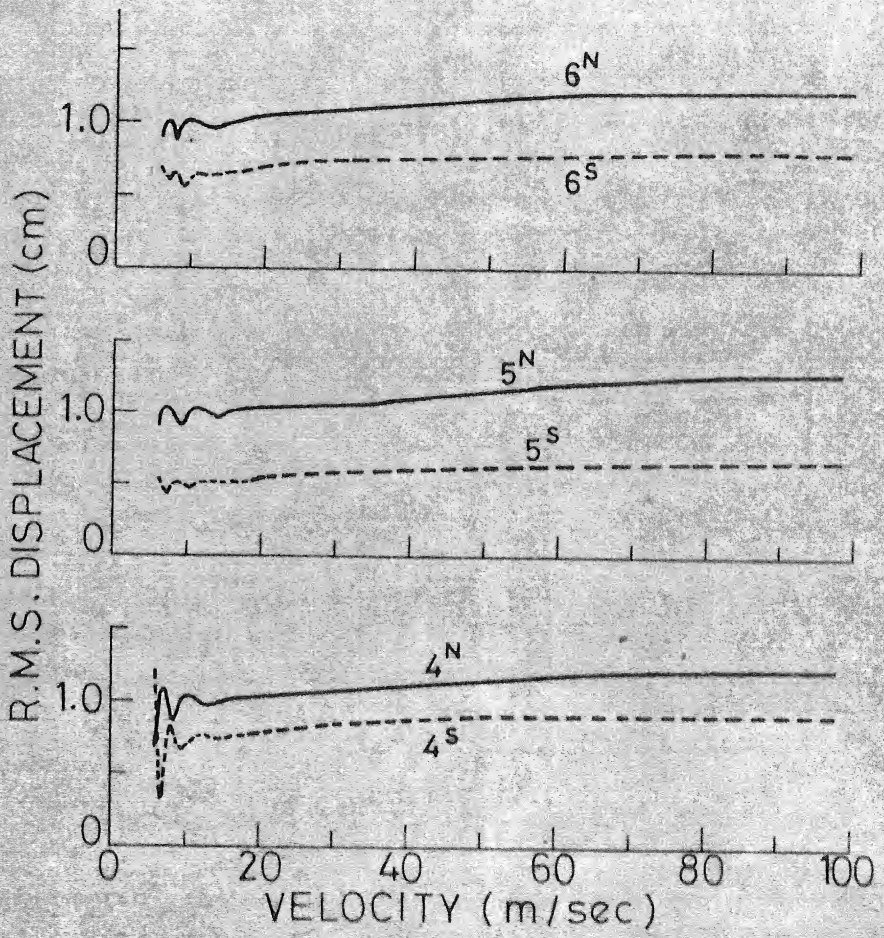

FIG 5.2a R.M.S. HEAVE RESPONSE FOR DISPLACEMENT AGAINST VEHICLE VELOCITY.

Empty vehicle c.g. at (o , o)
for liquid in container :

	Length	Height	c . g .
7	$\frac{a_l}{4}$	$\frac{h_l}{4}$	$(\frac{a_l}{4}, \frac{h_l}{8})$
8	,,	$\frac{h_l}{2}$	$(\frac{a_l}{4}, \frac{h_l}{4})$
9	,,	$\frac{h_l}{4}$	$(\frac{a_l}{4}, \frac{3}{8} h_l)$

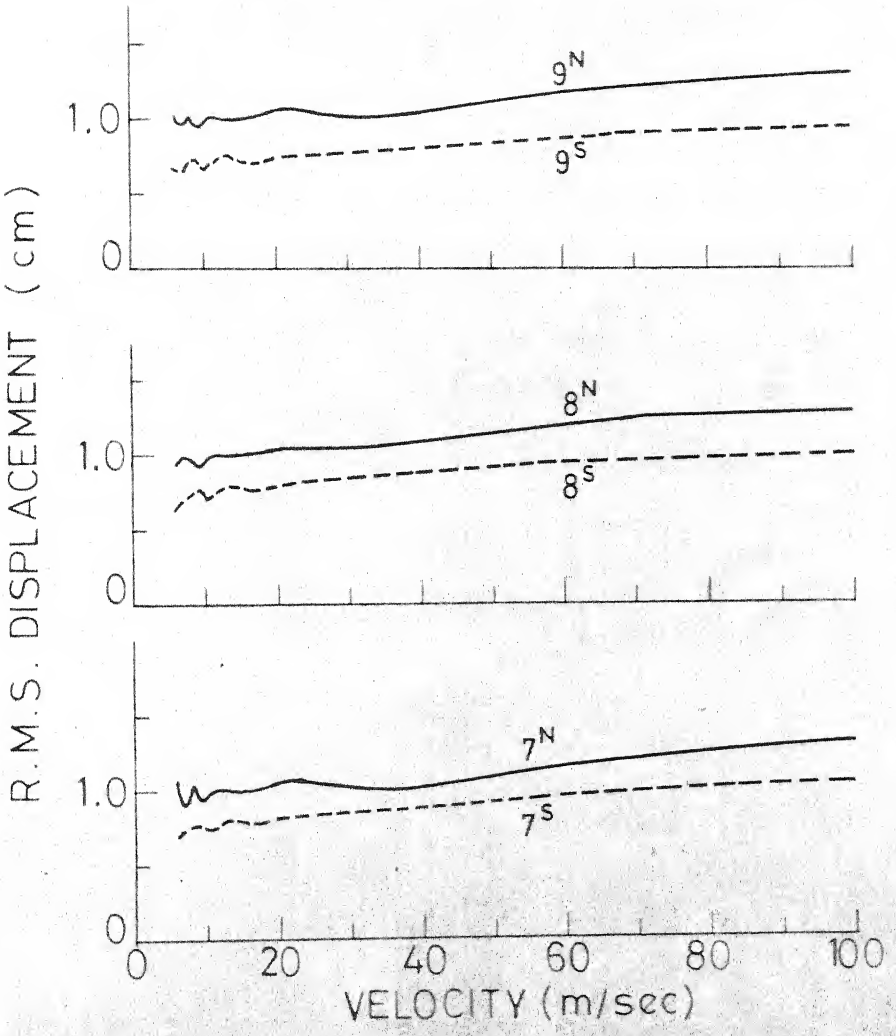

FIG.5.2a R.M.S. HEAVE RESPONSE FOR DISPLACEMENT AGAINST VEHICLE VELOCITY.

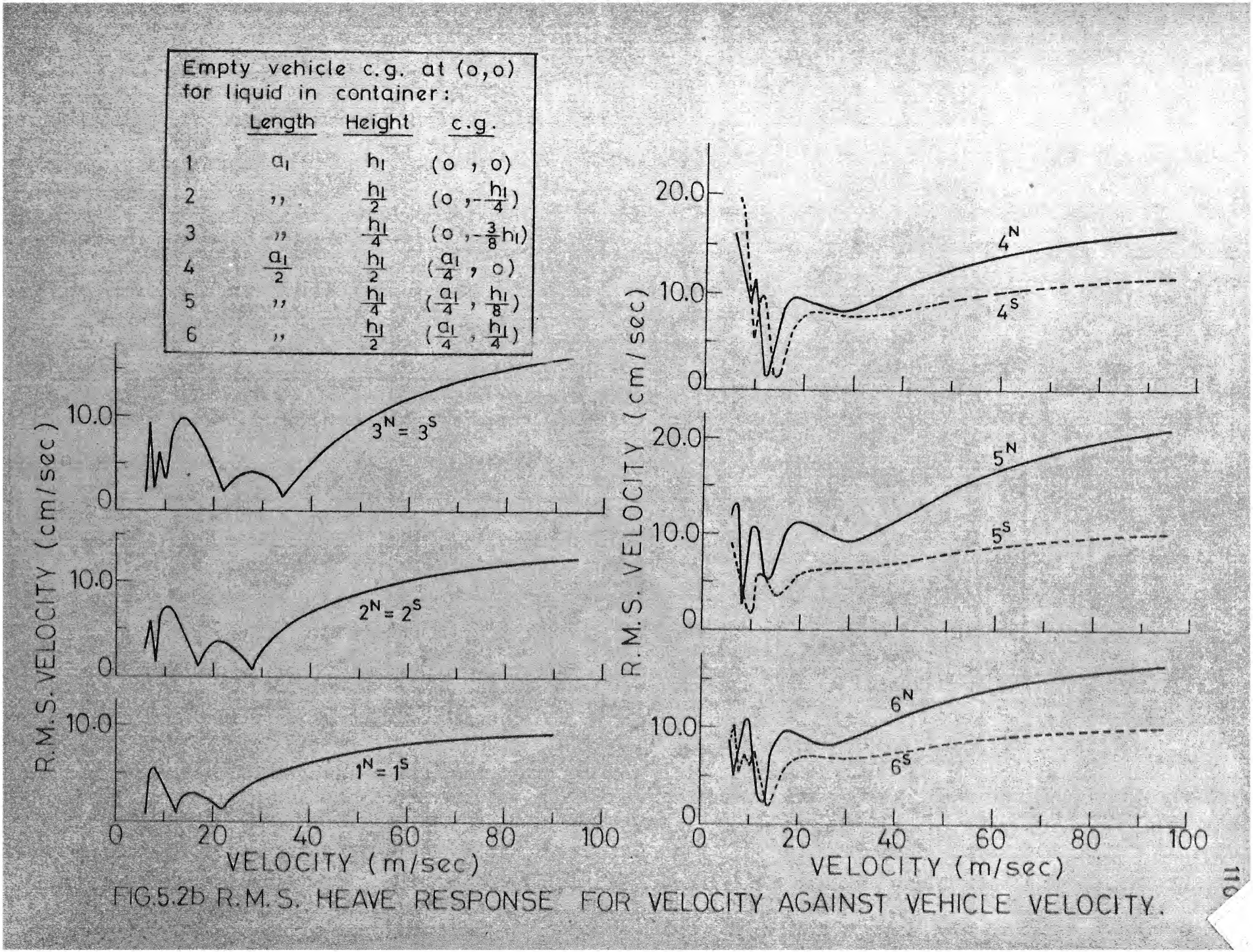

FIG.5.2b R.M.S. HEAVE RESPONSE FOR VELOCITY AGAINST VEHICLE VELOCITY.

Empty vehicle c.g. at (o,o) for liquid in container :	Length	Height	c.g.
7	$\frac{a_l}{4}$	$\frac{h_l}{4}$	$(\frac{a_l}{4}, \frac{h_l}{8})$
8	,,	$\frac{h_l}{2}$	$(\frac{a_l}{4}, \frac{h_l}{4})$
9	,,	$\frac{h_l}{4}$	$(\frac{a_l}{4}, \frac{3}{8}h_l)$

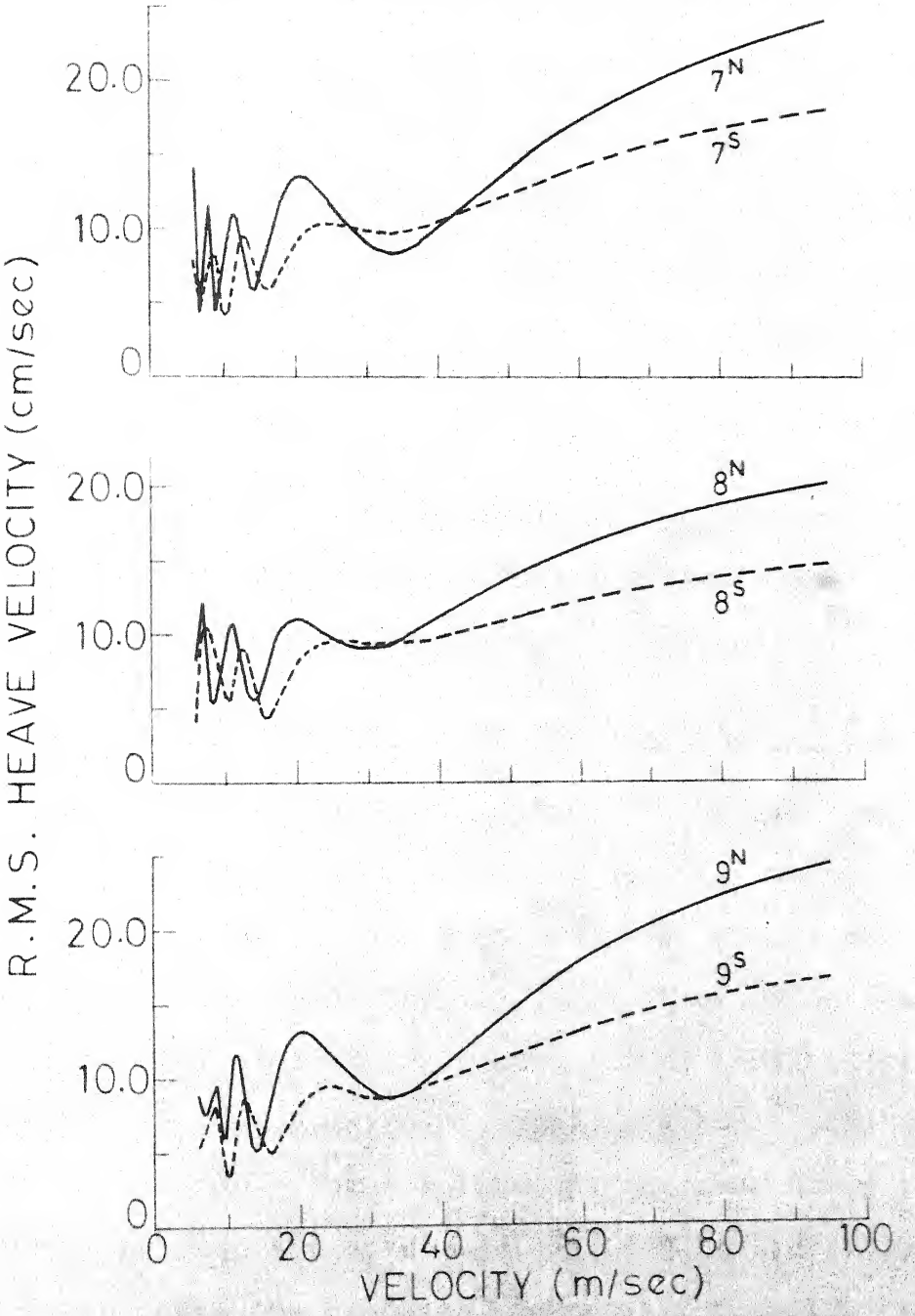

FIG.5.2b R.M.S. HEAVE RESPONSE FOR VELOCITY AGAINST VEHICLE VELOCITY.

than no-sloshing case (compare cases 4 to 9 in Fig. 5.2a). The r.m.s. velocity response for sloshing case is greater than no-sloshing case (cases 7,8) for some velocities. But the range of such velocities is narrow and towards lower end. Beyond vehicle velocity of 40 m/sec (144 km/hour), the response with sloshing is invariably less, as much as 45 to 50%; than without sloshing case. For the same horizontal eccentricity and mass of the liquid, larger vertical eccentricity causes greater reduction in the response for sloshing liquid (compare the cases (4,6) and (7,9) in Fig. 5.2a,b)). This implies that for larger eccentricity the absorption effect of the sloshing liquid on the heave response of the vehicle is significant for the cases considered.

5.11.1.2 R.M.S. pitch response for displacement and velocity

Nine vehicle-container configurations are chosen to present the r.m.s. displacement and velocity responses in Fig. (5.3a,b). It is seen that at small vehicle velocities, the response fluctuates rapidly. The fluctuation ceases around velocity of 15 to 20 m/sec. After this, the response increases and a peak is reached again in the velocity range of 20 to 40 m/sec. For displacement response there is gradual reduction in response after the peak (cases 1,2,3,7,9). In some other cases the response increases gradually (cases 4,5,6,8). For velocity response there is gradual reduction

Empty vehicle c.g. at (o,o)
for liquid in container:

	Length	Height	c.g.
1	a_1	h_1	(o , o)
2	,,	$\frac{h_1}{2}$	(o , $-\frac{h_1}{4}$)
3	,,	$\frac{h_1}{4}$	(o , $-\frac{3}{8}h_1$)

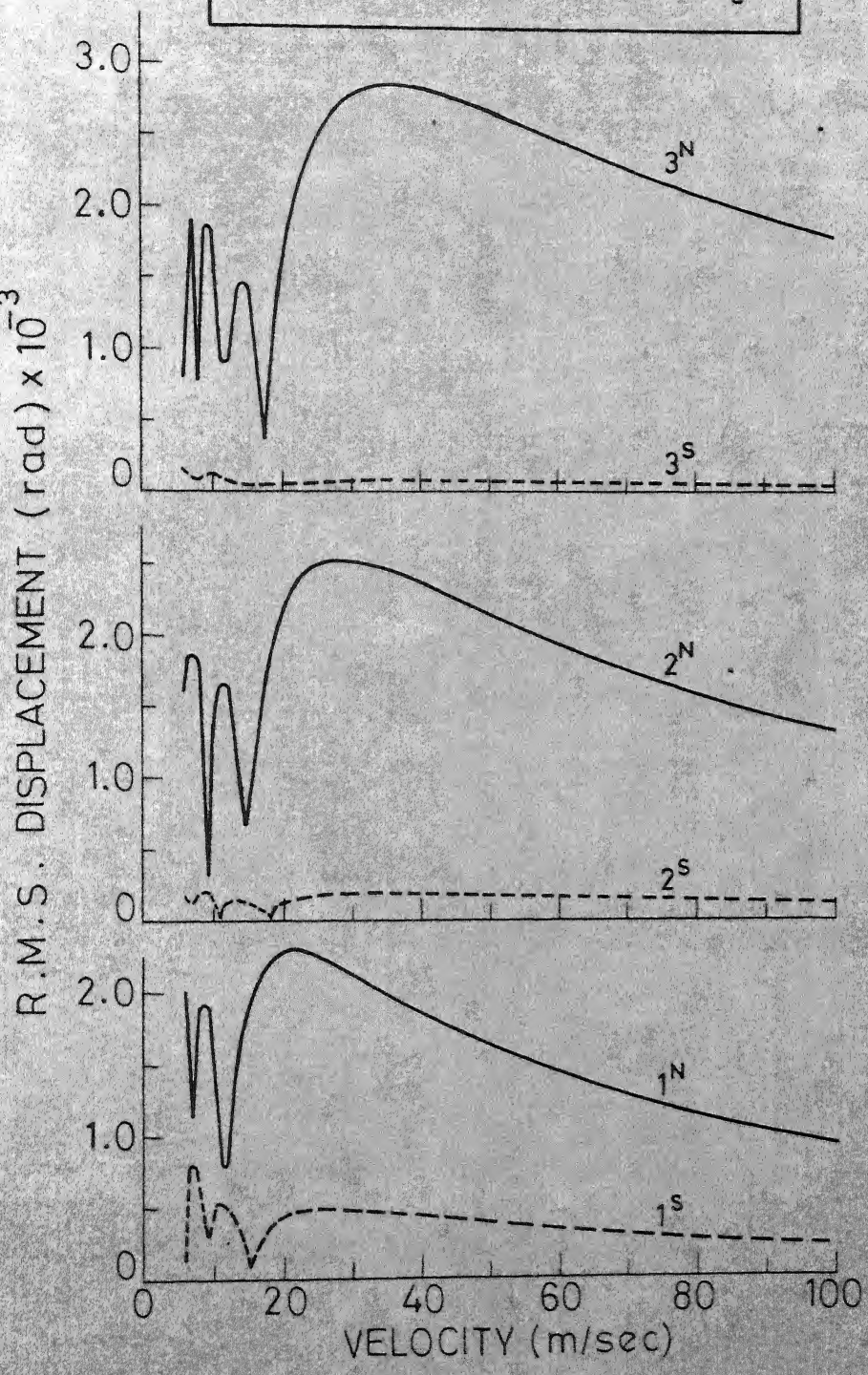

FIG. 5.3a R.M.S. PITCH RESPONSE FOR DISPLACEMENT AGAINST VEHICL VELOCITY.

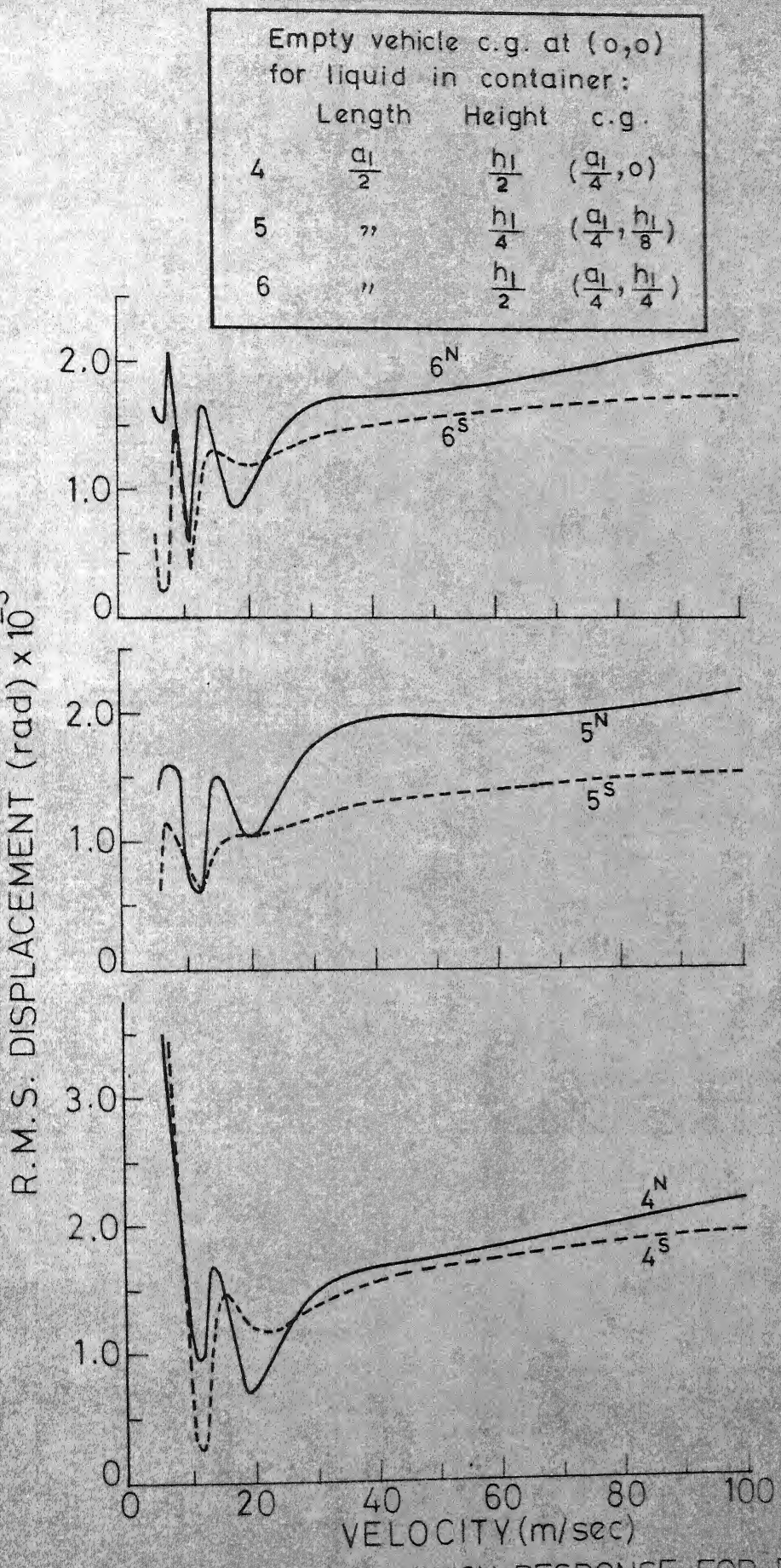

FIG.5.3a R.M.S. PITCH RESPONSE FOR DISPLACE--MENT AGAINST VEHICLE VELOCITY.

Empty vehicle c.g. at (o,o)
for liquid in container:

	Length	Height	c.g.
7	$\frac{a_1}{4}$	$\frac{h_1}{4}$	$(\frac{a_1}{4}, \frac{h_1}{8})$
8	"	$\frac{h_1}{2}$	$(\frac{a_1}{4}, \frac{h_1}{4})$
9	"	$\frac{h_1}{4}$	$(\frac{a_1}{4}, \frac{3}{8}h_1)$

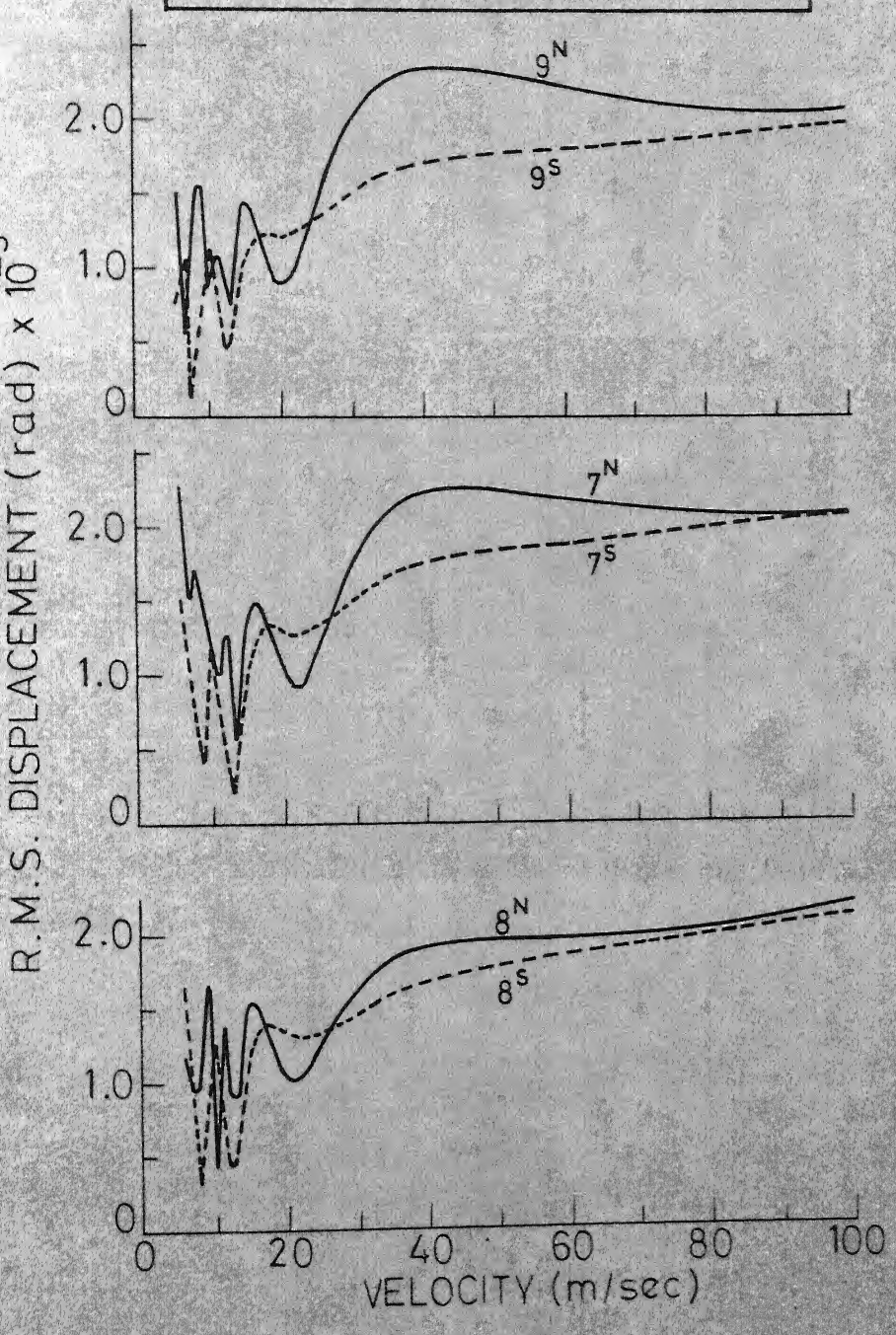

FIG. 5.3a R.M.S. PITCH RESPONSE FOR DISPLACEMENT AGAINST VEHICLE VELOCITY.

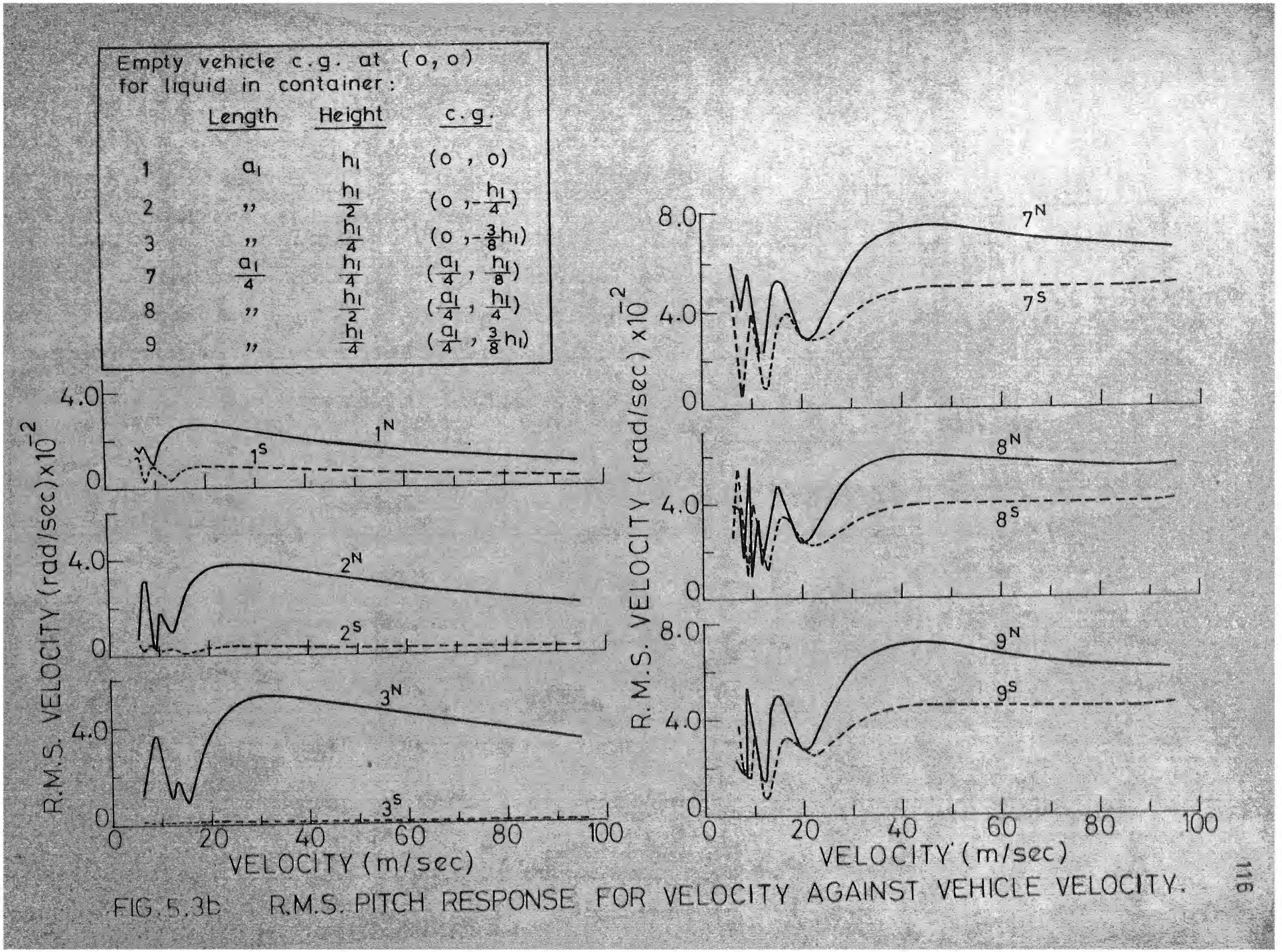

FIG. 5.3b R.M.S. PITCH RESPONSE FOR VELOCITY AGAINST VEHICLE VELOCITY.

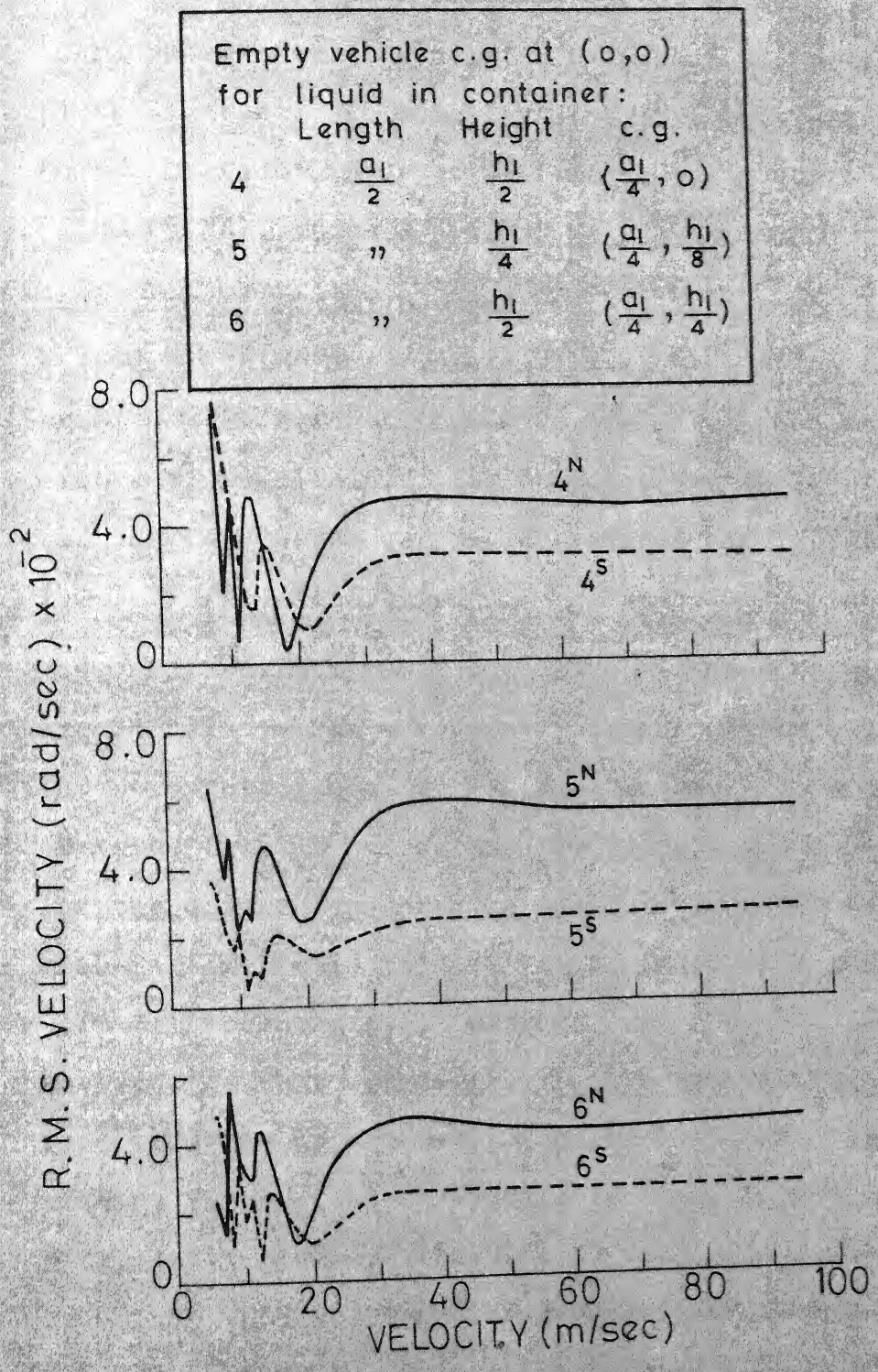

FIG. 5.3b R.M.S. PITCH RESPONSE FOR VELOCITY AGAINST VEHICLE VELOCITY.

in response after the peak which occurs in the range of 15 to 45 m/sec. In some cases, the velocity response tends to become independent of vehicle velocity quite early (Fig. (5.3b), cases 4,5,6,8).

For centrally mounted container, the equations of liquid sloshing and vehicle vibration in pitch mode are coupled. Sloshing brings down the pitch response by several orders of magnitude. With the decrease in liquid depth, the vehicle response in pitch reduces considerably (cases 1,2,3 of Fig. 5.3a,b).

For eccentrically mounted containers, the sloshing of liquid reduces the response over most of the velocities. For some velocities the response increases. But the range of velocities is narrow and towards lower end (cases 4 to 9). For the same mass of liquid and horizontal eccentricity, the sloshing of liquid reduces the response with increase in vertical eccentricity. Compare cases (4,6) and (7,9). It is expected that with increase in eccentricity, there is more of sloshing. Thus it implies that more the sloshing of liquid, larger is the reduction in vehicle response. For a typical vehicle velocity of 40 m/sec (144 km/hour), the reduction in displacement response is of the order of 6 to 33% and that of the velocity response is as much as 30 to 60% (cases 4 to 9).

5.11.1.3 R.M.S. free surface displacement response

Free surface displacement response statistics can be used to predict the spilling of contained liquid under random excitation. If the second order statistics of the response is known, the maximum response can be predicted.

The pendulum displacement represents the free surface displacement of the contained liquid. In Fig. (5.4a), the free surface response is presented. The non-dimensional parameter (radian· a/2h), represents the relative wave height at the free surface of the liquid (a = length of the container, h = depth of the liquid). The surface wave height decreases with velocity and approaches a constant value as the vehicle velocity increases. This is in conformity with the limits discussed in Sec. 5.7.2.

The surface wave height increases with decrease in liquid depth (cases 1,2,3; 5,6; 7,8). For eccentrically mounted container the relative surface wave height is much larger for same length and depth of the liquid (cases 4,6; 7,9). In general, the eccentrically mounted container offers more surface wave displacement than the centrally mounted container for most of the velocity range.

5.11.1.4 R.M.S. pendulum velocity response

The pendulum velocity represents the free surface velocity of the contained liquid. The response fluctuates

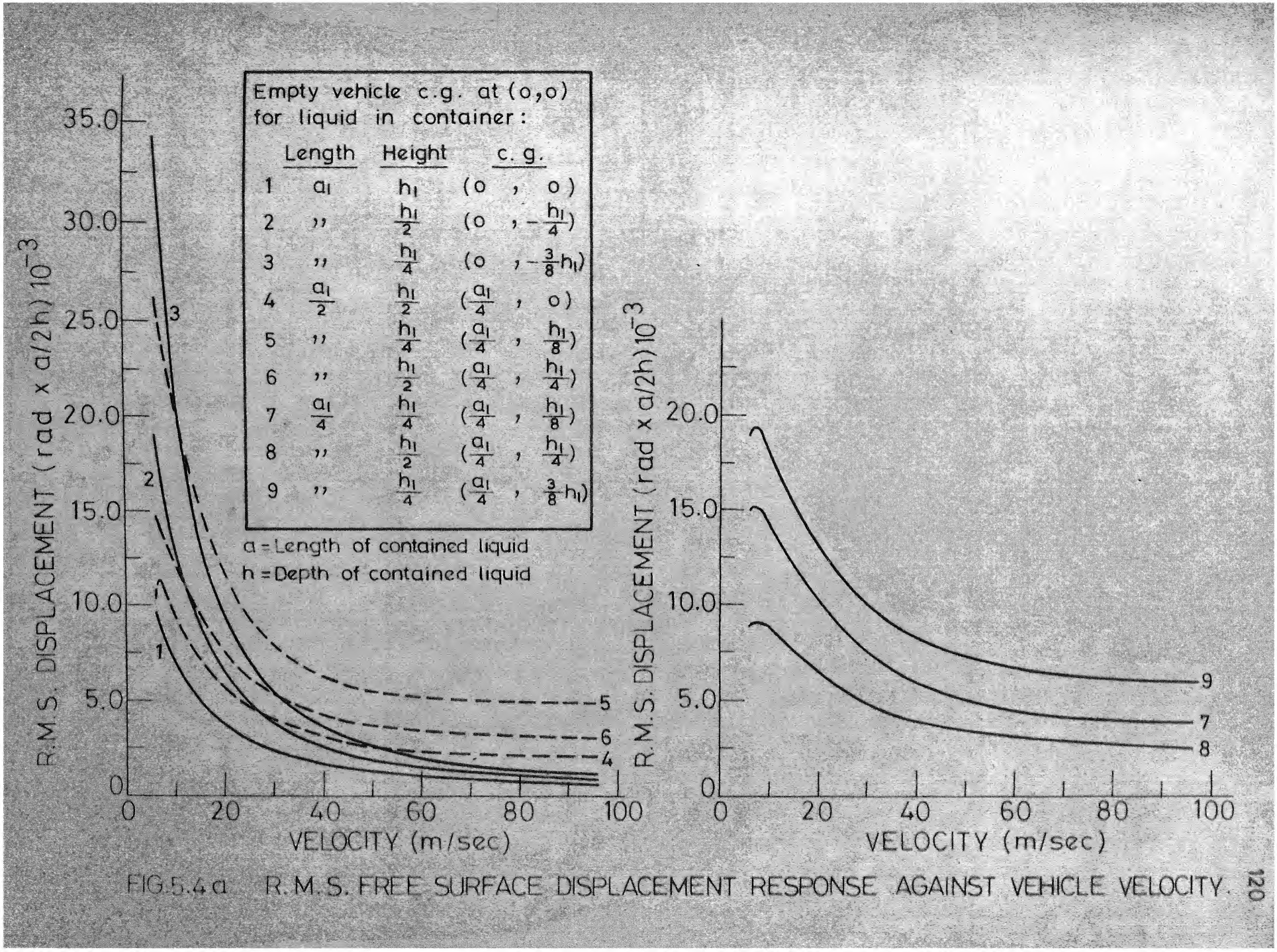

FIG.5.4a R.M.S. FREE SURFACE DISPLACEMENT RESPONSE AGAINST VEHICLE VELOCITY.

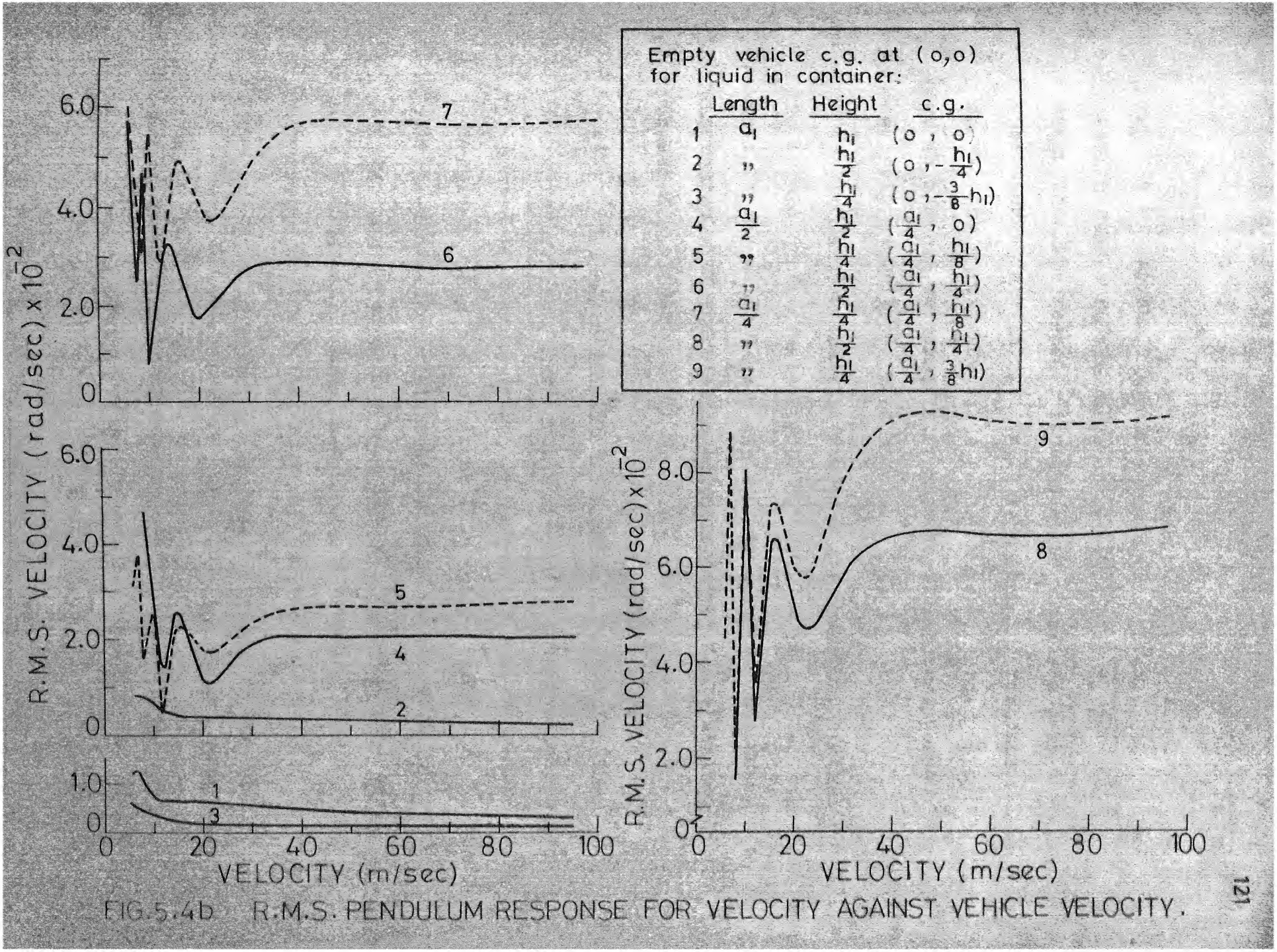

FIG.5.4b R.M.S. PENDULUM RESPONSE FOR VELOCITY AGAINST VEHICLE VELOCITY.

rapidly in the small velocity range (Fig. 5.4b). The fluctuation ceases in the range of velocities 10 to 25 m/sec. After this, the response increases and reaches a peak and then starts decreasing. It is seen that the response approaches a constant value rather early (approx. velocity of 45 m/sec.) as compared to the displacement response (approx. velocity of 80 m/sec.).

It is seen that the response decreases with decrease in liquid depth (cases 1,2,3; 5,6; 8,9). It is also seen that for same length and depth of liquid, the response increases with increase in eccentricity of the container (cases 4,6; 7,9).

5.11.1.5 R.M.S. shear force and bending moment response

The r.m.s. shear force and bending moment response are presented in Figs. 5.5 and 5.6 respectively. These are determined using the relations (5.67) and (5.68) for all the vehicle-container configurations. The total force exerted by the liquid is assumed to act on the vertical centre-line of the side wall. The shear force and bending moment are determined on the bottom edge of the side walls.

It is seen that the response is larger in the small velocities range and fluctuates rapidly. The fluctuations may continue up to a vehicle velocity of 25 m/sec. After this, the response increases to reach a peak and then starts

Empty vehicle c.g. at (o , o) for liquid in container	Length	Height	c.g.
1	a_l	h_l	(o , o)
2	,,	$\frac{h_l}{2}$	(o , $-\frac{h_l}{4}$)
3	,,	$\frac{h_l}{4}$	(o , $-\frac{3}{8}h_l$)
4	$\frac{a_l}{2}$	$\frac{h_l}{2}$	($\frac{a_l}{4}$, o)
5	,,	$\frac{h_l}{4}$	($\frac{a_l}{4}$, $\frac{h_l}{8}$)
6	,,	$\frac{h_l}{2}$	($\frac{a_l}{4}$, $\frac{h_l}{4}$)
7	$\frac{a_l}{4}$	$\frac{h_l}{4}$	($\frac{a_l}{4}$, $\frac{h_l}{8}$)
8	,,	$\frac{h_l}{2}$	($\frac{a_l}{4}$, $\frac{h_l}{4}$)
9	,,	$\frac{h_l}{4}$	($\frac{a_l}{4}$, $\frac{3}{8}h_l$)

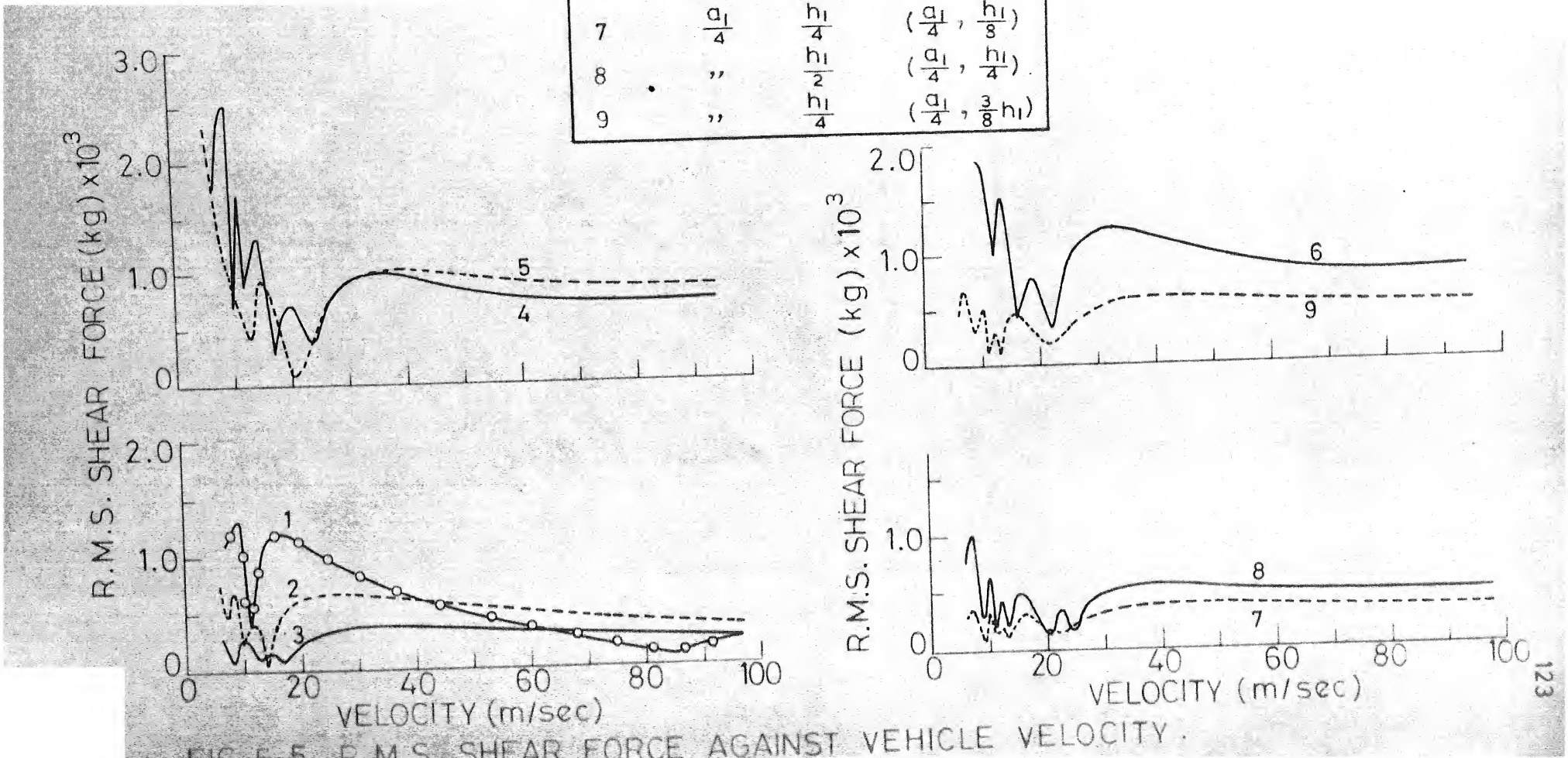

FIG. 5.5 R.M.S. SHEAR FORCE AGAINST VEHICLE VELOCITY.

Empty vehicle c.g. at (o , o)
for liquid in container :

	Length	Height	c. g.
1	a_l	h_l	(o , o)
2	"	$\frac{h_l}{2}$	(o , $-\frac{h_l}{4}$)
3	"	$\frac{h_l}{4}$	(o , $-\frac{3}{8}h_l$)
4	$\frac{a_l}{2}$	$\frac{h_l}{2}$	($\frac{a_l}{4}$, o)
5	"	$\frac{h_l}{4}$	($\frac{a_l}{4}$, $\frac{h_l}{8}$)
6	"	$\frac{h_l}{2}$	($\frac{a_l}{4}$, $\frac{h_l}{4}$)
7	$\frac{a_l}{4}$	$\frac{h_l}{4}$	($\frac{a_l}{4}$, $\frac{h_l}{8}$)
8	"	$\frac{h_l}{2}$	($\frac{a_l}{4}$, $\frac{h_l}{4}$)
9	"	$\frac{h_l}{4}$	($\frac{a_l}{4}$, $\frac{3}{8}h_l$)

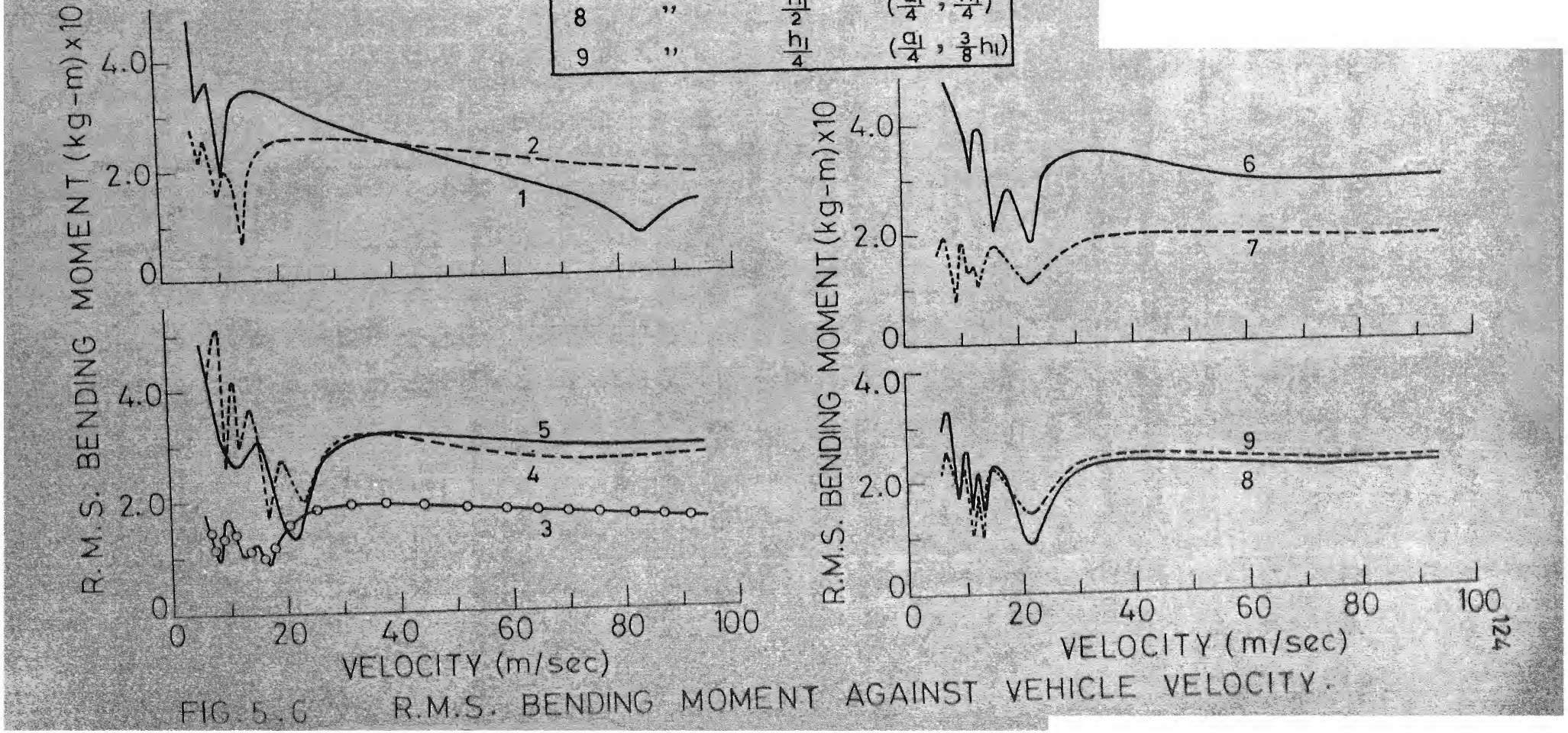

FIG. 5.6 R.M.S. BENDING MOMENT AGAINST VEHICLE VELOCITY.

decreasing. It is expected that the response will start increasing again (case 1). It is to be noted that at large velocity, the response tends to a large value in accordance with the limits discussed in Sec. 5.7.2.2(ii).

Table 5.1 gives the mechanical model parameters, hydrostatic and r.m.s. shear force and bending moment values for various depths of the liquid in the container. The hydrostatic values may be treated as the mean values. The coefficient of variation of dynamic forces can be defined as the ratio of the r.m.s. value to its mean value. Using the results of Figs. 5.5 and 5.6 the co-efficient of variation can be determined. In Table 5.1(iii), the co-efficient of variation for dynamic shear force and dynamic bending moment are given. A typical value corresponding to the peak-value observed in each of the nine cases is given in Table 5.1(iii). It is seen that the co-efficient of variation increases with decrease in liquid depth (cases 1,2,3; 4,5; 5,6; 7,8; 8,9). Similarly it increases with the increase in eccentricity (cases 4,6; 7,9). Although the co-efficient of variation increases with decrease in liquid depth, it is seen from Figs. 5.5 and 5.6 that the absolute value of the dynamic force increases with increase in liquid depth (cases 1,2,3; 5,6; 7,8). From Table 5.1(iii), it is seen that the co-efficient of variation for the shear force can be as large as 1.556 and for bending moment it can be 0.218.

The lowest value of the co-efficient of variation, corresponding to the centrally mounted and completely full container, is 0.113 for shear force and 0.004 for bending moment. If one assumes the maximum dynamic response as three times the standard deviation, the maximum dynamic bending moment (case 1, Table 5.1(iii)) is nearly 1.2% of the static bending moment. Similarly the maximum dynamic shear force will be nearly 34% of the static value for the same case. Thus the results indicate that the effect of liquid sloshing is not significant in the design of the container walls for strength. The dynamic effect of liquid sloshing may, however, be important from the point of view of fatigue.

5.11.2 Vehicle moving with constant acceleration

Vehicles generally accelerate and decelerate during starting and stopping respectively. For the dynamic analysis of the vehicle system under variable velocity run, equations of motion (5.4) to (5.6) are considered The parameters of vehicle and mechanical model considered are the same as for constant velocity case. The vehicle maintains constant acceleration and is assumed to achieve a velocity of 150 km/hour over a distance of 1 km from rest. The distance and velocity at any time, t, can be determined from Eqs. (4.8) and (4.9). The vehicle rolls over a railway track whose spectrum is given by Eq. (4.2). The track roughness provides vertical excitation to the vehicle system. Two sets of

equations of motion are considered for the study. The first set of equations (5.4) to (5.6) includes sloshing of liquid and the second set of equations (5.69) belongs to no-sloshing case.

5.11.2.1 Numerical solution of the equations of motion

Simulation

The two point input excitations, $y_1(t)$ and $y_2(t)$, are the road roughness at a distance, L, apart (L = base length of the vehicle). Using the power spectral density of railroad roughness, given by Eq. (4.2), the input excitations, $y_1(t)$ and $y_2(t)$, can be generated as discussed in Chapter 4.

Numerical integration and averaging

Equations of motion (5.4) to (5.6) and (5.59) are solved by Runge-Kutta algorithm for zero initial conditions. As the input excitation is random in nature ensemble average of sample functions are taken. 5 sample functions are considered for averaging. Further averaging is carried out over five consecutive readings of the sample response function.

Presentation of results

Three different vehicle-container configurations are chosen for the constant acceleration of the vehicle. As in constant velocity case, the results are presented for the sloshing and no-sloshing cases. These are distinguished with superscript 's' and 'N' respectively for sloshing and no-sloshing

cases. The three different configurations are numbered and tabulated in the various figures as in constant velocity case.

5.11.2.2 Displacement response

R.M.S. heave response

It is seen from Fig. 5.7, that the response with sloshing and without sloshing are almost identical. This implies that for centrally mounted container, the heave response remains virtually unaffected by the sloshing of the liquid. The response is a narrow band random process with the period same as the heave period of the vehicle (Table 5.1(ii)). The response is also compared with the vehicle having single base-point excitation described in Chapter 4. It is seen that the vehicle response with single-point base excitation is in general larger than the present case with two-point base excitations. This is in agreement with the results obtained in reference [53].

R.M.S. pitch response

For the same vehicle-container configurations, as for heave case, the results are presented in Fig. 5.8. The results are also compared with no-sloshing case. It is seen that, except for a very small period of time considered, the response without sloshing case is larger than with-sloshing case. The liquid depth has a considerable effect

Empty vehicle c.g. at (o,o)
for liquid in container

	Length	Height	c.g.	step length Δt
1	a_l	h_l	(o,o)	0.005 980
2	,,	$\frac{h_l}{2}$	$(o,-\frac{h_l}{4})$	0.003 332
3	,,	$\frac{h_l}{4}$	$(o,-\frac{3}{8}h_l)$	0.002 035

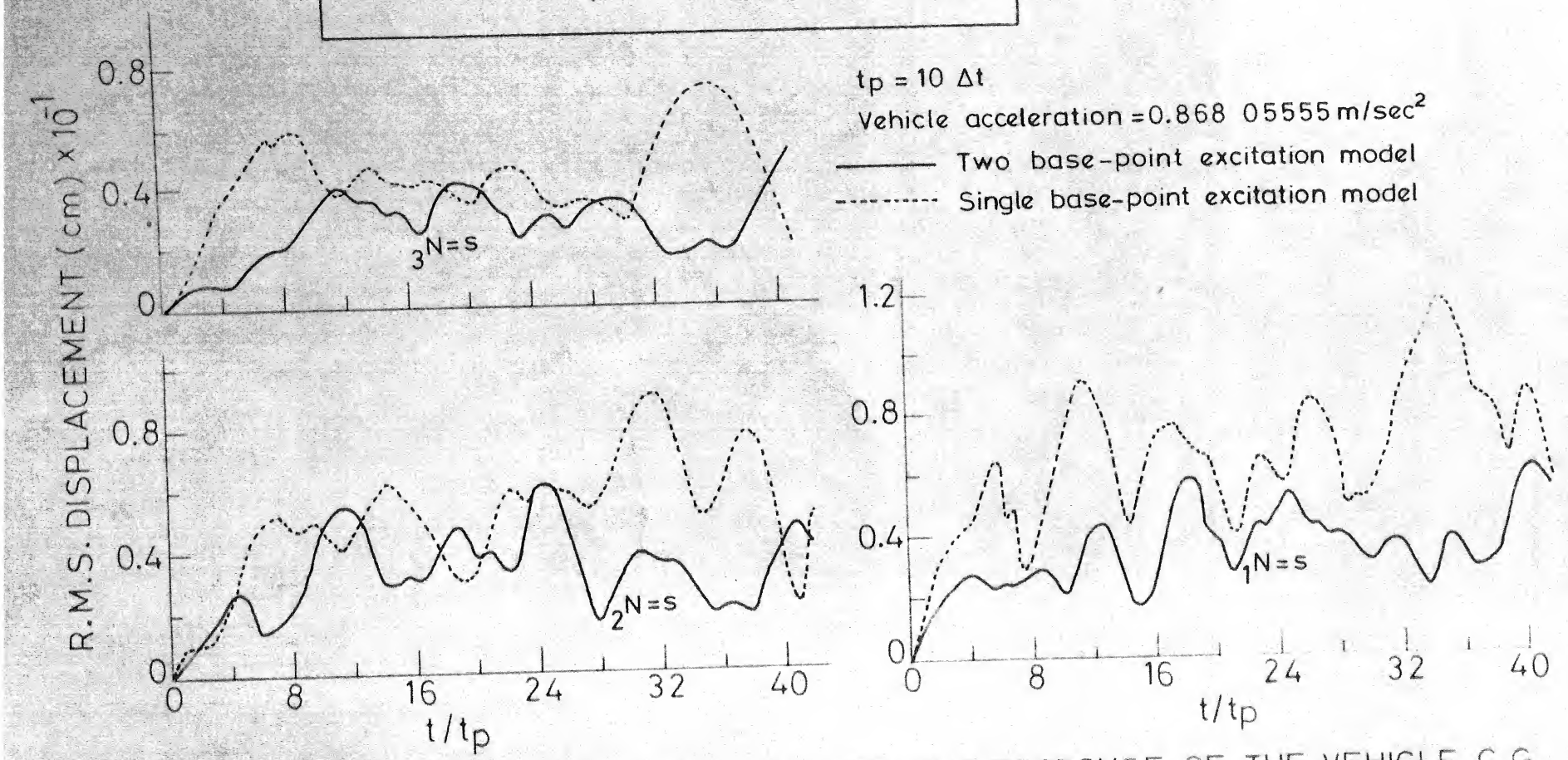

Fig 5.7 TIME Vs. R.M.S. HEAVE DISPLACEMENT RESPONSE OF THE VEHICLE C.G. MOVING WITH CONSTANT ACCELERATION.

Empty vehicle c.g. at (o , o)
for liquid in container :

	Length	Height	c.g.	Step length Δt
1	a_l	h_l	(o , o)	0.005 980
2	,,	$\frac{h_l}{2}$	$(o, -\frac{h_l}{4})$	0.003 332
3	,,	$\frac{h_l}{4}$	$(o, -\frac{3}{8}h_l)$	0.002 035

$t_p = 10\ \Delta t$

Vehicle acceleration = 0.86805555 m/sec^2

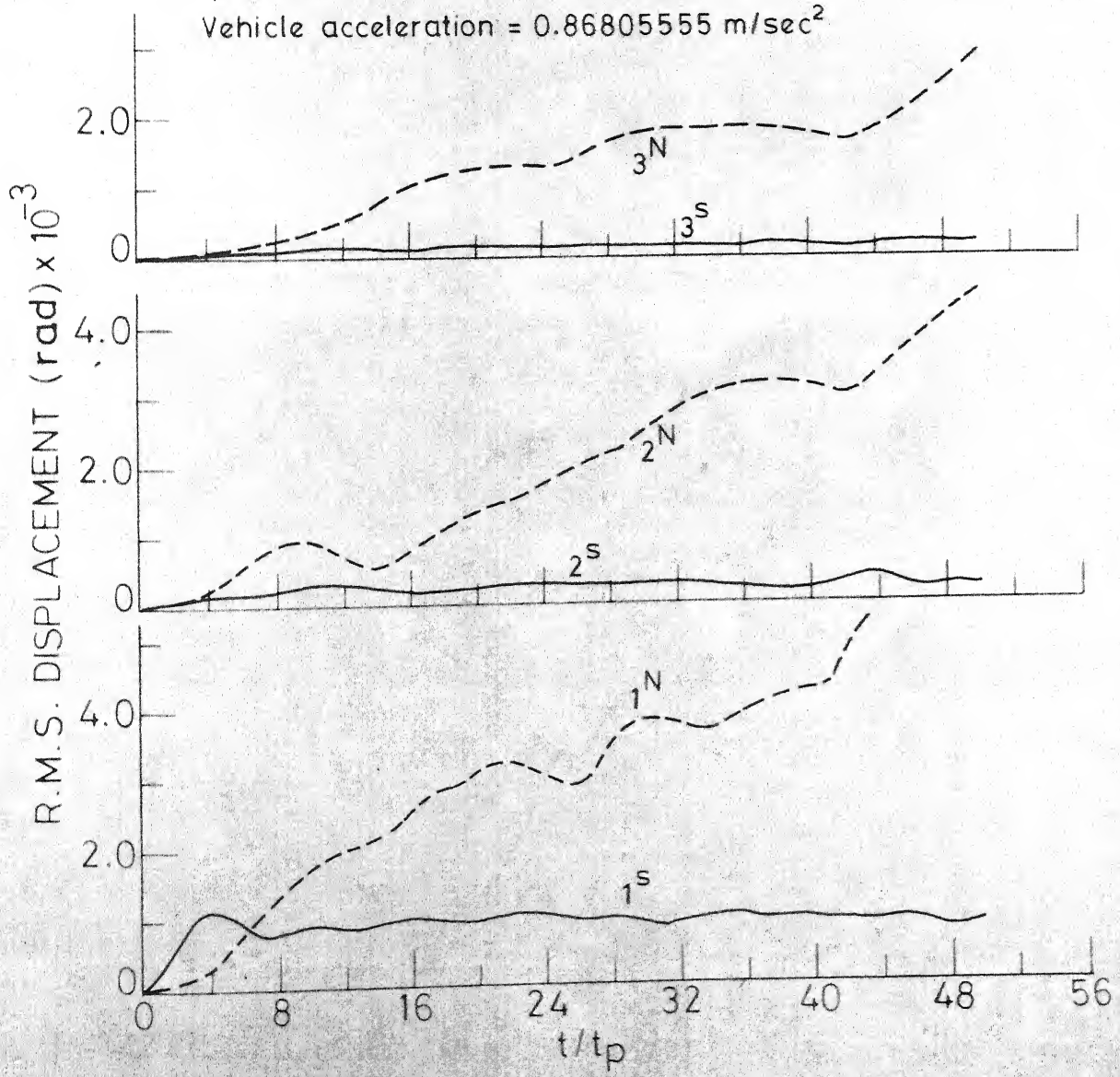

FIG.5.8 TIME Vs. R.M.S. PITCH DISPLACEMENT RESPONSE ABOUT THE C.G. OF THE VEHICLE.

Empty vehicle c.g. at (o , o)
for liquid in container :

	Length	Height	c.g.	Step length Δt
1	a_l	h_l	(o , o)	0.005 980
2	,,	$\frac{h_l}{2}$	$(o, -\frac{h_l}{4})$	0.003 332
3	,,	$\frac{h_l}{4}$	$(o, -\frac{3}{8}h_l)$	0.002 035

$t_p = 10\ \Delta t$

Vehicle acceleration = 0 86805555 m/sec^2

a = Length of contained liquid

h = Depth of contained liquid

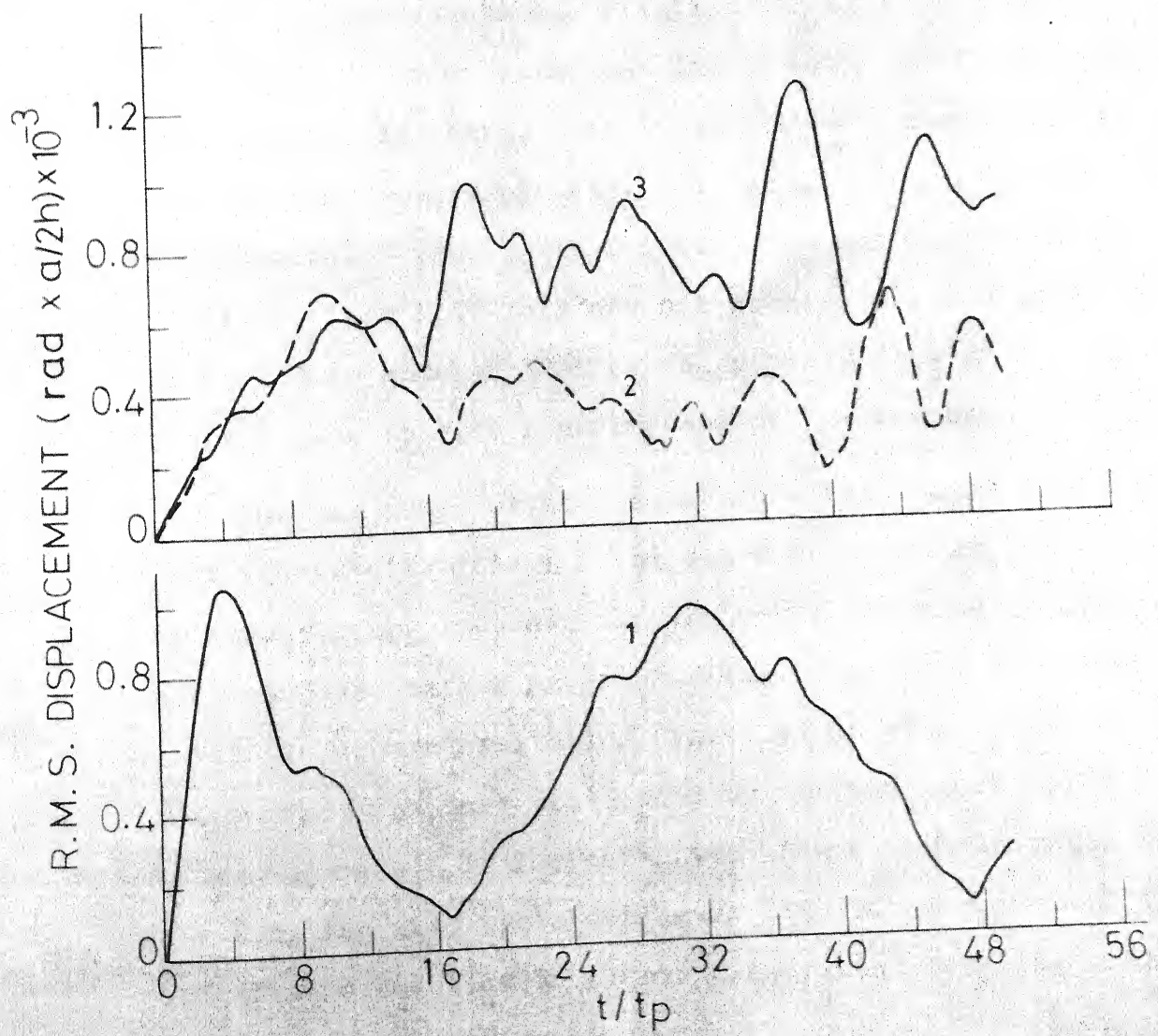

FIG. 5.9 TIME Vs. R.M.S. FREE SURFACE DISPLACE-MENT RESPONSE.

on the response statistics. Small liquid depth reduces the response by several orders. This is in accordance with the observations already made as in the constant velocity case.

R.M.S. free surface response

The results for this case are presented in Fig. 5.9. The pendulum displacement is the representative of the free surface displacement. The non-dimensional parameter (rad x a/2h) represents the relative liquid free surface displacement. It is seen that the liquid surface displacement reduces with the increase in liquid depth. The response is a narrow band random process. It has a same period as that of the pendulum (see Table 5.1(ii)) for the completely full container. For half-full and one-fourth full containers, the period is same as that of the pendulum but high frequency of excitation is also superimposed on the response.

One can compare the present case response, having two-point base excitations for the vehicle, with the corresponding free surface response for the vehicle having single point base excitation given in Fig. 4.4. It is seen that the single source excitation system of Chapter 4, keeps the free surface response unaffected by the randomness of the track roughness. It indicates that heave vehicle model has weak coupling with the sloshing of liquid. The present two-point base excitation model has significant coupling with the sloshing of liquid.

5.11.2.3 Acceleration response

R.M.S. heave response

In Fig. 5.10 the acceleration response, in non-dimensional form, is presented. The ordinate is the ratio of vertical acceleration to acceleration due to gravity. As expected, the vertical acceleration increases with decrease in liquid depth. The acceleration response is a narrow band random process and at the start has a impulsive nature. The response is same for sloshing and no-sloshing cases. It implies that coupling effect on heave response due to sloshing is negligible. Further the acceleration response is small (0.01 to 0.07 times the acceleration due to gravity) for the kind of vehicle under consideration.

R.M.S. pitch response

The acceleration response in pitch is shown in Fig. 5.11. As expected, the response reduces with increase in liquid depth and is a narrow band random process. For most of the time range covered, it is larger for no-sloshing case than the sloshing case. It is also seen that the difference between these cases increases with reduction in liquid depth. This is similar to the one observed for constant velocity case. Thus sloshing of liquid has an absorption effect.

R.M.S. pendulum response

The acceleration response characteristics of the pendulum represents the mean free surface acceleration of the contained

Empty vehicle c.g. at (o, o)
for liquid in container :

	Length	Height	c.g.	Step length Δt
1	a_l	h_l	(o, o)	0.061 298
2	,,	$\frac{h_l}{2}$	$(o, -\frac{h_l}{4})$	0.045 756
3	,,	$\frac{h_l}{4}$	$(o, -\frac{3}{8}h_l)$	0.036 450

$t_p = 10\ \Delta t$

Vehicle acceleration = 0.868 05555 m/sec^2

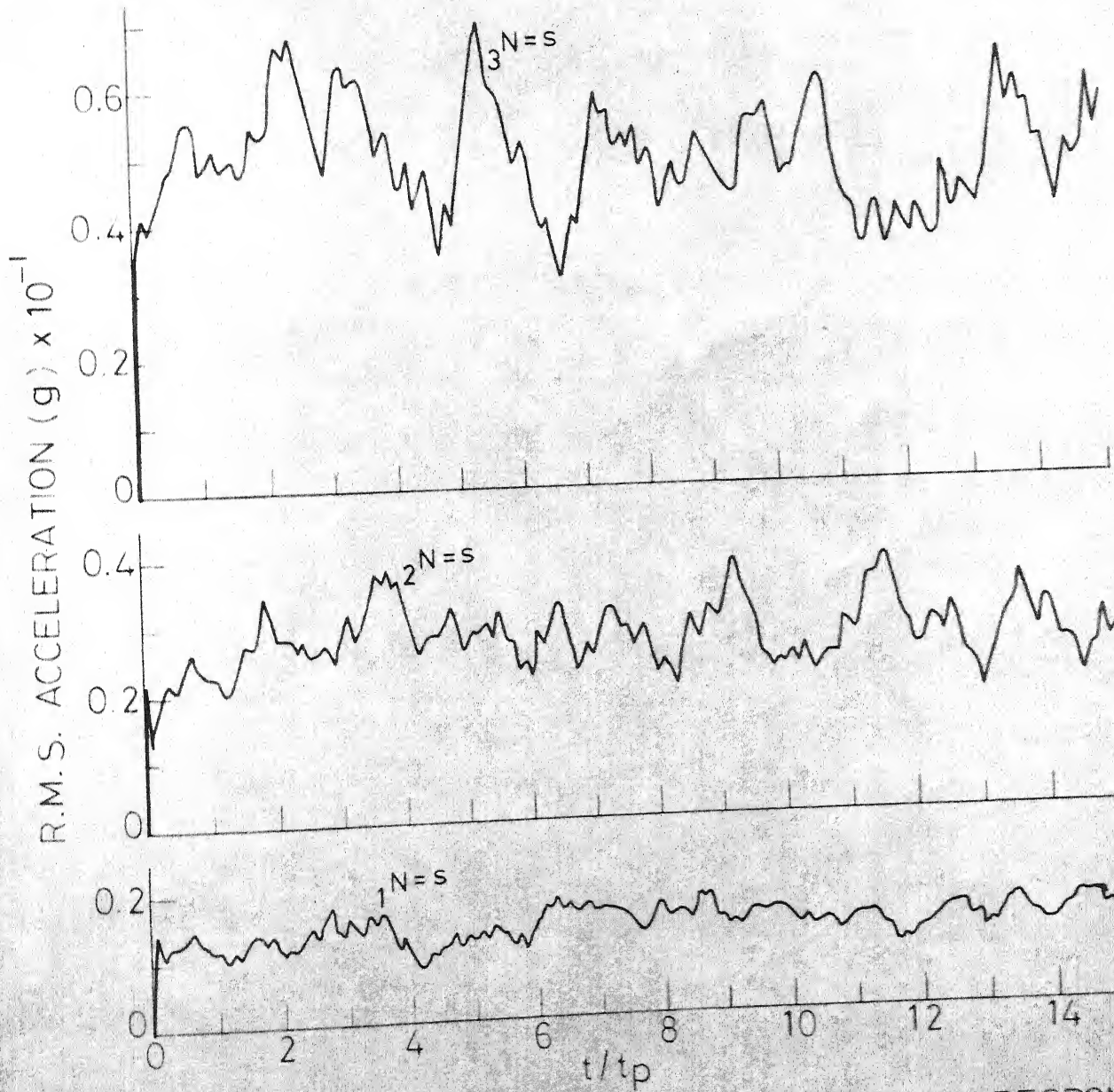

FIG. 5.10 TIME Vs R.M.S. HEAVE ACCELERATION RESPONSE OF THE VEHICLE C.G. MOVING WITH CONSTANT ACCELERATION.

Empty vehicle c.g. at (o, o)
for liquid in container:

	Length	Height	c.g.	Step length Δt
1	a_1	h_1	(o, o)	0.061 298
2	,,	$\frac{h_1}{2}$	$(o, -\frac{h_1}{4})$	0.045 756
3	,,	$\frac{h_1}{4}$	$(o, -\frac{3}{8}h_1)$	0.036 450

$t_p = 10\ \Delta t$

Vehicle acceleration = 0.868 05555 m/sec^2

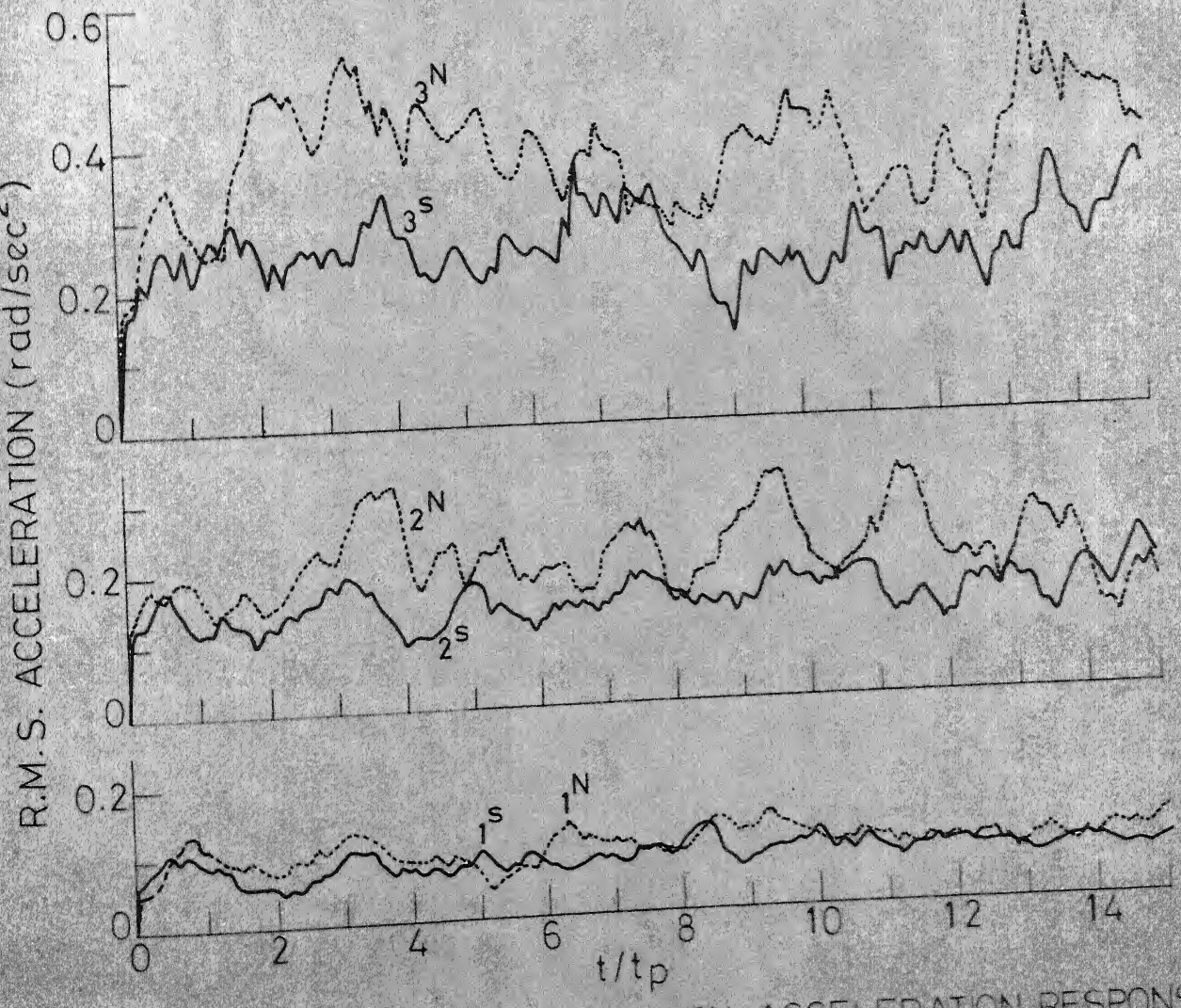

FIG. 5.11 TIME Vs. R.M.S. PITCH ACCELERATION RESPONSE ABOUT THE C.G. OF THE VEHICLE.

Empty vehicle c.g. at (o, o)
for liquid in container

	Length	Height	c. g.	Step length Δt
1	a_1	h_1	(o, o)	0.061 298
2	"	$\frac{h_1}{2}$	$(o, -\frac{h_1}{4})$	0.045 756
3	"	$\frac{h_1}{4}$	$(o, -\frac{3}{8}h_1)$	0.036 450

$t_p = 10\ \Delta t$

Vehicle acceleration = 0.868 05555 m/sec²

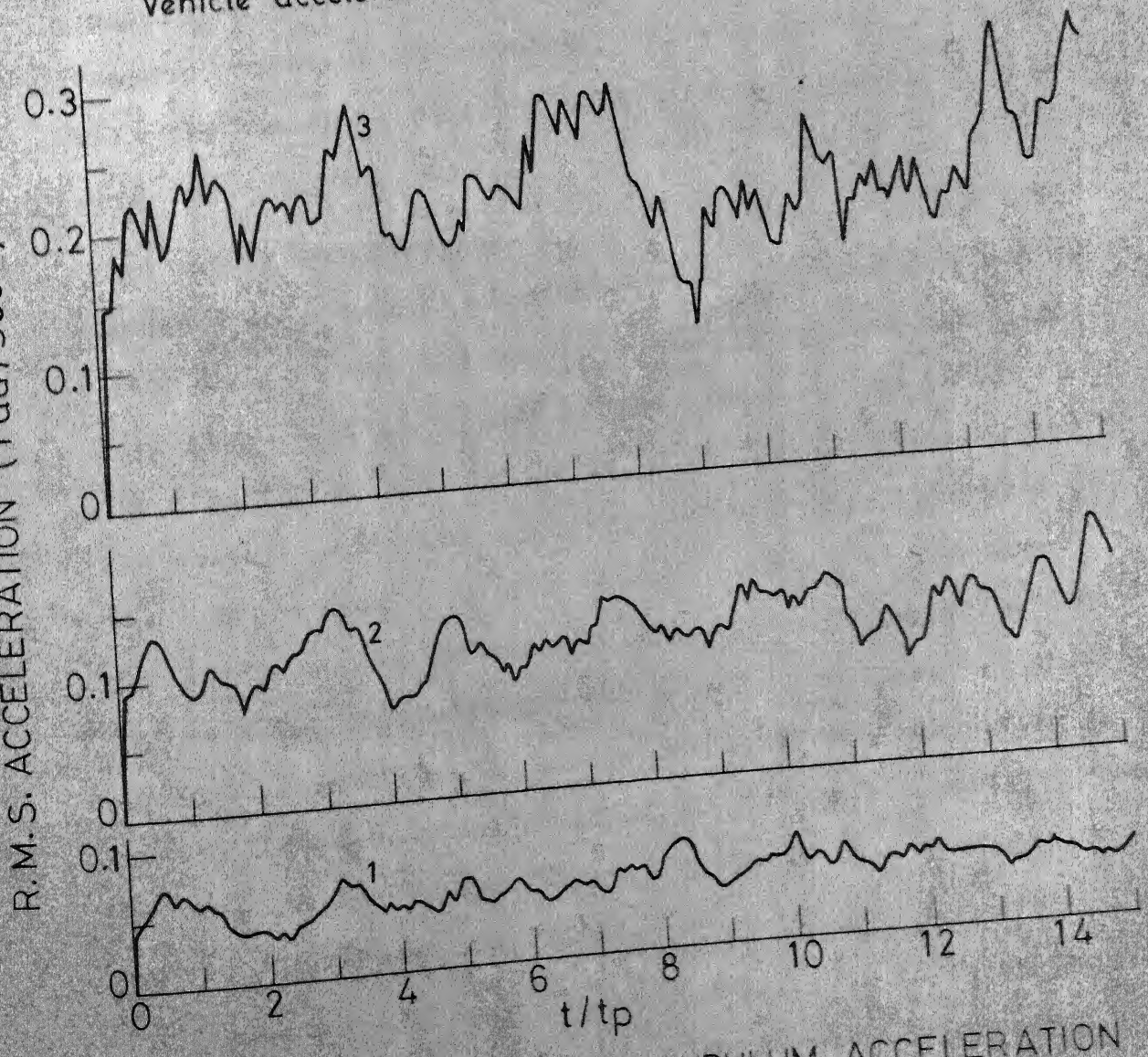

FIG. 5.12 TIME Vs. R.M.S. PENDULUM ACCELERATION RESPONSE.

liquid. It is seen that the acceleration of the pendulum increases with decrease in liquid depth. The relative increase in acceleration with decrease in liquid depth is almost of the same order.

5.12 Absorption Effect of the Sloshing Liquid

In Sec. (5.11.1) and (5.11.2) the response for constant velocity and acceleration of the vehicle are presented. The response in heave and pitch mode of the vehicle are compared with the two cases of sloshing liquid and equivalent solidified mass of the liquid.

It is observed that the sloshing of liquid has the tendency to reduce the response of vehicle in heave and pitch mode of the vehicle vis-a-vis the vehicle carrying equivalent solidified mass of the liquid. This implies that the sloshing of liquid acts as an absorbing mechanism for the vehicle. For the given input, the energy is shared by the vehicle mass in motion and the sloshing liquid mass. The energy to the sloshing liquid mass is transferred through the vehicle, thus reducing the vehicle response. In contrast to this phenomenon, the energy shared by the solidified mass of the liquid becomes the integral part of the energy shared by the vehicle system. Therefore the vehicle response reduces due to the sloshing of liquid.

The vehicle response reduces with the increase in sloshing of liquid. This is usually accompanied by reducing the

liquid depth. This observation is verified both for constant velocity case and constant acceleration case. It is known that the vibration absorption becomes more effective with a reduced ratio of the natural frequency to the exciting frequency [52]. A container mounted on a vehicle is subjected to narrow band vehicle excitation, as discussed in Sections 5.11.2.3 and also in 4.5.4, with the central frequency corresponding to the natural frequency of the vehicle. In table 5.1(ii), the natural periods of vibration, for the vehicle with solidified mass of the liquid in centrally mounted container, are given for heave and pitch modes. It is seen from Table 5.1 (see also Table 4.1) that the ratio of natural frequency of liquid sloshing to that of vehicle natural frequency reduces with decrease in liquid depth. This ratio, for liquid depths h_1 (=2.675 meter) to $h_1/4$; varies from 0.171 to 0.0584 for pitch mode and 0.174 to 0.0573 for heave mode of the vehicle. Thus sloshing of liquid is found to be an effective method of vibration absorption for the particular vehicle considered in the velocity range of interest.

Table 5.1

Parameters of Mechanical Model, Vehicle Natural Period, Shear Force and Bending Moment

Container dimensions (a_1 x b x h_1) = (7.89x2.946x2.675) meters

(i) Mechanical Model Parameters

Location of mechanical masses (e_4 and e_5) is measured from liquid c.g. as positive upwards.

Case	Length	Liquid height	Pendulum			Fixed mass		
			Mass m_v (Kg)	Rod length (meter)	Pivot location e_4 (meter)	Location e_5 (meter)	mass m_{ov} (kg)	Moment of inertia I_{ov} (kg-m^2)
1	a_1	h_1	3799.02	3.19	2.078	1.661	2539.16	12059.05
2	"	$h_1/2$	2350.63	5.15	4.515	1.832	818.46	10766.92
3	"	$h_1/4$	1254.86	9.65	9.323	1.258	329.68	6954.80
4	$a_1/2$	$h_1/2$	949.75	1.59	1.039	0.830	634.79	753.69
5	"	$h_1/4$	587.65	2.57	2.257	0.916	204.61	672.93
6	"	$h_1/2$	949.75	1.59	1.039	0.830	634.79	753.69
7	$a_1/4$	$h_1/4$	237.43	0.80	0.520	0.415	158.69	47.10
8	"	$h_1/2$	293.07	0.64	0.325	0.188	499.20	48.58
9	"	$h_1/4$	237.43	0.80	0.520	0.415	158.69	47.10

Table 5.1 (...Contd.)

(ii) Natural period and hydrostatic forces

Hydrostatic shear force (H.S.F.) = $\rho g h^2 / 2$

Hydrostatic bending moment (H.B.M.)= $\rho g h^3 / 6$

Case	Container Length (meter)	Liquid depth (meter)	Natural period in secs. Pendulum	Vehicle Heave	Vehicle Pitch	H.S.F. (kg)	H.B.M. (kg-meter)
1	a_1	h_1	3.582	0.624	0.613	10540.23	9398.37
2	"	$h_1/2$	4.554	0.464	0.457	2635.06	1174.78
3	"	$h_1/4$	6.232	0.357	0.364	658.76	146.85

(iii) R.M.S. Shear force and bending moment

Case	Liquid depth (m)	R.M.S. shear Force (=RMS S.F.) Velocity (m/sec)	$(\frac{\text{RMS S.F.}}{\text{H.S.F.}})$	R.M.S. Bending moment (=RMS B.M.) Velocity (m/sec)	$(\frac{\text{RMS B.M.}}{\text{H.B.M.}})$
1	h_1	17	0.113	16	0.004
2	$h_1/2$	26	0.253	26	0.022
3	$h_1/4$	34	0.547	34	0.129
4	$h_1/2$	34	0.380	36	0.027
5	$h_1/4$	40	1.556	38	0.218
6	$h_1/2$	32	0.470	32	0.030
7	$h_1/4$	44	0.592	44	0.135
8	$h_1/2$	40	0.214	40	0.020
9	$h_1/4$	42	0.936	42	0.169

CHAPTER 6

SUMMARY OF RESULTS AND CONCLUSIONS

In the preceding chapters the results of the investigations of the following problems in the sloshing of liquid in moving containers have been presented:

(i) The stability of the plane free surface of liquid in a rectangular container with flexible bottom, under periodic vertical excitation;

(ii) development of a mechanical model for liquid sloshing in a rectangular container under the simultaneous action of vertical excitation and horizontal motion, and

(iii) study of the dynamics of a vehicle carrying liquid as cargo and comparison of the results with a vehicle carrying an equivalent solidified mass of the liquid under identical random track induced excitation.

The results have been discussed in detail in each chapter. In the sequel some of the important results, conclusions and recommendations for further investigation are presented.

(1) The stability of the plane free surface of liquid in a rectangular container with flexible bottom under vertical harmonic excitation has been investigated. Stability boundaries have been established and compared with that of container with rigid bottom. Since a container mounted on a vehicle is subjected to narrow band vehicle excitation with the central frequency corresponding to heave degree of freedom, the results of the stability analysis can be used as a guide for the behavior of liquid in vehicle mounted containers. The work presented in the thesis may be extended to include the flexibility of the side walls and consider narrow band random excitation.

(2) The sloshing of incompressible and inviscid liquid in a rigid rectangular container, under simultaneous action of constant horizontal acceleration and vertical periodic acceleration, can be represented through its equivalent mechanical model. The model consists of a fixed mass and infinite number of oscillating pendulum masses. The parameters of the mechanical model are independent of the excitation characteristics. The fixed mass location of the mechanical model can be decided on the assumption that the mechanical model c.g. is the same as that of the liquid. This is assumed in the present analysis. The model is valid for small displacement and stable free surface conditions of the containing liquid. It is capable of incorporating important

modal characteristics of the oscillating free surface of the containing liquid and, forces and moments exerted by the sloshing liquid on container walls.

(3) The vehicle unevenness of the track is treated as a homogenous random process. For an analytical treatment of vehicle response, it is convenient to represent the power spectral density of the vertical unevenness of the track by the following expression:

$$\Phi_{YY}(f) = \frac{C}{\gamma^2+f^2}, \text{ one sided p.s.d., } ft^2/(cycle/ft);$$

where C and γ are constants. It is shown that the above expression fits the measured p.s.d. closely.

The equations of motion of the vehicle-container system, with liquid replaced by an equivalent mechanical elements are non-linear. The vehicle response is studied in two ways under constant acceleration motion. In the first the vehicle is assumed to respond under heave mode and, in the second it is assumed to respond under heave and pitch modes. In the heave mode alone, the vehicle is exposed to single point base excitation and in the second it is exposed to two-point base excitations. The response of the equations of motion is determined numerically using the simulated track unevenness. In case where acceleration is not constant, it can be approximated by segments of constant acceleration to determine the response.

It is found that the effect of liquid sloshing on the vehicle response is negligible for the heave model. The response characteristics of the vehicle model with heave and pitch degrees of freedom are, however, significantly affected by the liquid sloshing. The sloshing of liquid reduces the vehicle response due to absorber effect. The free surface response in heave model remains unaffected by the randomness of the track unevenness whereas in the heave-pitch model, the free surface response has random characteristics.

(4) The vehicle response with heave model is found to be larger than the heave-pitch model. The heave model has single point base excitation and the heave-pitch model has two-point base excitations.

(5) The coupled vehicle-liquid sloshing behaviour is investigated for a vehicle model with heave and pitch degrees of freedom under constant velocity and acceleration over a railway track. Nine different configurations of the container location and liquid depth are considered. The liquid is replaced by an equivalent mechanical model. The governing equations of motion of vehicle-container system contain non-linearities in inertia, damping and stiffness terms. The equations are linearized using the stochastic linearization technique. The response statistics are determined after transforming the equations to space co-ordinate. With space co-ordinate as independent variable, the input process

is homogeneous and a unified treatment is possible for determining the response statistics both for a vehicle moving with constant velocity and constant acceleration.

Some of the important results obtained from the investigation of the response of a railway wagon carrying liquid as cargo are:

(i) Sloshing has a significant effect on vehicle dynamics for eccentrically located containers;

(ii) the liquid acts as a vibration absorber at velocities more than 40 m/sec. The vehicle response is reduced due to transfer of energy from vehicle to liquid as in the case of two degrees of freedom system. The absorber effect is more pronounced in pitch-degree of freedom. In some cases, for velocities less than 40 m/sec, liquid sloshing increases the response; and

(iii) the relative wave height at the free surface increases with decrease in liquid depth and with increase in eccentricity of the container c.g. w.r.t. vehicle c.g.

The liquid sloshing is found to reduce the vehicle response under certain conditions. Hence it may be effectively used as a means of vibration absorption to improve the riding quality of vehicles.

(6) It is found that the effect of liquid sloshing is not significant in the design of the container walls for strength.

The dynamic effect of liquid sloshing may, however, be important from the point of view of fatigue.

(7) For the design of the wagon under-carriage, the effect of liquid sloshing on vehicle dynamics may be neglected. For the specific case considered, the model with no-sloshing gives conservative results at high velocities.

(8) The model of the railway wagon considered in the study includes only heave and pitch degrees of freedom. The actual wagon has all the six degrees of freedom and is subjected to track induced excitation at each wheel due to vertical and lateral irregularities. A more realistic analysis must take into account other degrees of freedom of the wagon, particularly lateral and rolling, and lateral track irregularities also. Such an investigation will require a more general equivalent mechanical model for liquid sloshing. The investigation should be extended to cover the effect of various parameters, such as the stiffness and damping of vehicle suspension, on the vehicle dynamics.

REFERENCES

1. Abramson, H.N. (ed), 'The Dynamic Behavior of Liquids in Moving Containers', NASA SP-106 (1966).

2. Abramson, H.N., 'The Dynamic Behavior of Liquids in Moving Containers', App. Mechanics Review, 16(7), 501-506 (1963).

3. Aslam, M., Godden, W.G., Scalise, D.T., 'Earthquake Sloshing in Annular and Cylindrical Tanks', J. Engg. Mech. Div., EM3, 105, 371-389 (June 1979).

4. Atalik, T.S. and Utku, S., 'Stochastic Linearization of Multi-Degree-of-Freedom Systems', Earthquake Engineering and Structural Dynamics, 4, 411-420 (1976).

5. Basu, S., 'Power Spectrum Algorithm', Private Communication, Dept. of Civil Engg., Univ. of Roorkee, Roorkee, India.

6. Bäth, M., 'Spectral Analysis in Geophysics', Elsevier Scientific Publishing Company (1974).

7. Bauer, H.F., Hsu, T.M., Wang, J.T.S., 'Liquid Sloshing in Elastic Containers', NASA CR-882 (1967).

8. Benjamin, T.B. and Ursell, F., 'The Stability of the Plane Free Surface of a Liquid in Vertical Periodic Motion', Proc. Roy. Soc. London, Series A, 225, 505-515 (1954).

9. Bentley, P.G. and Firth, D., 'Acoustically Excited Vibrations in a Liquid Filled Cyclindrical Tank', Jour. Sound and Vibration, 19(2), 179-191 (1971).

10. Berry, J.G. and Reissner, E., 'The Effect of an Internal Fluid Column on the Breathing Vibrations of a Thin Pressurized Cylindrical Shell', J. Aero. Sci., 25, 288-294 (1958).

11. Bhuta, P.G., and Yeh, G.C.K., 'Liquid Sloshing due to a Time-Dependent Discontinuous Boundary', International Jr. of Mech. Scie., 7(7), 475-488 (1965).

12. Bleich, H.H., 'Longitudinal Forced Vibrations of Cylindrical Fuel Tanks', Jet Propulsion 26(2), 109-111 (1956).

13. Bolotin, V.V., 'The Dynamic Stability of Elastic Systems', San-Francisco, Holden-Day Inc. (1964).

14. Caughey, T.K., 'Equivalent Linearization Techniques', Journal of Acou. Soc. of America, 35(11), 1706-1711 (1963).

15. Chakrabarti, P. and Chopra, A.K., 'Earthquake Analysis of Gravity Dams Including Hydrodynamic Interaction', Earthquake Engg. and Structural Dynamics, 2, 143-160 (1973).

16. Cole, H.A., Jr., 'On the Fundamental Lamping Law for Fuel Sloshing', NASA TRD-3240 (1966).

17. Cooper, R.M., 'The Dynamics of Liquids in Moving Containers', A.R.S. Jour., 30, 725-729 (1960).

18. Dahlberg, T., 'Ride Comfort and Road Holding of a 2-DOF Vehicle Travelling on a Randomly Profiled Road', J. Sound and Vibration, 58(2), 179-187 (1978).

19. Dodds, C.J. and Robson, J.D., 'The Description of Road Surface Roughness', J. Sound and Vibration, 31(2), 175-183 (1973).

20. Foss, K., 'Co-ordinates which Uncouple the Equations of Motion of Damped Linear System', J. App. Mech. 25, 361-364 (1955).

21. Garivaltis, D.S., Garg, V.K., D'Souza, A.F., 'Dynamic Response of a Six-Axle Locomotive to Random Track Inputs', Dynamic Research Division, Association of American Railroads, Chicago, Illinois (1977).

22. Graham, E.W., and Rodrigue, A.M., 'The Characteristics of Fuel Motion which Affect Airplane Dynamics', J. App. Mech., 19, 381-388 (1952).

23. Houbolt, J.C., 'Runway Roughness Studies in Aeronautical Field', J. Air Transport Division, Am. Soc. Civil Engr., 87, 11-31 (1961).

24. Housner, G.W., 'Dynamic Pressures on Accelerated Fluid Containers', Bull. Seismo. Soc. Ame., 57, 15-35 (1955).

25. Hurty, W.C. and Rubinstein, M.F., 'Dynamics of Structures', Prentice Hall of India (1967).

26. Iwan, W.D. and Yang, I., 'Application of Statistical Linearization Technique to Non-linear Multi-Degree-of-Freedom System', J. App. Mech. 39, 545-550 (1972).

27. Jenkins, G.M. and Watts, D.G., 'Spectral Analysis and its Applications', Holden-Day (1968).

28. Kirk, C.L., 'The Random Heave-Pitch Response of Aircraft to Runway Roughness', Aeronautical Jour. of R.A.S., 75, 476-483 (1971).

29. Koelle, H.H. (ed.), 'Handbook of Astronautical Engineering', McGraw Hill (1961).

30. Kreyszig, E., 'Advanced Engineering Mathematics', Wiley Eastern Pvt. Ltd., Second ed., (1967).

31. Lamb, H.G., 'Hydrodynamics', Sixth ed., Dover Pub., New York (1945).

32. Lin, Y.K., 'Probabilistic Theory of Structural Dynamics', McGraw Hill (1967).

33. Mark, A., 'Transient Eigenfrequencies in Liquid-Filled Containers', AIAA Jour., 13(2), 217-219 (1975).

34. Meirovitch, L., 'Analytical Methods in Vibrations', Macmillan Company, New York (1967).

35. Miles, J.W., 'On the Sloshing of Liquid in a Flexible Tank', J. App. Mech., 25, 277-283 (1958).

36. NASA Space Vehicle Design Criteria (Structures), 'Propellant Slosh Loads', NASA SP-8009 (1968).

37. Papoulis, A., 'Probability, Random Variables, and Stochastic Processes', McGraw Hill (1965).

38. Perumalswami, P.R. and Kar, L., 'Earthquake Hydrodynamic Forces on Arch Dams', Jr. EMD, Proc. ASCE, EM5, 99, 965-977 (1973).

39. Priestley, B.M., 'Evolutionary Spectra and Non-stationary Processes', J. Royal Statistical Soc., B27, 204-237 (1965).

40. Pritsker, A.A.B., 'Compilation of Definitions of Simulation', SCS Simulation, 33, 61-63 (Aug. 1979).

41. Rayleigh, Lord, 'On Waves', Phil. Mag. Series 5, 1, 257-279 (1876).

42. R.D.S.O., Lucknow, 'Research and Development into the Design of a 20T Axle-Load BG Covered Four Wheeled Wagon', Mech. Engg. Report M-264, R.D.S.O. Lucknow, Govt. of India, Ministry of Railways (April 1971).

43. Saleme, E. and Liber, T., 'Breathing Vibrations of Pressurized, Partially Filled Tanks', AIAA Jour., 3, 132-136 (1965).

44. Shinozuka, M., 'Monte-Carlo Solution of Structural Dynamics', Tech. Rep. No. 19, Dept. of Civil Engg. and Engg. Mechanics, Columbia University (1972).

45. Shinozuka, M. and Jan, C.M., 'Digital Simulation of Random Processes and its Applications', Jour. Sound and Vibration, 25(1), 111-128 (1972).

46. Sobczyk, K., Macvean, D.B. and Robson, J.D., 'Response of Profile-Imposed Excitation with Randomly Traversal Velocity', J. Sound and Vibration, 52(1), 37-49 (1977).

47. Stoker, J.J., 'Water Waves', Interscience Publishers Inc., New York, (1957).

48. Virchis, V.J. and Robson, J.D., 'Response of an Accelerating Vehicle to Random Road Undulation', J. Sound and Vibration, 18(3), 423-527 (1971).

49. Werner, P.W. and Sundquist, K.J., 'On Hydrodynamic Earthquake Effects', Trans. Amer. Geophysical Union, 30, 636-657 (1949).

50. Westergard, H.M., 'Water Pressures on Dams During Earthquakes', Trans. Am. Soc. Civil Engineers, 98, 418-433 (1933).

51. Yadav, D., 'Response of Moving Vehicles to Ground Induced Excitation', Ph.D. Thesis submitted to I.I.T. Kanpur (India), Dept. of Aeronautical Engineering (1976).

52. Bykhovsky, I.I., 'Fundamentals of Vibration Engineering', Mir Publishers, Moscow, pp 343-48 (1972).

53. Goyal, S.K., 'Response of Aircraft to Ground Environment', M.Tech. Thesis submitted to the Dept. of Aeronautical Engg., I.I.T. Kanpur, May 1973.

APPENDIX A

SOME PROPERTIES OF MATHIEU-HILL EQUATION

Following Mathieu-Hill equation is considered to study the stability characteristics.

$$\frac{d^2y}{dt^2} + \Omega_o^2 [1 - 2\varepsilon f(t)]y = 0, \qquad \text{(A-2.1)}$$

where f(t) is a periodic function with a period

$$T = \frac{2\pi}{\omega} .$$

Since f(T+t) = f(t), equation (A-2.1) does not change its form on addition of the period T to t. This implies that if y(t) is the solution then y(t+T) is also the solution of (A-2.1).

Equation (A-2.1) is of second order and is linear in y. Hence if $y_1(t)$ and $y_2(t)$ are two independent solutions of (A-2.1) then $y_1(t+T)$ and $y_2(t+T)$ are also its solutions. These last two solutions can be expressed in the linear combinations of $y_1(t)$ and $y_2(t)$ as follows.

$$y_1(t+T) = a_{11}\, y_1(t) + a_{12}\, y_2(t), \qquad \text{(A-2.2.1)}$$

$$y_2(t+T) = a_{21}\, y_1(t) + a_{22}\, y_2(t), \qquad \text{(A-2.2.2)}$$

where a_{ij} are constants.

Thus, the addition of the period T to t results in a linear transformation of the initial system of solutions. It is to be noted that other combinations of independent solutions are possible on the right hand side of the last two equations. In particular, one can try to choose solutions $y_1^*(t)$ and $y_2^*(t)$ such that the co-efficients a_{12} and a_{21} in equations (A-2.2) vanish. The transformation in this case will take its simplest form and will be reduced to the multiplication of initially chosen solutions by certain constants. These are sometimes known as Floquet solutions.

$$y_1^*(t+T) = \rho_1 \, y_1^*(t) \qquad \text{(A-2.3.1)}$$

$$y_2^*(t+T) = \rho_2 \, y_2^*(t) \qquad \text{(A-2.3.2)}$$

From the theory of linear transformations, the transformation of the type (A-2.2) can be reduced to the diagonal form (A-2.3), where the constants $\rho_{1,2}$ are known from the characteristic equation

$$\begin{vmatrix} a_{11} - \rho & a_{12} \\ a_{21} & a_{22} - \rho \end{vmatrix} = 0$$

which can be written in the following form,

$$\rho^2 - 2A\rho + B = 0, \qquad \text{(A-2.4)}$$

where,

$$A = \frac{1}{2}(a_{11} + a_{22}),$$

$$B = a_{11}\, a_{22} - a_{12}\, a_{21}.$$

The characteristic equation (A-2.4) defines the character of the solution of the equation (A-2.1). Hence it is desired to get the form of equation (A-2.4) from the independent linear solutions, $y_1(t)$ and $y_2(t)$. Let us assume the most general initial conditions for $y_1(t)$ and $y_2(t)$ as follows.

$$\begin{aligned} y_1(0) &= \alpha_1, & y_2(0) &= \alpha_2, \\ \dot{y}_1(0) &= \beta_1, & \dot{y}_2(0) &= \beta_2, \end{aligned} \qquad \text{(A-2.5)}$$

where $(\cdot)$ denotes differentiation with respect to t. These initial conditions are required to be satisfied by the solutions (A-2.2). Hence one gets using (A-2.2) and (A-2.5),

$$a_{11}\,\alpha_1 + a_{12}\,\alpha_2 = y_1(T), \qquad \text{(A-2.6.1)}$$

$$a_{11}\,\beta_1 + a_{12}\,\beta_2 = \dot{y}_1(T), \qquad \text{(A-2.6.2)}$$

$$a_{21}\,\alpha_1 + a_{22}\,\alpha_2 = y_2(T), \qquad \text{(A-2.6.3)}$$

$$a_{21}\,\beta_1 + a_{22}\,\beta_2 = \dot{y}_2(T). \qquad \text{(A-2.6.4)}$$

Equations (A-2.6) determine the constants a_{ij} as follows.

$$a_{11} = \frac{\alpha_2 \dot{y}_1(T) - \beta_2 y_1(T)}{\alpha_2\beta_1 - \alpha_1\beta_2} ,$$

$$a_{12} = \frac{\beta_1 y_1(T) - \alpha_1 \dot{y}_1(T)}{\alpha_2\beta_1 - \alpha_1\beta_2} ,$$

$$a_{21} = \frac{\alpha_2 \dot{y}_2(T) - \beta_2 y_2(T)}{\alpha_2\beta_1 - \alpha_1\beta_2} ,$$

and $$a_{22} = \frac{\beta_1 y_2(T) - \alpha_1 \dot{y}_2(T)}{\alpha_2\beta_1 - \alpha_1\beta_2} .$$

Using the values of constants a_{ij}, the constant B in (A-2.4) is given by

$$B = a_{11} a_{22} - a_{12} a_{21}$$

$$= \frac{y_1(T) \dot{y}_2(T) - y_2(T) \dot{y}_1(T)}{\alpha_1\beta_2 - \alpha_2\beta_1} . \qquad \text{(A-2.7)}$$

In the following it is proved that B is always equal to unity. Since $y_{1,2}(t)$ are solutions of equation (A-2.1) hence,

$$\ddot{y}_1 + \Omega_o^2 [1 - 2\varepsilon f(t)] y_1 = 0, \qquad \text{(A-2.8.1)}$$

$$\ddot{y}_2 + \Omega_o^2 [1 - 2\varepsilon f(t)] y_2 = 0. \qquad \text{(A-2.8.2)}$$

Multiplying (A-2.8.1) by $y_2(t)$ and (A-2.8.2) by $y_1(t)$, and subtracting one from the other, one gets

$$y_1(t)\ \ddot{y}_2(t) - y_2(t)\ \ddot{y}_1(t) = 0.$$

On integrating once, one obtains,

$$y_1(t)\ \dot{y}_2(t) - y_2(t)\cdot \dot{y}_1(t) = C, \qquad \text{(A-2.9)}$$

where C is the integration constant.

Using initial conditions (A-2.5) (at t=0), one obtains

$$C = \alpha_1\beta_2 - \alpha_2\beta_1 ,$$

and at t=T, equation (A-2.9) gives

$$y_1(T)\ \dot{y}_2(T) - y_2(T)\ \dot{y}_2(T) = \epsilon = \alpha_1\beta_2 - \alpha_2\beta_1.$$

Hence from (A-2.7),

$$B = 1.$$

Thus, the characteristic equation (A-2.4) becomes

$$\rho^2 - 2A\rho + 1 = 0, \qquad \text{(A-2.10)}$$

and its roots are related by

$$\rho_1\rho_2 = 1 \qquad \text{(A-2.11)}$$

It has been already shown that among the particular solutions of (A-2.1) two linearly independent solutions $y^*_{1,2}(t)$ exist which satisfy equations (A-2.3).

$$y_k^*(t+T) = \rho_k\, y_k^*(t), \quad k = 1,2 .$$

These solutions, which acquire a constant multiplier by the addition of the period T to t, can be represented in the form

$$y_k(t) = \chi_k(t)\; e^{(t/T)\,\ln \rho_k}, \quad k = 1,2, \qquad (A.2.12)$$

where $\chi_{1,2}(t)$ are certain periodic functions of period T.

It follows from equation (A-2.12) that the behavior of the solutions as $t\to\infty$ depends on the value of characteristic roots (more precisely, on the value of its moduli). In fact, taking into account that

$$\ln \rho = \ln|\rho| + i \arg\rho ,$$

one can write equation (A-2.12) in the following form

$$y_k(t) = f_{1k}(t)\; e^{(t/T)\ln|\rho_k|}, \quad k = 1,2 \qquad (A-2.13)$$

where,

$$f_{1k}(t) = \chi_k(t)\; e^{(it/T)\arg\rho}$$

and is bounded.

Looking to (A-2.13) one can establish the stability criteria. If the characteristic number $\rho_k > 1$, then the corresponding solution (A-2.13) increases unboundedly with time. If $\rho_k < 1$, then a bounded decaying solution with time

is obtained. If $\rho_k = 1$, then a periodic and bounded solution with time is obtained.

B is always equal to unity as noted earlier. Hence on the basis of the characteristic value ρ_k one can establish the limits on the values of A for stability using equation (A-2.4).

If $|A| > 1$, then the characteristic roots will be real, and one of them will be greater than unity. Hence the general solution of equation (A-2.1) will increase unboundedly with time.

If $|A| < 1$, the characteristic equation has complex conjugate roots and since their products must be equal to B=1, their moduli will be equal to unity (Eq. A-2.11). Thus the case of complex characteristic roots corresponds to the region of bounded solutions. On the boundaries separating the regions of bounded solutions, condition $|A| = 1$ must be satisfied [Ref. [13]].

For $|A| = 1$, multiple roots occur, moreover, it follows from equation (A-2.11) that such roots can be either $\rho_1 = \rho_2 = 1$ or $\rho_1 = \rho_2 = -1$. In the first case, as seen from (A-2.5), the solution will be periodic with a period $T = \frac{2\pi}{\omega}$; whereas in the second case the period will be $2T$.

Therefore, the regions of unbounded solutions are separated from the regions of bounded solutions by the periodic solutions with period T and 2T. In other words, two solutions of identical period bound the region of instability ($|A| > 1$), and two solutions of different periods bound the region of stability ($|A| \leq 1$).

Bolotin [13] has shown similarly for the coupled type of homogeneous Mathieu-Hill equations, that the solutions of an identical period bound the region of instability and two solutions of different periods bound the region of stability.

APPENDIX B

SOLUTION OF MATHIEU'S EQUATION

Following Mathieu's equation is considered to find the solution by small perturbation method.

$$\ddot{x} + \Omega^2 (1 - \varepsilon \cos \omega t)\, x = A, \tag{B.1}$$

in which A is constant and ε is a small parameter. Initial conditions for (B.1) are

$$x(0) = \dot{x}(0) = 0 . \tag{B.2}$$

One assumes the solution of (B.1) in a power series of ε as given below.

$$x = x_o + \varepsilon x_1 + \varepsilon^2 x_2 + \ldots + \varepsilon^k x_k \tag{B.3}$$

On substituting (B.3) into (B.1) and (B.2) and comparing the powers of ε^k on both sides of the equations, one obtains

$$\ddot{x}_o + \Omega^2 x_o = A, \tag{B.4.1}$$

with, $x(0) = \dot{x}(0) = 0,$ (B.4.2)

and

$$\ddot{x}_k + \Omega^2 x_k = \Omega^2 x_{k-1} \cos \omega t, \qquad (B.5.1)$$

with,

$$x_k(0) = \dot{x}_k(0) = 0, \quad k = 1,2,3,... \qquad (B.5.2)$$

The solution of (B.4.1) with initial conditions (B.4.2) is

$$x_o(t) = \frac{A}{\Omega^2}(1 - \cos \Omega t) \qquad (B.6)$$

Similarly the solution of x_1 using (B.6) one obtains from (B.5.1) and (B.5.2),

$$x_1(t) = A\left[\frac{\cos \omega t}{(\Omega^2-\omega^2)} + \frac{1}{2}\left(\frac{\cos(\Omega+\omega)t}{(2\Omega+\omega)\omega} - \frac{\cos(\Omega-\omega)t}{\omega(2\Omega-\omega)}\right)\right.$$

$$\left. - \frac{3\Omega^2 \cos \Omega t}{(\Omega^2-\omega^2)(4\Omega^2-\omega^2)}\right] \qquad (B.7)$$

Proceeding the same way as for x_1 one obtains the solution of x_2 as

$$x_2(t) = \frac{A\Omega^2}{2}\left[\frac{3}{(\Omega^2-\omega^2)(4\Omega^2-\omega^2)}\left(1 - \frac{\Omega^2}{\omega^2}\left(\frac{\cos(\Omega-\omega)t}{(2\Omega-\omega)} - \frac{\cos(\Omega+\omega)t}{(2\Omega+\omega)}\right)\right)\right.$$

$$- \frac{1}{8\omega^2}\left(\frac{\cos(\Omega+2\omega)t}{(2\Omega+\omega)(\Omega+\omega)} + \frac{\cos(\Omega-2\omega)t}{(2\Omega-\omega)(\Omega-\omega)}\right) + \frac{\cos 2\omega t}{(\Omega^2-\omega^2)(\Omega^2-4\omega^2)}$$

$$\left. + \frac{(\Omega^2 - 9\omega^2)}{\omega^2(4\Omega^2-\omega^2)(\Omega^2-4\omega^2)} \cos \Omega t\right] \qquad (B.8)$$

One may confine up to the terms containing ε^2 in the series of x and thus approximating x as,

$$x \simeq x_0 + \varepsilon x_1 + \varepsilon^2 x_2 \tag{B.9}$$

On substituting for x_0, x_1, x_2 in (B.9) one obtains

$$x = A\left[\frac{1}{\Omega^2}(1 - \cos\Omega t) + \varepsilon\left(\frac{-3\Omega^2 \cos\Omega t}{(\Omega^2-\omega^2)(4\Omega^2-\omega^2)} + \frac{\cos\omega t}{(\Omega^2-\omega^2)}\right.\right.$$

$$+ \frac{1}{2}\left(\frac{\cos(\Omega+\omega)t}{\omega(2\Omega+\omega)} - \frac{\cos(\Omega-\omega)t}{\omega(2\Omega-\omega)}\right)\Big) + \varepsilon^2 \frac{\Omega^2}{2}\left(\frac{3}{(\Omega^2-\omega^2)(4\Omega^2-\omega^2)}\right\{$$

$$1 - \frac{\Omega^2}{\omega}\left(\frac{\cos(\Omega-\omega)t}{(2\Omega-\omega)} - \frac{\cos(\Omega+\omega)t}{(2\Omega+\omega)}\right)\Big\} - \frac{1}{8\omega^2}\left(\frac{\cos(\Omega+2\omega)t}{(2\Omega+\omega)(\Omega+\omega)}\right.$$

$$+ \frac{\cos(\Omega-2\omega)t}{(2\Omega-\omega)(\Omega-\omega)}) + \frac{\cos 2\omega t}{(\Omega^2-\omega^2)(\Omega^2-4\omega^2)}$$

$$\left.\left.\left. + \frac{(\Omega^2-9\omega^2)\cos\Omega t}{\omega^2(4\Omega^2-\omega^2)(\Omega^2-4\omega^2)}\right)\right)\right] \tag{B.10}$$